NON-LINEAR FLEXURAL VIBRATIONS OF THIN CIRCULAR RINGS

Thesis by

David Arthur Evensen

In Partial Fulfillment of the Requirements

For the Degree of

Doctor of Philosophy

California Institute of Technology

Pasadena, California

1964

(Submitted May 22, 1964)

ACKNOWLEDGMENT

Throughout his graduate study, the author has benefited from the guidance and counsel of Dr. E. E. Sechler; this continued support during the present investigation is sincerely appreciated. The author is similarly indebted to Dr. T. K. Caughey, who made many helpful comments and suggestions concerning both the theoretical and experimental phases of this work. The advice of Dr. Y. C. Fung, and discussions with Dr. C. D. Babcock, Dr. L. V. Schmidt, and other members of the Aeronautics Staff is also appreciated.

The experimental program would not have succeeded without the support of Mr. M. E. Jessey and the other members of the Electronics Laboratory. Thanks are also due Miss Helen Burrus for typing the manuscript and Mrs. Betty Wood for the graphs and figures.

The financial support of the California Institute of Technology, the National Science Foundation, and the Space Technology Laboratories, Inc. made it possible for the author to continue his graduate study; this assistance is gratefully acknowledged.

Finally, the author is indebted to his wife and children and to his mother, who have provided continuing encouragement throughout this study. The work itself is dedicated to the memory of my father.

ABSTRACT

The non-linear flexural vibrations of thin circular rings are analyzed by means of the appropriate "shallow shell" equations. These partial differential equations are reduced to non-linear ordinary differential equations by assuming vibration modes and applying Galerkin's procedure. Vibrations involving primarily a single bending mode are investigated for three distinct cases, and the results indicate that the basic features of the problem are exhibited by an inextensional analysis.

This information is then applied to simplify the analysis of vibrations in which several modes participate. A study of "self-coupled" bending modes shows that the single mode solution is valid only for certain combinations of amplitude and frequency: when the single mode exceeds a "critical amplitude", its companion mode is parametrically excited and participates in the motion.

The general inextensional case (involving an infinite number of modes) is examined for two important sets of forces, and possible solutions are shown to be the excitation of primarily one or two bending modes. Stability analyses of these solutions indicate that when certain restrictions are met, all other bending modes play only a minor part in the vibration.

An experimental study of the problem was also conducted. Theory and experiment both indicate a non-linearity of the softening type, the presence of ultraharmonic responses, and the appearance of the companion mode. Measurements of the steady-state response

are in good agreement with the calculated values, and the experimentally determined mode shapes agree with the form of the assumed deflection.

The analytical and experimental results exhibit several features that are common to the non-linear vibration of axisymmetric systems in general and to circular cylindrical shells in particular.

TABLE OF CONTENTS

LIST OF FIGURES

LIST OF FIGURES (cont'd)

NOTATION

u, v, w	Displacements of the mid-surface of the ring; Fig. 1
x, y, z	Coordinate directions; Fig. 1
t	Time
$\dot{(\,)} = \frac{\partial (\,)}{\partial t}$ $\ddot{(\,)} = \frac{\partial^2 (\,)}{\partial t^2}$	Derivatives with respect to time
∇^2, ∇^4	$\nabla^2 = \frac{\partial^2}{\partial x^2} + \frac{\partial^2}{\partial y^2}$; $\nabla^4 = \nabla^2 \nabla^2$
n	Circumferential wave number; mode number
E	Young's Modulus
ν	Poisson's Ratio
ρ	Density
R	Radius of the ring
h	thickness
b	Width of the ring
$D = \frac{E h^3}{12 (1-\nu^2)}$	Bending stiffness
N_y	Circumferential force/unit length
q(y, t)	Load applied to the ring; see (1.4) - (1.6)
$A_n(t)$, $B_n(t)$	Time dependent coefficients; see (2.1)
$\varphi = \frac{A_n}{h} = \varphi_c = \varphi_{cn}$	Non-dimensional amplitude of the $\cos \frac{ny}{R}$ mode
$\varphi_s = \frac{B_n}{h} = \varphi_{sn}$	Non-dimensional amplitude of the $\sin \frac{ny}{R}$ mode

$\eta = \frac{n^2 h}{R} = \eta_n$, $\epsilon = \eta^2$ — Non-Linearity parameters

$\eta_0 = \frac{A_0}{h} = \eta r$ — Non-Dimensional amplitude

τ — Non-Dimensional time

ω — Frequency, radians/sec.

$\omega_s^2 = \frac{E}{\rho R^2} \frac{n^4 h^2}{12(1-\nu^2)R^2} = \frac{E}{\rho R^2} \frac{\eta^2}{12(1-\nu^2)}$

$\omega_M^2 = \frac{E}{\rho R^2} \frac{(n^2-1)^2 h^2}{12(1-\nu^2)R^2} = \frac{E}{\rho R^2} \frac{(1-\frac{1}{n^2})^2 \eta^2}{12(1-\nu^2)}$

Ω — Non-Dimensional frequency

$Q_n(t) = \int_0^{2\pi R} q(y,t) \cos \frac{ny}{R} dy = C_n(t)$

$Q_0(t) = \int_0^{2\pi R} q(y,t)\, dy$

$S_n(t) = \int_0^{2\pi R} q(y,t) \sin \frac{ny}{R} dy$

$\frac{1}{F} = \frac{(1-\frac{1}{n^2})^2}{12(1-\nu^2)}$

$\gamma = \frac{n C_n}{h}$, $\delta_0 = \frac{n D_n}{h} = \eta \delta$ — Non-Dimensional coefficients; see (2.32)

F_n, F_0, G_n, G_0 — Amplitude of the loading; see (3.1) and (3.3)

$A(\tau), B(\tau), \phi(\tau), \psi(\tau)$ — Slowly varying amplitudes and phase angles

$\bar{A}, \bar{B}, \bar{\phi}, \bar{\psi}$ — Average values of $A(\tau)$, etc. over one period

$\bar{\Delta} = \bar{\psi} - \bar{\phi}$ — Average phase difference

$\beta, \beta_c, \beta_{cn}$ — Per cent critical damping in the $\cos \frac{ny}{R}$ mode

β_s β_{sm}	Per cent critical damping in the sin $\frac{ny}{R}$ mode
$\zeta(\tau)$, $\zeta_m(t)$	Perturbation in the cos $\frac{ny}{R}$ mode
$x(\tau)$, $x_m(t)$	Perturbation in the sin $\frac{ny}{R}$ mode

Other symbols used are defined as they occur in the text.

I. INTRODUCTION

The flexural vibrations of circular rings were first considered by Hoppe (Ref. 1) in 1871. In 1894, Rayleigh's "Theory of Sound" (Ref. 2) included calculation of the linear vibration modes and frequencies, making use of the approximation that the mid-surface of the ring was inextensional. Since that time, the effects of mid-plane extension (Ref. 3), shear deformation (Ref. 4), and rotary inertia (Ref. 5) have been investigated.

The first study of the elastic, non-linear flexural vibrations of rings appears to be the 1959 paper of Federhofer (Ref. 6), who considered the free vibration problem. The same problem was examined by Shkenev (Ref. 7), who also investigated parametrically excited vibrations, as did McIvor and Goodier (Ref. 8). Although the linear vibrations have been studied experimentally (Refs. 9 and 10), no experiments on the non-linear vibration of rings have been reported in the literature.

The present work is concerned with the forced, non-linear flexural vibrations of thin circular rings. Only vibrations in the plane of the ring are considered. The material of the ring is assumed to obey Hooke's Law; that is, the relation between stress and strain in the ring is taken to be linear. The non-linearities examined here are geometric in nature, arising from the non-linear terms of the general strain-displacement relations.

The problem was studied in detail theoretically and experimentally. Both aspects of the work were carried out concurrently, and as

a result they complemented each other considerably. Before proceeding with the discussion, however, it seems appropriate to mention the events which led up to this particular study.

It began in 1962 with some experiments that were run on the non-linear vibration of thin cylindrical shells. The experimental results were at variance with the available analyses (Refs. 11 to 13); this led to a re-examination of the theoretical work. Apparently, a boundary condition was neglected in these studies (Ref. 14). When the problem was reformulated to satisfy this constraint, qualitative agreement with the experiments was obtained.

At this point, it was suggested that the non-linear vibration of a thin ring be investigated, since the ring and the shell would be expected to have much in common. A first attempt at the ring analysis was done, and some preliminary experiments were conducted. It was found that the shell and ring analyses did indeed possess several similarities. More promising than that, however, was the agreement indicated between the ring analysis and experiments. As the work progressed, the decision was made to concentrate on the ring problem, leaving the shell study for another report. Thus, while the primary goal of this thesis is to analyze the forced, non-linear flexural vibrations of a thin circular ring, it was hoped that some light would be shed on the cylindrical shell problem as well.

II. THE MATHEMATICAL PROBLEM

The non-linear flexural vibrations of a thin circular ring may be analyzed mathematically, providing certain assumptions are made. It is the purpose of this part of the thesis to present these assumptions and the analysis which results.

First, the partial differential equations which govern the motion of a circular ring are presented. By assuming that the vibration involves only certain vibration modes, the equations of motion can be reduced to ordinary differential equations. Such equations are derived for three distinct cases which involve the vibration of primarily a single bending mode. Comparison of the solutions to these equations shows that the basic non-linear behavior of the ring may be obtained from an inextensional analysis. This facilitates the study of vibrations which involve several bending modes, and the equations governing such vibrations are derived. Approximate solutions to these equations are presented, for the case of some important forcing functions. With some relatively minor restrictions, it can be shown that only one or two vibration modes will participate in the motion, even though the ring is forced to vibrate to large amplitudes. Finally, the effects of some additional non-linearities, shear deformation, and rotary inertia are discussed, and comparisons are made with some analogous problems.

2.1. The Equations of Motion

Since this work originated with a study on thin cylindrical shells, it was only natural to obtain a set of ring equations by

specializing the well-known shallow shell equations to the case of a ring. Preliminary analyses using these equations indicated qualitative agreement with the experiments in several areas.

The shallow shell equations are, of course, subject to the approximations made in their development. The assumption that $\frac{1}{n^2}$ is negligible in comparison to unity (where n is the circumferential wave number) is inherent in these equations. As a result, when specialized to a ring, they do not yield the correct expression for the vibration frequency. This discrepancy is most noticeable for low values of n (e.g. $n < 6$) and has been pointed out for shell vibrations as well. Yet, because of their relative simplicity, one is reluctant to abandon the shallow shell equations in favor of another set.

Faced with a similar problem, Morley (Ref. 15) found that he could significantly improve the linearized form of these equations without impairing their simplicity. By modifying the shallow shell equations as Morley's work suggests, one obtains a set of equations that yield the correct linear vibration frequencies and that have the same non-linear terms as the original set. This amounts to rejecting the approximation that $\frac{1}{n^2} << 1$ where the linear terms are concerned, but retaining it for the non-linear terms. While this is inconsistent, it is extremely useful from the standpoint of attempting to solve the equations.

Finally, a somewhat more exact set of equations for a ring are presented herein. These equations retain all the linear terms and do not assume that $\frac{1}{n^2} << 1$. They possess the properties that

(a) when linearized, they reduce to the linear, extensional ring equations, and

(b) when the approximation $\frac{1}{n^2} << 1$ is made throughout, they reduce to the shallow shell equations specialized to a ring.

The major portion of this work employs the shallow shell equations and the modified form of them. It is possible to treat both these cases simultaneously, since the equations differ only in a linear term. The more exact set of equations serve primarily for comparison purposes and to indicate the effects of additional non-linearities.

An alternative to using the differential equations of motion is to employ an energy method. Both approaches can be made to coincide (Ref. 16), and the results presented herein can be obtained by either technique.

2.1.1 The Shallow Shell Equations and their Specialization to a Ring

The shallow shell equations have long been employed in non-linear analyses of thin cylindrical shells. In terms of stress resultants, they are (see Ref. 12)

$$\frac{\partial N_x}{\partial x} + \frac{\partial N_{xy}}{\partial y} = \rho h \ddot{u}$$

$$\frac{\partial N_{xy}}{\partial x} + \frac{\partial N_y}{\partial y} = \rho h \ddot{v}$$

$$\frac{\partial^2 M_x}{\partial x^2} + 2\frac{\partial^2 M_{xy}}{\partial x\,\partial y} + \frac{\partial^2 M_y}{\partial y^2}$$
$$+ \frac{\partial}{\partial x}\left(N_x \frac{\partial w}{\partial x} + N_{xy}\frac{\partial w}{\partial y}\right) + \frac{\partial}{\partial y}\left(N_y \frac{\partial w}{\partial y} + N_{xy}\frac{\partial w}{\partial x}\right) \qquad (1.0)$$
$$- \frac{N_y}{R} + q(x,y,t) = \rho h \ddot{w}$$

where u, v, and w are the mid-plane displacements in the axial, circumferential, and radial directions respectively (see Fig. 1). The stress-resultants are defined in the usual way*

$$N_x = \int_{-\frac{h}{2}}^{\frac{h}{2}} \sigma_{xx}\,dz \qquad N_{xy} = \int_{-\frac{h}{2}}^{\frac{h}{2}} \sigma_{xy}\,dz \qquad N_y = \int_{-\frac{h}{2}}^{\frac{h}{2}} \sigma_{yy}\,dz$$
$$M_x = \int_{-\frac{h}{2}}^{\frac{h}{2}} \sigma_{xx}\,z\,dz \qquad M_{xy} = \int_{-\frac{h}{2}}^{\frac{h}{2}} \sigma_{xy}\,z\,dz \qquad M_y = \int_{-\frac{h}{2}}^{\frac{h}{2}} \sigma_{yy}\,z\,dz \qquad (1.1)$$

and q(x, y, t) is the applied load, which acts in the radial direction. The strain-displacement relations are taken in the form

---

* It might be noted at this point that the stresses and stress-resultants in (1.1) are all referred to an undeformed element of the shell, in its original position. Since shallow shell theory assumes that all strains and all slopes are small in comparison with unity, the stresses and forces on the deformed element are, in a first approximation, equal to their counterparts for the undeformed element. For a general discussion of this point, the reader is referred to Novozhilov (Ref. 33).

$$\varepsilon_{xx} = \frac{\partial u}{\partial x} + \frac{1}{2}\left(\frac{\partial w}{\partial x}\right)^2 - z\frac{\partial^2 w}{\partial x^2}$$

$$\varepsilon_{yy} = \frac{\partial v}{\partial y} + \frac{w}{R} + \frac{1}{2}\left(\frac{\partial w}{\partial y}\right)^2 - z\frac{\partial^2 w}{\partial y^2} \qquad (1.2)$$

$$\varepsilon_{xy} = \frac{\partial v}{\partial x} + \frac{\partial u}{\partial y} + \frac{\partial w}{\partial x}\cdot\frac{\partial w}{\partial y} - 2z\frac{\partial^2 w}{\partial x\,\partial y}$$

Transverse shear deformation is neglected, and the transverse normal stress is assumed to be negligible. That is, one assumes

$$\varepsilon_{xz} = 0, \qquad \varepsilon_{yz} = 0, \qquad \sigma_{zz} = 0$$

Hooke's Law is used to relate the stresses to the strains; with the preceding assumptions, it yields

$$\sigma_{yy} = \frac{E}{1-\nu^2}\left[\varepsilon_{yy} + \nu\varepsilon_{xx}\right] \qquad \sigma_{xx} = \frac{E}{1-\nu^2}\left[\varepsilon_{xx} + \nu\varepsilon_{yy}\right]$$

$$\sigma_{xy} = \frac{E}{2(1+\nu)}\varepsilon_{xy}$$

where E is Young's modulus and ν is Poisson's ratio. Employing these stresses and equations (1.2) and (1.1) and carrying out the integration through the thickness yields

$$N_y = \frac{Eh}{1-\nu^2}\left[\frac{\partial v}{\partial y} + \frac{w}{R} + \frac{1}{2}\left(\frac{\partial w}{\partial y}\right)^2 + \nu\left\{\frac{\partial u}{\partial x} + \frac{1}{2}\left(\frac{\partial w}{\partial x}\right)^2\right\}\right]$$

$$N_x = \frac{Eh}{1-\nu^2}\left[\frac{\partial u}{\partial x} + \frac{1}{2}\left(\frac{\partial w}{\partial x}\right)^2 + \nu\left\{\frac{\partial v}{\partial y} + \frac{w}{R} + \frac{1}{2}\left(\frac{\partial w}{\partial y}\right)^2\right\}\right]$$

$$N_{xy} = \frac{Eh}{2(1+\nu)}\left[\frac{\partial v}{\partial x} + \frac{\partial u}{\partial y} + \frac{\partial w}{\partial x}\cdot\frac{\partial w}{\partial y}\right]$$

$$M_y = -D\left[\frac{\partial^2 w}{\partial y^2} + \nu\frac{\partial^2 w}{\partial x^2}\right] \qquad (1.3)$$

$$M_x = -D\left[\frac{\partial^2 w}{\partial x^2} + \nu\frac{\partial^2 w}{\partial y^2}\right]$$

$$M_{xy} = -D(1-\nu)\frac{\partial^2 w}{\partial x\,\partial y}$$

$$\text{WHERE} \quad D = \frac{Eh^3}{12(1-\nu^2)}$$

These relations can be inserted in (1.0) to give the shell equations of motion completely in terms of the displacements u, v, and w.

To specialize the shallow shell equations to the case of a ring, the following assumptions will be made:

a. The displacements w and v are taken to be functions of only the circumferential coordinate (y) and the time. That is, all derivatives of these displacements with respect to x are assumed to be zero*.

b. The transverse load, q, is likewise taken to be a function of only the circumferential coordinate and the time.

c. The thickness of the ring, h, and the ring width, b, are both taken to be constant. The ring is assumed to be thin, such that $(\frac{h}{R})^2$ is negligible in comparison to unity.

d. The stress resultants N_x and N_{xy} are assumed to be zero throughout the ring. The boundary conditions at the ends of the ring (at x = 0, x = b, Fig. 1) require that N_x and N_{xy} vanish there; for flexural vibrations, one does not anticipate rapid variations in the x-direction and is thus led to assume $N_x = 0$, $N_{xy} = 0$ throughout.

Using these assumptions, equations (1.3) may be written in the form

$$N_y = Eh\left[\frac{\partial v}{\partial y} + \frac{w}{R} + \frac{1}{2}\left(\frac{\partial w}{\partial y}\right)^2\right], \quad N_x = 0, \quad N_{xy} = 0$$

$$M_y = -D\frac{\partial^2 w}{\partial y^2}, \qquad M_x = -\nu D\frac{\partial^2 w}{\partial y^2}, \qquad M_{xy} = 0$$

---

* Since we intend to discuss the flexural vibrations of rings, one might legitimately ask if bending in the circumferential direction would give rise to a curvature in the x-direction (anticlastic curvature) and thereby invalidate the assumption above. However, in problems concerning the large deflection of thin plates with free edges, it has been shown (see Ref. 34) that a boundary layer phenomenon occurs which inhibits the anticlastic behavior. Based upon the results of Ref. 34, one suspects that for thin rings, assumption (a) will be valid in all but a very narrow region near the edges.

Using assumption (a) and inserting the results for N_y, etc. in equations (1.0) gives the displacement equations of motion for a thin ring:

$$0 = \rho h \ddot{u}$$

$$Eh \frac{\partial}{\partial y}\left[\frac{\partial v}{\partial y} + \frac{w}{R} + \frac{1}{2}\left(\frac{\partial w}{\partial y}\right)^2\right] = \rho h \ddot{v} \qquad (1.4a)$$

$$D\frac{\partial^4 w}{\partial y^4} + \frac{Eh}{R}\left[\frac{\partial v}{\partial y} + \frac{w}{R} + \frac{1}{2}\left(\frac{\partial w}{\partial y}\right)^2\right]$$

$$- Eh \frac{\partial}{\partial y}\left[\frac{\partial v}{\partial y} + \frac{w}{R} + \frac{1}{2}\left(\frac{\partial w}{\partial y}\right)^2\right] + \rho h \ddot{w} = q(y,t) \qquad (1.4b)$$

The first of these equations is unimportant for the problems dealt with herein, and henceforth it will be dropped.

2.1.2 Modification of the Shallow Shell and Ring Equations

When in-plane inertia is neglected, the shallow shell equations (1.0) can be written in terms of two variables, w and F. They are derived by many authors (see Refs. 11 and 12, for example) and will simply be quoted here:

$$D\nabla^4 w + \rho h \ddot{w} = -\frac{1}{R}\frac{\partial^2 F}{\partial x^2} + \frac{\partial^2 F}{\partial y^2}\frac{\partial^2 w}{\partial x^2} - 2\frac{\partial^2 F}{\partial x \partial y}\frac{\partial^2 w}{\partial x \partial y} + \frac{\partial^2 F}{\partial x^2}\frac{\partial^2 w}{\partial y^2} + q(x, y, t)$$

$$\frac{\nabla^4 F}{Eh} = \frac{1}{R}\frac{\partial^2 w}{\partial x^2} + \left[\left(\frac{\partial^2 w}{\partial x \partial y}\right)^2 - \frac{\partial^2 w}{\partial x^2}\frac{\partial^2 w}{\partial y^2}\right]$$

$D = \dfrac{Eh^3}{12(1-\nu^2)}$ is the familiar bending stiffness, and F is a stress function: $N_x = \dfrac{\partial^2 F}{\partial y^2}$, $N_{xy} = -\dfrac{\partial^2 F}{\partial x \partial y}$, and $N_y = \dfrac{\partial^2 F}{\partial x^2}$.

Morley (Ref. 15) improved the linearized form of these equations by replacing $D\nabla^4 w$ with $D(\nabla^2 + \frac{1}{R^2})^2 w$. (see Section 2.1.). The resulting equations compare favorably with the more exact (and more complicated) equations of Flugge for both static and dynamic problems (Ref. 16).

The analogous improvement in the displacement equations of motion for a ring results in the following equations:

$$Eh\frac{\partial}{\partial y}\left[\frac{\partial v}{\partial y} + \frac{w}{R} + \frac{1}{2}\left(\frac{\partial w}{\partial y}\right)^2\right] = \rho h \ddot{v} \qquad (1.5a)$$

$$D\left(\frac{\partial^2}{\partial y^2} + \frac{1}{R^2}\right)\left(\frac{\partial^2 w}{\partial y^2} + \frac{w}{R^2}\right) + \frac{Eh}{R}\left[\frac{\partial v}{\partial y} + \frac{w}{R} + \frac{1}{2}\left(\frac{\partial w}{\partial y}\right)^2\right]$$

$$-Eh\frac{\partial}{\partial y}\left\{\left[\frac{\partial v}{\partial y} + \frac{w}{R} + \frac{1}{2}\left(\frac{\partial w}{\partial y}\right)^2\right]\frac{\partial w}{\partial y}\right\} + \rho h \ddot{w} = q(y, t) \qquad (1.5b)$$

2.1.3 A More Exact Set of Ring Equations

By making approximations similar to those used in deriving the shallow shell equations but not assuming that $\frac{1}{n^2} << 1$, a more exact set of ring equations can be obtained. The derivation of these equations is outlined in Appendix A. They are presented here for comparison with (1.4) and (1.5); they are

$$Eh\frac{\partial}{\partial y}\left[\frac{\partial v}{\partial y}+\frac{w}{R}+\frac{1}{2}\left(\frac{\partial w}{\partial y}\right)^2\right]+\frac{Eh}{R}\left\{\frac{w}{R}\left(\frac{\partial w}{\partial y}-\frac{v}{R}\right)-v\frac{\partial^2 w}{\partial y^2}+\left(\frac{\partial w}{\partial y}-\frac{v}{R}\right)^3\right\}=\rho h\ddot{v} \tag{1.6a}$$

and

$$D\left[\frac{\partial^4 w}{\partial y^4}+\frac{2}{R^2}\frac{\partial^2 w}{\partial y^2}-\frac{1}{R^3}\frac{\partial v}{\partial y}\right]+\frac{Eh}{R}\left[\frac{\partial v}{\partial y}+\frac{w}{R}+\frac{1}{2}\left(\frac{\partial w}{\partial y}\right)^2\right]$$

$$-Eh\frac{\partial}{\partial y}\left\{\left[\frac{\partial v}{\partial y}+\frac{w}{R}+\frac{1}{2}\left(\frac{\partial w}{\partial y}\right)^2\right]\frac{\partial w}{\partial y}\right\}+\rho h\ddot{w}$$

$$+\frac{Eh}{R}\left\{\frac{\partial v}{\partial y}\left[\frac{\partial v}{\partial y}+\frac{w}{R}+\frac{1}{2}\left(\frac{\partial w}{\partial y}\right)^2\right]+v\left[\frac{\partial^2 v}{\partial y^2}\right.\right. \tag{1.6b}$$

$$\left.+\frac{v}{2R^2}+3\frac{\partial w}{\partial y}\frac{\partial^2 w}{\partial y^2}-\frac{3}{R}\frac{\partial w}{\partial y}\frac{\partial v}{\partial y}-\frac{3}{2R}v\frac{\partial^2 w}{\partial y^2}\right.$$

$$\left.\left.+\frac{3}{2R^2}v\frac{\partial v}{\partial y}\right]+\frac{\partial v}{\partial y}\left(\frac{\partial w}{\partial y}\right)^2\right\}=q(y,t)$$

The brackets which are underlined indicate the non-linear terms which (1.4) and (1.5) do not contain; the simplification which results from the $\frac{1}{n^2} << 1$ approximation is quite evident.

2.1.4 Boundary and Initial Conditions

The boundary conditions on w and v are of the "periodic" type. They are

$$w(0,t) = w(2\pi R, t); \quad \frac{\partial w}{\partial y}(0,t) = \frac{\partial w}{\partial y}(2\pi R, t)$$

$$\frac{\partial^2 w}{\partial y^2}(0,t) = \frac{\partial^2 w}{\partial y^2}(2\pi R, t); \quad \frac{\partial^3 w}{\partial y^3}(0,t) = \frac{\partial^3 w}{\partial y^3}(2\pi R, t) \tag{1.7}$$

and

$$v(0,t) = v(2\pi R, t); \quad \frac{\partial v}{\partial y}(0,t) = \frac{\partial v}{\partial y}(2\pi R, t) \tag{1.8}$$

From a physical standpoint, these boundary conditions insure that the displacements, slope, bending moment, transverse shear force, and circumferential strain remain continuous in going around the ring. The above conditions arise naturally in a derivation of the equations of motion by variational methods. (see Appendix A, for example).

Only "steady-state" vibrations are considered herein; i. e., the motion is assumed to have been going on for such a long time that the "starting transients" have disappeared. Steady-state vibrations imply that the motion of the ring is periodic in time. This requires

$$w(y,t) = w(y, t+T) \qquad \frac{\partial w}{\partial y}(y,t) = \frac{\partial w}{\partial y}(y, t+T)$$

$$\frac{\partial^2 w}{\partial y^2}(y,t) = \frac{\partial^2 w}{\partial y^2}(y, t+T) \qquad \frac{\partial^3 w}{\partial y^3}(y,t) = \frac{\partial^3 w}{\partial y^3}(y, t+T) \tag{1.9}$$

$$v(y,t) = v(y, t+T) \qquad \frac{\partial v}{\partial y}(y,t) = \frac{\partial v}{\partial y}(y, t+T)$$

where T is the period of the motion.

2.1.5 An Alternative to using the Equations of Motion

After choosing a set of equations to use, one is faced with finding their solution, subject to the conditions just discussed. Since we are dealing with non-linear partial differential equations, exact solutions are difficult to obtain. Furthermore, the equations themselves are already inexact, which suggests attempting approximate solutions. One approximate approach is to first solve the linearized problem and use its results to estimate the non-linear terms in the non-linear equations. This yields a second set of linear equations; their solution is a first improvement on the original, linear one. An iteration scheme of this type was used by Federhofer (Ref. 6).

An approach that has proved useful for the study of other structures is to assume the shape of the deflection in space. By then applying various approximate techniques, one can reduce the problem to one involving non-linear ordinary (in lieu of partial) differential equations, with time as the independent variable. This approach has been employed in the non-linear vibration of strings (Ref. 18), beams (Ref. 19), plates (Ref. 20), and shells (Refs. 11 - 13).

An alternative to using the equations of motion directly is to apply an energy method. Using approximations similar to those made in deriving the differential equations, one can write expressions for the kinetic energy of the ring (T), its strain energy (V), and the potential energy of the external forces (W). If one then assumes the shape of the deflection in space, it is possible to express T, V, and W as functions of time only. These expressions are then used in Lagrange's Equations, and non-linear ordinary differential equations result.

The present work assumes the shape of the deflection (the vibration "mode"), and ordinary differential equations are obtained either by (a) applying Galerkin's procedure on the equations of motion or (b) by the energy method just indicated.

2.2. Ordinary Differential Equations which Result from Various "Single Bending Mode" Assumptions

As was just noted, assuming the shape of the deflection makes it possible to reduce the problem to one involving ordinary differential equations. The usefulness of this technique depends greatly on how successful one is in estimating the actual deflection shape. Perhaps the most general radial deflection that is compatible with the constraints (1.7 - 1.9) is

$$w(y,t) = \sum_{n=0}^{\infty} \left[A_n(t) \cos \frac{2n\pi y}{2\pi R} + B_n(t) \sin \frac{2n\pi y}{2\pi R} \right]$$

$$= \sum_{n=0}^{\infty} \left[A_n(t) \cos \frac{ny}{R} + B_n(t) \sin \frac{ny}{R} \right] \qquad (2.1)$$

where A_n and B_n are periodic functions of time, with period T. Each A_n and B_n can in turn be expanded as a Fourier Series in time; thus it is possible to represent virtually any radial deflection of interest here in the form (2.1).

The functions $\cos \frac{ny}{R}$ and $\sin \frac{ny}{R}$ correspond to the nth linear vibration mode of a ring. From the study of linear vibrations, one knows it is possible to excite a single mode in a structure by proper arrangement of the forcing function in space and by a proper choice of the driving frequency. In considering non-linear vibrations of the structure, one frequently limits himself to the case where primarily one mode (one deflection function, say) is excited. This is the approach which has been employed in other non-linear vibration studies and verified experimentally in the case of strings and beams (see Refs. 18 and 21).

Applying this to the present problem, one is led to replace the series (2.1) by

$$w(y,t) = A_m(t) \cos \frac{ny}{R} \quad \text{or} \quad B_m(t) \sin \frac{ny}{R} \tag{2.2}$$

and limit the discussion to vibrations that involve primarily the nth linear bending mode. However, when finite amplitude vibrations are considered, mode shapes of the form (2.2) involve appreciable stretching of the mid-surface of the ring. Yet, for the linear case at least, it has long been known that thin rings vibrate in such a manner that the mid-surface of the ring remains very nearly inextensional! With this in mind, a more realistic deflection form in which the nth

bending mode vibrates to finite amplitudes is

$$w(y,t) = \left\{ \begin{matrix} A_m(t)\cos\frac{ny}{R} \\ B_m(t)\sin\frac{ny}{R} \end{matrix} \right\} + A_o(t) \qquad (2.3)$$

In this section, ordinary differential equations for the $A_n(t)$ are derived by assuming $w(y,t)$ in the form (2.3). This automatically limits the discussion to vibrations involving primarily a single bending mode. Initially, the effect of tangential inertia is neglected, and the cases of an inextensional ring and extensional ring are discussed. Finally, the effects of both tangential inertia and extension are included. The resulting differential equations are discussed and compared. Approximate solutions for them are presented in Section 2.3.

Comparison of the solutions indicates that the approximation of an inextensional mid-surface is a good one even for finite amplitude vibrations of thin rings. This approximation facilitates the study of vibrations involving multiple bending modes (including the series, (2.1)), which is discussed in Section 2.5.

2.2.1 Equations in which Tangential Inertia is Neglected

As a first step in obtaining approximate solutions to the equations of motion, consider the case in which the effect of tangential inertia is negligible.

When the frequency of flexural vibration is well below the frequency of the first extensional mode of the ring, the extensional

modes respond essentially statically. In this case, it is a good approximation to neglect the effect of tangential inertia*. Thus, when

$$\omega^2 << \frac{E}{\rho R^2} \tag{2.4}$$

($\frac{1}{R}\sqrt{\frac{E}{\rho}}$ is the frequency of the first extensional mode of the ring) holds, the equation for tangential displacements from (1.4) or (1.5) reads

$$E h \frac{\partial}{\partial y}\left[\frac{\partial v}{\partial y} + \frac{w}{R} + \frac{1}{2}\left(\frac{\partial w}{\partial y}\right)^2\right] = \rho h \ddot{v} \cong 0$$

Or, since $N_y = E h \left[\frac{\partial v}{\partial y} + \frac{w}{R} + \frac{1}{2}\left(\frac{\partial w}{\partial y}\right)^2\right]$,

one has

$$\frac{\partial N_y}{\partial y} = 0 \tag{2.5}$$

which can be integrated immediately, giving

$$N_y = q(t) \tag{2.6}$$

That is, the stress resultant N_y is a function of time only and does not vary around the circumference of the ring. This result will be employed in the two specific cases which follow.

(a) The Inextensional Ring

To obtain inextensional vibrations, one stipulates that the mid-plane strain in the circumferential direction shall be zero for all y and t. As a result, the circumferential length of the ring remains

---

* The reader familiar with the non-linear vibration of strings and beams will recall that it is common to neglect longitudinal inertia on similar grounds in those studies.

constant*. For the present treatment, then, inextensional vibrations means that

$$\epsilon_{yy}\Big|_{z=0} = \frac{\partial v}{\partial y} + \frac{w}{R} + \frac{1}{2}\left(\frac{\partial w}{\partial y}\right)^2 = 0 \qquad (2.7)$$

This condition is applicable for both (1.4) and (1.5). Solving for $\frac{\partial v}{\partial y}$, one has

$$\frac{\partial v}{\partial y} = -\frac{w}{R} - \frac{1}{2}\left(\frac{\partial w}{\partial y}\right)^2$$

Now, if one attempts to use the deflection shape

$$w(y,t) = A_n(t)\cos\frac{ny}{R} \qquad (2.2)$$

he sees that

$$\frac{\partial v}{\partial y} = -\frac{A_n}{R}\cos\frac{ny}{R} - \frac{1}{2}\left(-\frac{nA_n}{R}\sin\frac{ny}{R}\right)^2$$

$$= -\frac{n^2A_n^2}{4R^2} + \text{terms periodic in } y.$$

By direct integration, this is seen to be incompatible with the boundary condition $v(0,t) = v(2\pi R,t)$. For inextensional vibrations, (2.2) must be modified such that $\frac{\partial v}{\partial y}$ contains no terms that are functions of time alone. This can be accomplished by taking w in the form

$$w(y,t) = A_n(t)\cos\frac{ny}{R} + A_0(t) \qquad (2.3)$$

---

* A slightly more general problem would be to consider vibrations in which the length of the ring remained constant but where the mid-plane strain was not identically zero at every point; however, this is incompatible with neglecting tangential inertia.

Then,

$$\frac{\partial v}{\partial y} = -\frac{A_0}{R} - \frac{n^2 A_n^2}{4R^2} \qquad + \text{terms periodic in y}$$

and to satisfy the constraint on v, the terms that depend only on time are equated to zero:

$$-\frac{A_0}{R} - \frac{n^2 A_n^2}{4R^2} = 0, \qquad \text{OR} \qquad A_0 = -\frac{n^2 A_n^2}{4R}$$

Thus, (2.3) becomes

$$w(y,t) = A_n(t)\cos\frac{ny}{R} - \frac{n^2 A_n^2(t)}{4R} \tag{2.8}$$

Having found a deflection shape that allows the ring to vibrate inextensionally, it is possible to employ it and (2.7) in the equations of motion and apply Galerkin's procedure. Rather than do that, however, let us use this case to demonstrate the energy method.

With tangential inertia neglected, the kinetic energy is approximated by

$$T = \frac{\rho h b}{2}\int_0^{2\pi R}\left[\frac{\partial w}{\partial t}\right]^2 dy \tag{2.9}$$

For inextensional vibrations, the strain energy expression is

$$V = \frac{E b h^3}{24(1-\nu^2)}\int_0^{2\pi R}\left[\frac{\partial^2 w}{\partial y^2}\right]^2 dy \tag{2.10}$$

where the z integration has been carried out. Finally, the potential

energy of the applied load is

$$W = -b \int_0^{2\pi R} q(y,t)\, dy \tag{2.11}$$

By substituting (2.8) into these expressions, it is possible to express T, V, and W as functions of $A_n(t)$. Then one simply writes Lagrange's Equations for the motion, considering $A_n(t)$ as the generalized displacement. That is, one has

$$\frac{d}{dt}\left(\frac{\partial L}{\partial \dot{A}_n}\right) - \frac{\partial L}{\partial A_n} = 0 \tag{2.12}$$

where $L = T - (V + W)$.

Carrying out the various operations, (2.9 - 2.12) combine to yield

$$\ddot{A}_n + \frac{n^4}{2R^2} A_n \left(A_n \ddot{A}_n + \dot{A}_n^2\right) + \omega_s^2 A_n + \frac{n^2}{2R} A_n \frac{Q_0(t)}{\pi R \rho h} = \frac{Q_n(t)}{\pi R \rho h} \tag{2.13}$$

where

$$\omega_s^2 = \frac{E}{\rho R^2}\left[\frac{n^4 h^2}{12(1-\nu^2)R^2}\right], \quad Q_0(t) = \int_0^{2\pi R} q(y,t)\, dy, \tag{2.14}$$

$$\text{AND} \quad Q_n(t) = \int_0^{2\pi R} q(y,t) \cos\frac{ny}{R}\, dy$$

Equation (2.13) can be obtained by substituting (2.8) into (1.4) and applying Galerkin's procedure with $\frac{\partial w}{\partial A_n}$ as the weighting function. Analogous results are obtained by taking $w = B_n(t) \sin \frac{ny}{R} - \frac{n^2 B_n^2}{4R}$. If (1.5) is used, ω_s^2 is replaced by

$$\omega_M^2 = \frac{E}{\rho R^2}\left[\frac{(n^2-1)^2 h^2}{12(1-\nu^2)R^2}\right].$$

Now, define $\gamma = \frac{A_n(t)}{h}$, $\eta = \frac{n^2 h}{R}$, $\tau = \omega_s t$. Then (2.13) gives

$$\gamma_{\tau\tau} + \frac{\eta^2}{2}\gamma\left[\gamma\gamma_{\tau\tau} + \gamma_\tau^2\right] + \gamma + \frac{\eta\gamma}{2}\frac{Q_o(\tau)}{\pi R\rho h^2 \omega_s^2} = \frac{Q_n(\tau)}{\pi R\rho h^2 \omega_s^2} \tag{2.15}$$

and, from (2.8),

$$r_o = \frac{A_o}{h} = -\frac{\eta\gamma^2}{2} \tag{2.16}$$

For free vibrations, (2.15) becomes

$$\gamma_{\tau\tau} + \frac{\epsilon}{2}\gamma\left[\gamma\gamma_{\tau\tau} + \gamma_\tau^2\right] + \gamma = 0 \tag{2.17}$$

where $\epsilon = \eta^2$. This equation can be integrated, and for all $\epsilon > 0$ it indicates non-linearity of the "softening" type. For thin rings, (say $\frac{h}{R} < 100$), ϵ may be much less than unity, in which case (2.15) and (2.17) demonstrate only slight non-linearity.

Finally, note that (2.8) predicts the occurrence of a "contraction" at the zeros of $\cos \frac{ny}{R}$; if $A_n(t)$ vibrates with a frequency ω, the contraction will take place with frequency 2ω. A

slight non-linearity (of the softening type) and the double frequency contraction were readily detected experimentally.

For the ring that was tested, the assumption of inextensionality and the neglecting of tangential inertia appeared to be qualitatively correct. In order to determine when these approximations break down, however, both effects were investigated theoretically.

(b) The Extensional Ring

As before, w is assumed in the form

$$w(y,t) = A_n(t)\cos\frac{ny}{R} + A_o(t) \qquad (2.3)$$

Now $A_n(t)$ and $A_o(t)$ are separate, distinct variables, since in this case we cannot use the inextensionality condition to relate them. Thus, two coupled equations result, both involving $A_n(t)$ and $A_o(t)$. By fixing $A_o(t) = -\frac{n^2 A_n^2}{4R}$ in these equations, the results of the inextensional case can be regained.

From (2.6), one has

$$N_y = g(t) = Eh\left[\frac{\partial v}{\partial y} + \frac{w}{R} + \frac{1}{2}\left(\frac{\partial w}{\partial y}\right)^2\right] = Eh\,f(t)$$

With w(y,t) as given by (2.3),

$$\frac{\partial v}{\partial y} = f(t) - \frac{A_o}{R} - \frac{1}{2}\left(\frac{n^2 A_n^2}{2R^2}\right) \quad + \text{terms periodic in } y$$

Since $\frac{\partial v}{\partial y}$ can contain no terms that are functions solely of t, f(t) satisfies $f(t) - \frac{A_o}{R} - \frac{n^2 A_n^2}{4R^2} = 0$. Thus

$$N_y(t) = Eh\, f(t) = Eh\left[\frac{A_o}{R} + \frac{n^2 A_n^2}{4R^2}\right] \tag{2.18}$$

Rewriting equation (1.5b) gives

$$D\left(\frac{\partial^2}{\partial y^2} + \frac{1}{R^2}\right)\left(\frac{\partial^2 w}{\partial y^2} + \frac{w}{R^2}\right) - \frac{\partial}{\partial y}\left[N_y \frac{\partial w}{\partial y}\right] + \frac{N_y}{R} + \rho h \ddot{w} = q(y,t) \tag{2.19}$$

Substituting the expressions for w and N_y (and recalling that $\frac{\partial N_y}{\partial y}$ was taken to be zero) yields

$$\frac{Eh^3}{12(1-\nu^2)R^4}(n^2-1)^2 A_n \cos\frac{ny}{R} + \frac{Eh^3}{12(1-\nu^2)R^4} A_o + \frac{Eh}{R}\left[A_o + \frac{n^2 A_n^2}{4R}\right]\frac{n^2}{R^2} A_n \cos\frac{ny}{R} + \frac{Eh}{R^2}\left[A_o + \frac{n^2 A_n^2}{4R}\right] + \rho h \ddot{A}_n \cos\frac{ny}{R} + \rho h \ddot{A}_o = q(y,t) \tag{2.20}$$

In keeping with the assumption that the ring is thin, $\frac{h^2}{12R^2}$ is neglected in comparison to unity. That is

$$\frac{Eh A_o}{R^2}\left[1 + \frac{h^2}{12R^2}\right] \cong \frac{Eh}{R^2} A_o$$

Applying Galerkin's Method to (2.20), using first $\frac{\partial w}{\partial A_n}$ and then $\frac{\partial w}{\partial A_o}$ as weighting functions, one finds

$$\ddot{A}_n + \frac{E}{\rho R^2}\left[\frac{(n^2-1)^2 h^2}{12(1-\nu^2)R^2}\right] A_n$$

$$+ \frac{n^2 A_n}{R}\left(\frac{E}{\rho R^2}\right)\left[A_o + \frac{n^2 A_n^2}{4R}\right] = \frac{Q_n(t)}{\pi R \rho h} \qquad (2.21)$$

and

$$\ddot{A}_o + \frac{E}{\rho R^2}\left[A_o + \frac{n^2 A_n^2}{4R}\right] = \frac{Q_o(t)}{\pi R \rho h} \qquad (2.22)$$

with $Q_n(t) = \int_0^{2\pi R} q(y,t) \cos\frac{ny}{R}\, dy$, $Q_o(t) = \int_0^{2\pi R} q(y,t)\, dy$ as defined previously.

Let $\gamma = \frac{A_n}{h}$, $r_o = \frac{A_o}{h}$, $\eta = \frac{n^2 h}{R}$

Then (2.21) and (2.22) become

$$\ddot{\gamma} + \frac{E}{\rho R^2}\frac{\eta^2}{F}\gamma + \frac{E}{\rho R^2}\eta\gamma\left[r_o + \frac{\eta\gamma^2}{4}\right] = \frac{Q_n(t)}{\pi R \rho h^2} \qquad (2.23a)$$

and

$$\ddot{r}_o + \frac{E}{\rho R^2}\left[r_o + \frac{\eta\gamma^2}{4}\right] = \frac{Q_o(t)}{\pi R \rho h^2} \qquad (2.23b)$$

where $\frac{1}{F} = \frac{\left(1 - \frac{1}{n^2}\right)^2}{12(1-\nu^2)}$

The same equations resulted from application of the energy method. If (1.4b) is used instead of (1.5b), $\left(1 - \frac{1}{n^2}\right)^2$ is replaced by unity in $\frac{1}{F}$. Analogous results hold for $w(y,t) = B_n(t) \sin\frac{ny}{R} + A_o(t)$.

At first glance, (2.23) suggests defining $t' = \frac{1}{R}\sqrt{\frac{E}{\rho}}\,t$. However, a more convenient non-dimensional time is $\tau = \omega_M t$ where

$$\omega_M^2 = \frac{E}{\rho R^2}\left[\frac{(n^2-1)^2 h^2}{12(1-\nu^2)R^2}\right] = \frac{E}{\rho R^2}\frac{\eta^2}{F}$$

Simultaneously, let $r_o = \eta r$, and divide the first of (2.23) by η^2, the second by η. Then one has

$$\frac{1}{F}[\gamma_{\tau\tau} + \gamma] + \gamma\left[r + \frac{\gamma^2}{4}\right] = \frac{Q_n(\tau)}{\frac{E}{\rho R^2}(\pi R\rho h^2)\eta^2} \qquad (2.24a)$$

and

$$\frac{\eta^2}{F} r_{\tau\tau} + \left[r + \frac{\gamma^2}{4}\right] = \frac{Q_o(\tau)}{\frac{E}{\rho R^2}(2\pi R\rho h^2)\eta} \qquad (2.24b)$$

By manipulating these equations and then setting $A_o = \frac{-n^2 A_n^2}{4R}$ i.e., $r = -\frac{\gamma^2}{4}$, (2.24) can be combined to give

$$\gamma_{\tau\tau} + \gamma + \frac{\eta^2}{2}\gamma\left[\gamma\gamma_{\tau\tau} + \gamma_\tau^2\right] + \frac{\eta\gamma}{2}\frac{Q_o(\tau)}{\pi R\rho h^2} = \frac{Q_n(\tau)}{\pi R\rho h^2} \qquad (2.15)$$

which is the inextensional result.

It is not immediately apparent that (2.24) and (2.15) possess nearly identical solutions. Various approximate techniques can be used to demonstrate this similarity; however, it is convenient to postpone such a discussion until the effects of tangential inertia are also included.

2.2.2 Equations in which Tangential Inertia is Included

For reasons of simplicity, the effect of tangential inertia was assumed negligible in the previous calculations. In so doing, a linear term in the equations has been neglected; including the tangential inertia corrects this discrepany. More significant, however, are the conditions under which tangential inertia effects are small and their effect (if any) on the non-linear terms. Treating the more complete problem yields this information.

Thus, one is led to consider the first of (1.4) or (1.5):

$$Eh \frac{\partial}{\partial y}\left[\frac{\partial v}{\partial y} + \frac{w}{R} + \frac{1}{2}\left(\frac{\partial w}{\partial y}\right)^2\right] = \rho h \ddot{v}$$

One can rewrite this as

$$\frac{1}{c^2}\ddot{v} - \frac{\partial^2 v}{\partial y^2} = \frac{1}{R}\frac{\partial w}{\partial y} + \frac{\partial w}{\partial y}\frac{\partial^2 w}{\partial y^2} \qquad (2.25)$$

where $c^2 = \frac{E}{\rho}$.

Using $$w(y,t) = A_n(t)\cos\frac{ny}{R} + A_0(t) \qquad (2.3)$$

one has

$$\frac{1}{c^2}\ddot{v} - \frac{\partial^2 v}{\partial y^2} = -\frac{n A_n}{R^2}\sin\frac{ny}{R} + \frac{n^3 A_n^2}{2R^3}\sin\frac{2ny}{R} \qquad (2.26)$$

which has the solution*

---

* Only the particular solution is of interest here.

$$w(y,t) = C_n(t) \sin \frac{ny}{R} + D_n(t) \sin \frac{2ny}{R} \tag{2.27}$$

where $C_n(t)$ and $D_n(t)$ satisfy

$$\begin{aligned} \frac{\ddot{C}_n}{c^2} + \frac{n^2}{R^2} C_n &= -\frac{n A_n}{R^2} \\ \frac{\ddot{D}_n}{c^2} + \frac{(2n)^2}{R^2} D_n &= \frac{n^3 A_n^2}{2R^3} \end{aligned} \tag{2.28}$$

Until some additional information concerning $A_n(t)$ is given, one cannot proceed beyond (2.28). Accordingly, the second of equations (1.4) or (1.5) must be examined. Substituting (2.3) and (2.27) into (1.5b) yields

$$\begin{aligned} &\frac{E h^3 (n^2-1)^2}{12(1-\nu^2)R^4} A_n \cos \frac{ny}{R} + \frac{E h^3 A_0}{12(1-\nu^2)R^4} \\ &E h \left(\frac{n^2 A_n}{R^2}\right) \left\{ \left(\frac{n C_n}{R} + A_n\right) \frac{1}{2} \left(1 + \cos \frac{2ny}{R}\right) \right. \\ &+ \frac{1}{2} \left(\cos \frac{ny}{R} + \cos \frac{3ny}{R}\right) \left(\frac{2n D_n}{R} - \frac{n^2 A_n^2}{4R^2}\right) \\ &+ \left(\frac{A_0}{R} + \frac{n^2 A_n^2}{4R^2}\right) \cos \frac{ny}{R} - \frac{1}{2} \left(\frac{n C_n}{R} + A_n\right) \left(1 - \cos \frac{2ny}{R}\right) \\ &\left. - \left(\frac{2n D_n}{R} - \frac{n^2 A_n^2}{4R}\right) \left(\cos \frac{ny}{R} - \cos \frac{3ny}{R}\right) \right\} \\ &+ \frac{Eh}{R} \left[\left(\frac{n C_n}{R} + A_n\right) \cos \frac{ny}{R} + \left(\frac{A_0}{R} + \frac{n^2 A_n^2}{4R^2}\right) \right. \\ &\left. + \left(\frac{2n D_n}{R} - \frac{n^2 A_n^2}{4R}\right) \cos \frac{2ny}{R} + \rho h \left(\ddot{A}_n \cos \frac{ny}{R} \right.\right. \\ &\left.\left. + \ddot{A}_0\right) - q(y,t) = 0 \end{aligned} \tag{2.29}$$

Equation (2.29) will be satisfied approximately, by the application of Galerkin's Method. Using a weighting function $\frac{\partial w}{\partial A_n} = \cos \frac{ny}{R}$ and setting $\int_0^{2\pi R} (2.29) \frac{\partial w}{\partial A_m} dy = 0$ gives

$$\frac{Eh^3(n^2-1)^2}{12(1-\nu^2)R^4} A_n + \frac{Eh}{R^2}(n^2 A_n)\left\{\frac{A_0}{R} + \frac{n^2 A_n^2}{4R^2} + \frac{1}{2}\left(\frac{n^2 A_n^2}{4R^2} - \frac{2n D_n}{R}\right)\right\} + \frac{Eh}{R}\left[\frac{n C_n}{R} + A_n\right] + \rho h \ddot{A}_n = \frac{Q_n(t)}{\pi R} \tag{2.30}$$

Similarly, setting $\int_0^{2\pi R} (2.29) \frac{\partial w}{\partial A_0} dy = 0$ gives

$$\frac{Eh}{R} A_0 \left[1 + \frac{h^2}{12(1-\nu^2)R^2}\right] + \frac{Eh}{R}\frac{n^2 A_n^2}{4R^2} + \rho h \ddot{A}_0 = \frac{Q_0(t)}{2\pi R} \tag{2.31}$$

As before, let

$$\gamma = \frac{A_n}{h}, \quad \delta_0 = \frac{A_0}{h}, \quad \eta = \frac{n^2 h}{R} \tag{2.32}$$

Also, define $\gamma = \frac{n C_n}{h}$, $\delta_0 = \frac{n D_n}{h}$

Employing these dimensionless variables in (2.28), (2.30), and (2.31), one has

$$\ddot{\gamma} + \frac{E}{\rho R^2}(n^2)\gamma = -\frac{E}{\rho R^2}(n^2)\gamma$$

$$\ddot{\delta}_0 + \frac{E}{\rho R^2}(2n)^2 \delta_0 = \frac{E}{\rho R^2}(n^2)\frac{\eta\gamma^2}{2} \tag{2.33}$$

$$\ddot{\gamma} + \frac{E}{\rho R^2}\frac{(1-\frac{1}{m^2})^2}{12(1-\nu^2)}\eta^2\gamma + \frac{E}{\rho R^2}[\gamma+\gamma] + \frac{E}{\rho R^2}\eta\gamma\left[\left(\delta_0+\frac{3\gamma^2}{4}\right)-\left(\delta_0-\frac{3\gamma^2}{8}\right)\right] = \frac{Q_n(t)}{\pi R\rho h^2} \qquad (2.34)$$

$$\ddot{\delta}_0 + \frac{E}{\rho R^2}\left[\delta_0+\frac{3\gamma^2}{4}\right] = \frac{Q_0(t)}{2\pi R\rho h^2} \qquad (2.35)$$

where $\frac{h^2}{12R^2}$ is neglected in comparison to unity, in keeping with the assumption of a thin ring.

As in the previous cases, identical results are obtained with the energy method. By appropriate manipulations, (2.33 - 2.35) can be specialized to the extensional and inextensional equations. To estimate the effect of including the tangential inertia, suppose for the moment that γ was of the form $\gamma = A_o \cos\omega t$. Putting $\delta = \delta_o \cos\omega t$ into (2.33) gives

$$\left[-\omega^2 + \frac{E}{\rho R^2}(n^2)\right]\delta_0\cos\omega t = -\frac{E}{\rho R^2}A_0\cos\omega t \qquad (2.36)$$

Neglecting tangential inertia means to disregard $\ddot{\gamma}$ and $\ddot{\delta}_o$ in comparison with $\gamma\frac{E}{\rho R^2}(n^2)$ and $\frac{E\delta_o}{\rho R^2}(2n)^2$ in (2.33). From (2.36) it is evident that such an approximation appears valid when

$$\omega^2 << \frac{E}{\rho R^2}(n^2)$$

which was assumed in the previous cases.

Now that the ordinary differential equations corresponding to various "single bending mode" assumptions have been obtained, one is in a position to evaluate the usefulness of each. In the next section, a comparison of the approximate solutions shows that the inextensional case gives results that (for thin rings) agree favorably with the more refined analyses. Armed with this information, one feels that reasonably good results might be obtained by using inextensionality in the "multiple bending mode" cases.

2.3. Approximate Solutions to the Equations Resulting from the "Single Bending Mode" Approaches

The previous section indicated the manner in which the equations of motion are reduced from non-linear partial to ordinary differential equations. The present section deals with the approximate solutions of these equations.

Two approaches are used: the perturbation method, and the method of averaging. The discussion is centered on the forced vibration problem, with the forcing function taken to be harmonic in time. Solutions including the effect of damping are presented, as well as discussions of the stability of the vibrations.

The results of the three cases (inextensional, extensional, tangential inertia) are compared and found to be identical in form up to first order in the parameter η. This indicates that even for large amplitude flexural vibrations, (involving primarily a single bending mode) thin circular rings vibrate very nearly inextensionally.

The non-linearity exhibited by the solutions is of the "softening" type, with its degree dependent on $\eta = \frac{n^2 h}{R}$. One must bear in mind that these solutions all assume that the vibration involves primarily one bending mode. It can be shown that when the ring vibrates to sufficiently large amplitudes, more than one bending mode participates in the motion.

Thus, the results presented in this section are valid only when the amplitude of vibration is less than some "critical amplitude". A discussion of the vibrations with several modes participating and determination of the critical amplitude for the single mode solution are given in Sections 2.4 and 2.5.

In order to discuss forced vibrations, the applied loading must be specified. The loadings which will be considered herein are restricted to the form $q(y, t) = Y(y) \cos \omega t$. That is, the loading is fixed in space and harmonic in time. With this form of $q(y,t)$, (2.14) gives

$$Q_n(t) = \cos\omega t \int_0^{2\pi R} Y(y) \cos \frac{ny}{R} dy = F_n \cos \omega t \qquad (3.1)$$

and

$$Q_0(t) = \cos\omega t \int_0^{2\pi R} Y(y)\, dy = F_0 \cos\omega t \qquad (3.2)$$

where

$$F_n = \int_0^{2\pi R} Y(y) \cos \frac{ny}{R} dy, \quad F_0 = \int_0^{2\pi R} Y(y)\, dy$$

Finally, define*

$$\Omega = \frac{\omega}{\omega_M}, \quad G_n = \frac{F_n}{\pi R \rho h^2 \omega_M^2}, \quad G_o = \frac{F_o}{\pi R \rho h^2 \omega_M^2} \tag{3.3}$$

2.3.1 Perturbation Solutions

Perturbation methods provide a convenient technique for obtaining approximate solutions in two of the cases at hand. Both (2.15) and (2.24) contain the parameter $\eta = \frac{n^2 h}{R}$. For thin rings and for sufficiently small n values, η can be made much less than unity, and it becomes the logical candidate for the perturbation parameter.

When (3.1) - (3.3) are substituted in (2.15), the latter becomes

$$\gamma_{\tau\tau} + \frac{\eta^2 \gamma}{2}\left[\gamma\gamma_{\tau\tau} + \gamma_\tau^2\right] + \gamma + \frac{\eta\gamma}{2} G_o \cos\Omega\tau = G_n \cos\Omega\tau \tag{3.4}$$

for the inextensional ring. Similarly, multiplying (2.24) through by F, using (3.1) - (3.3), and recalling $\omega_M^2 = \frac{E}{\rho R^2}\frac{\eta^2}{F}$, one has

$$\gamma_{\tau\tau} + \gamma + F\gamma\left[\lambda + \frac{\gamma^2}{4}\right] = G_n \cos\Omega\tau \tag{3.5a}$$

$$\eta^2 \lambda_{\tau\tau} + F\left[\lambda + \frac{\gamma^2}{4}\right] = G_o \frac{\eta}{2} \cos\Omega\tau \tag{3.5b}$$

for the extensional case.

---

* If (1.4) is used, ω_M is replaced by ω_s in (3.3).

Notice that (3.4) and (3.5) can give rise to three types of non-linear vibrations:

(1) $G_o = 0,\ G_n \neq 0$ forced non-linear vibrations

(2) $G_o \neq 0,\ G_n = 0$ parametrically excited vibrations

(3) $G_o \neq 0,\ G_n \neq 0$ a combination of the above

A particular example of the first case is when $q(y, t)$ is such to excite a single mode in linear vibrations: $q(y,t) = q_o \cos \frac{ny}{R} \cos \omega t$. The second occurs when $q(y,t)$ is a uniform pressure, oscillating in time: $q(y,t) = q_o \cos \omega t$. This is the case of parametric excitation, and it will not be examined here. The third combination is the general case; a specific example will be used to illustrate it, namely $G_o = G_n$.

To obtain perturbation solutions to (3.4) or (3.5), define

$$\theta = \Omega \tau \tag{3.6}$$

and expand φ and r in powers of η:

$$\varphi = \varphi_0 + \eta \varphi_1 + \eta^2 \varphi_2 + \eta^3 \varphi_3 + \cdots \tag{3.7}$$

$$r = \rho_0 + \eta \rho_1 + \eta^2 \rho_2 + \eta^3 \rho_3 + \cdots \tag{3.8}$$

(a) Vibrations near Resonance

For perturbation solutions near $\Omega = 1$, the frequency is also expanded in terms of η:

$$\Omega = 1 + \eta \omega_1 + \eta^2 \omega_2 + \eta^3 \omega_3 + \cdots \tag{3.9}$$

Similarly, the forcing function must be redefined:

$$G_n = \eta^2 P_n \text{ WHEN } G_o = 0, \text{ OR}$$
$$G_n = \eta P_n \text{ WHEN } G_o = G_n \tag{3.10}$$

Finally, the solutions are required to satisfy

$$\begin{aligned} &\text{(a)} \quad \varphi(\vartheta+2\pi) = \varphi(\vartheta) \\ &\text{(b)} \quad \varphi(0) = A \\ &\text{(c)} \quad \varphi_\vartheta(0) = 0 \end{aligned} \tag{3.11}$$

since steady-state solutions are being sought. The first of these conditions is just a statement that φ be periodic, as required by (1.9). Conditions (b) and (c) fix the origin of the time scale; they are specified as above for convenience.

To proceed with the solution, one substitutes the expansions (3.7) - (3.9) into equations (3.4) or (3.5) together with the definitions (3.6) and (3.10). In keeping with the perturbation method, the resulting equation is then satisfied for terms having like powers of η. This results in a series of linear equations, which can be solved in succession. The integration constants which appear in these equations are determined by the subsidiary conditions (3.11), expanded in terms of η:

$$\begin{aligned} &\varphi_i(\vartheta+2\pi) = \varphi_i(\vartheta) \quad \text{FOR ALL } i \\ &\varphi_0(0) = A, \quad \frac{d\varphi_0}{d\vartheta}(0) = 0 \\ &\varphi_i(0) = 0, \quad \frac{d\varphi_i}{d\vartheta}(0) = 0 \quad \text{FOR } i > 0 \end{aligned} \tag{3.12}$$

The details of the calculations are presented in Appendix B; only the results will be given here.

Case I: $G_0 = 0$; put $\epsilon = \eta^2$

In this case,

$$y(\tau) = A\cos\Omega\tau + \frac{\epsilon A^3}{32}(\cos\Omega\tau - \cos 3\Omega\tau) + O(\epsilon^2) \tag{3.13}$$

and

$$h(\tau) = -\frac{A^2}{8}(1+\cos 2\Omega\tau) - \frac{\epsilon A^4}{64}(1-\cos 4\Omega\tau) - \underline{\frac{\epsilon A^2}{2F}\cos 2\Omega\tau} + O(\epsilon^2) \tag{3.14}$$

where the underlined term is contained in the solution to (3.5) but not (3.4). The remaining terms are common to both. Similarly, the frequency is given by

$$\Omega = 1 - \epsilon\left(\frac{P_m}{2A} + \frac{A^2}{8}\right) + \epsilon^2\omega_2 + O(\epsilon^3) \tag{3.15}$$

where

ω_2 satisfies $\left[\omega_1^2 + 2\omega_2\right]A + \frac{9}{16}\omega_1 A^3 + \underline{\frac{A^3}{F}} = 0$

and $\omega_1 = -\left(\frac{P_m}{2A} + \frac{A^2}{8}\right)$

Case II: $G_n = G_o$

The solutions are

$$\psi(\tau) = A\cos\Omega\tau + \eta^2\left[\frac{A^3}{32}(\cos\Omega\tau - \cos 3\Omega\tau)\right.$$
$$\left. + \frac{AP_m}{2}\left(\frac{\cos\Omega\tau}{3} + \frac{\cos 2\Omega\tau}{6} - \frac{1}{2}\right)\right]$$
$$+ \eta^3\left[\frac{P_m A^2}{256}(\cos\Omega\tau - \cos 3\Omega\tau) - \frac{P_m^2}{9}(\cos\Omega\tau\right. \qquad (3.16)$$
$$\left. - \cos 2\Omega\tau)\right] + O(\eta^4)$$

$$h(\tau) = -\frac{A^2}{8}(1+\cos 2\Omega\tau) - \eta^2\left\{\frac{A^2}{8}\left[\frac{A^2}{16} + \frac{P_m}{3}\right]\right.$$
$$- \frac{P_m}{2}\left[\frac{5A^2}{48} + \underline{\frac{1}{F}}\right]\cos\Omega\tau + \frac{A^2}{2}\left[\frac{P_m}{12} + \underline{\frac{1}{F}}\right]\cos 2\Omega\tau \qquad (3.17)$$
$$\left. + \frac{A^2 P_m \cos 3\Omega\tau}{48} - \frac{A^4}{128}\cos 4\Omega\tau\right\} + O(\eta^3)$$

and

$$\Omega = 1 - \frac{\eta P_m}{2A} - \eta^2\left[\frac{A^2}{8} + \frac{P_m^2}{4A^2}\right]$$
$$+ \eta^3\left[\frac{P_m^2}{12A} - \frac{5P_m A}{64} - \frac{P_m^3}{8A^3}\right] + O(\eta^4) \qquad (3.18)$$

Again, the underlined terms result from (3.5), and the other terms are common to both solutions.

For free vibrations, both Case I and Case II yield

$$\Omega = 1 - \frac{\epsilon A^2}{8} + \frac{7\epsilon^2 A^4}{256} + O(\epsilon^3) \qquad (3.19)$$

by putting $G_n = 0$. Equation (3.19) is the so-called "backbone curve" for the non-linear vibrations. It is plotted in Fig. 2 for various values of $\epsilon - \eta^2$.

(b) Vibrations away from Resonance

When the frequency of the forcing function is not in the vicinity of the resonant frequency of the system, a somewhat simpler perturbation analysis is used. The details of the calculations are outlines in Appendix B; the results are given here.

Case I: $G_o = 0$; put $\epsilon = \eta^2$

Both (3.4) and (3.5) give

$$y(\tau) = \frac{G_n \cos\Omega\tau}{1-\Omega^2} + \frac{\epsilon G_n^3 \Omega^2}{4(1-\Omega^2)^3}\left[\frac{\cos\Omega\tau}{1-\Omega^2} + \frac{\cos 3\Omega\tau}{1-9\Omega^2}\right] + O(\epsilon^2) \tag{3.20}$$

but differ in the expressions for $r(\tau)$:

$$r(\tau) = -\frac{G_n^2}{8(1-\Omega^2)^2}(1+\cos 2\Omega\tau) - \frac{\epsilon\Omega^2 G_n^4}{16(1-\Omega^2)^4}\left\{\frac{1}{1-\Omega^2} + \left[\frac{1}{1-\Omega^2} + \frac{1}{1-9\Omega^2}\right]\cos 2\Omega\tau + \frac{\cos 4\Omega\tau}{1-9\Omega^2}\right\} \tag{3.21}$$

$$\underline{- \frac{\epsilon G_n^2 \Omega^2 \cos 2\Omega\tau}{F}} + O(\epsilon^2)$$

where the underlined term results when (3.5) is used.

Case II: $G_o = G_n$

For $y(\tau)$, (3.4) and (3.5) both give

$$y(\tau) = \frac{G_n \cos\Omega\tau}{1-\Omega^2} - \frac{\eta G_n^2}{4(1-\Omega^2)}\left[1 + \frac{\cos 2\Omega\tau}{1-4\Omega^2}\right] + O(\eta^3) \tag{3.22}$$

but again differ in the expression for $r(\tau)$:

$$r(\tau) = -\frac{G_n^2}{8(1-\Omega^2)^2}[1+\cos 2\Omega\tau] + \eta\left\{\frac{G_n \cos\Omega\tau}{F}\right.$$

$$\left. + \frac{G_n^3}{8(1-\Omega^2)^2}\left[\cos\Omega\tau + \frac{(\cos\Omega\tau + \cos 3\Omega\tau)}{1-4\Omega^2}\right]\right\} \qquad (3.23)$$

$$+ O(\eta^2)$$

Since the above solutions were developed for Ω away from 1 it is not surprising that they break down at $\Omega = 1$. It will also be noted that they break down at other discrete values of Ω ($\Omega = \frac{1}{2}, \frac{1}{3}$) which is a familiar occurrence in non-linear vibrations. In order to obtain solutions that are valid in these regions, additional analyses are required. Such a solution (valid near $\Omega = \frac{1}{2}$) is presented in Section 2.3.5.

The results for vibrations both near and away from resonance clearly demonstrate the close agreement of the inextensional and extensional analyses. Non-linearity of the "softening" type is indicated, depending on η (or ϵ) as a parameter. The solutions converge most rapidly when $\frac{n^2 h}{R} << 1$; this confines the analysis to "thin" rings and/or low mode numbers. Ultraharmonic resonances are predicted near $\Omega = \frac{1}{2}, \frac{1}{3}$, etc., by both sets of equations. At worst, the solutions differ in the $0(\eta)$ term of the expression for r. Since the physical variable of interest is

$$r_o = \frac{A_o}{h} = \eta r = \eta(\rho_0 + \eta\rho_1 + \cdots)$$

one is not too concerned about variations in the ρ_1 term. Furthermore, it appears that the variations which do occur in ρ_1 are of little significance.

2.3.2 Solutions by the Method of Averaging

The equations which include tangential inertia effects (2.33) - (2.35) can also be solved by a perturbation scheme. In lieu of perturbing four equations simultaneously, however, it is much simpler to employ the method of averaging. This technique has been successfully applied to many non-linear problems since its introduction by Krylov and Bogoliubov in the 1930's. A detailed explanation of the method itself is given in several texts; see reference 23, for example.

When (2.33) - (2.35) are analyzed in this fashion, the results are found to agree in form with the perturbation solutions. This agreement is further demonstrated by a comparison of approximate solutions to (3.4), (3.5), and (3.25) - (3.27), all obtained by the method of averaging. The details of the calculations are outlined in Appendix B.

Vibration of the Ring with Tangential Inertia Included

The forcing function is taken to be the same as that used previously; (see (3.1) and (3.2)). To be consistent with the other analyses, define

$$\tau = \omega_M t, \quad \Omega = \frac{\omega}{\omega_M}, \quad t_0 = \eta t, \quad \delta_0 = \eta \delta$$

$$\omega_M^2 = \frac{E}{\rho R^2}\frac{\eta^2}{F} = \frac{E}{\rho R^2}\,\frac{(1-\frac{1}{n^2})^2}{12(1-\nu^2)}\,\eta^2 \qquad (3.24)$$

$$G_n = \frac{F_n}{\pi R \rho h^2 \omega_M^2} \qquad G_0 = \frac{F_0}{\pi R \rho h^2 \omega_M^2}$$

Then (2.33) - (2.35) become

$$\frac{\eta^2}{F}\gamma_{\tau\tau} + n^2\gamma = -n^2\varphi \tag{3.25a}$$

$$\frac{\eta^2}{F}\delta_{\tau\tau} + (2n)^2\delta = n^2\left(\frac{\varphi^2}{2}\right) \tag{3.25b}$$

$$\frac{\eta^2}{F}r_{\tau\tau} + \left[r + \frac{\varphi^2}{4}\right] = \frac{\eta G_0}{2}\cos 2\Omega\tau \tag{3.26}$$

$$\frac{\eta^2}{F}\left[\varphi_{\tau\tau} + \varphi\right] + (\gamma + \varphi) + \eta^2\varphi\left[r + \frac{\varphi^2}{4} - \left(\delta - \frac{\varphi^2}{8}\right)\right] = \frac{\eta^2}{F}G_m\cos\Omega\tau \tag{3.27}$$

To obtain an approximate solution to these equations by the method of averaging, let

$$\varphi(\tau) = A(\tau)\cos\Omega\tau \tag{3.28}$$

as a first approximation for φ. Equations (3.25) then suggest the form of γ and δ:

$$\begin{aligned}\gamma(\tau) &= c(\tau)\cos\Omega\tau \\ \delta(\tau) &= d_0(\tau) + d_2(\tau)\cos 2\Omega\tau\end{aligned} \tag{3.29}$$

The choice of the functional form of r is not as obvious. It is apparent that one should include $\rho_0(\tau)$ and $\rho_2(\tau)\cos 2\Omega\tau$, but the forcing function in (3.26) suggests including $\rho_1(\tau)\cos\Omega\tau$ as well. To a first approximation, however, it is sufficient to use

$$r(\tau) = \rho_0(\tau) + \rho_2(\tau)\cos 2\Omega\tau \tag{3.30}$$

which can be seen from the perturbation solutions.

Substituting for γ and φ in (3.25a), multiplying by $\cos\Omega\tau$, and averaging over one period gives

$$\bar{c} = -\frac{\bar{A}}{1-\frac{\eta^2\Omega^2}{n^2F}} \cong -\bar{A}\left[1+\frac{\eta^2\Omega^2}{n^2F}+\frac{\eta^4\Omega^4}{n^4F^2}+\cdots\right] \tag{3.31}$$

where $\bar{A}$ and $\bar{c}$ are average values of the functions $A(\tau)$ and $c(\tau)$. The product $\frac{\eta^2\Omega^2}{n^2F}$ is found to be

$$\frac{\eta^2\Omega^2}{n^2F} = \frac{\omega^2}{n^2\frac{E}{\rho R^2}} = \left(\frac{\omega}{\omega_{vn}}\right)^2$$

where $\omega_{vn} = \frac{n}{R}\sqrt{\frac{E}{\rho}}$, which is the natural frequency of the nth extensional mode of the ring. The theory again points out that the extensional modes respond essentially statically (i.e., $\bar{c} \cong -\bar{A}$) when $\omega^2 << \frac{n^2E}{\rho R^2}$.

Similarly, substituting for δ and φ in (3.25b) and averaging directly gives

$$\bar{d}_0 = \frac{\bar{A}^2}{16} \tag{3.32}$$

whereas averaging with $\cos 2\Omega\tau$ as a weighting function gives

$$\bar{d}_2 = \frac{\bar{A}^2}{16}\left[1-\frac{\eta^2\Omega^2}{n^2F}\right]^{-1} \cong \frac{\bar{A}^2}{16}\left[1+\frac{\eta^2\Omega^2}{n^2F}+\cdots\right] \tag{3.33}$$

When the approximations for r and γ are substituted into (3.26) and appropriate averages taken, one finds

$$\bar{\rho}_0 = -\frac{\bar{A}^2}{8} \tag{3.34}$$

and

$$\bar{\rho}_2 = -\frac{\bar{A}^2}{8}\left[1 - \frac{4\Omega^2\eta^2}{F}\right]^{-1}$$

$$\cong -\frac{\bar{A}^2}{8}\left[1 + \frac{4\Omega^2\eta^2}{F} + \cdots\right] \tag{3.35}$$

where $\dfrac{4\Omega^2\eta^2}{F} = \left(\dfrac{2\omega}{\omega_0}\right)^2 = \dfrac{\omega^2}{\frac{1}{4}\frac{E}{\rho R^2}}$

Thus, when $\omega \ll \frac{1}{2}\sqrt{\dfrac{E}{\rho R^2}}$, the bending vibrations are basically inextensional; i.e., $\bar{\rho}_2 = -\dfrac{\bar{A}^2}{8}$.

Finally, one must substitute the approximations for γ, r, δ, and γ' into (3.27) and average with $\cos\Omega\tau$. This leads to

$$\frac{\eta^2}{F}\left[1-\Omega^2\right]\bar{A} + (\bar{C} + \bar{A}) + \eta^2\bar{A}\left[\bar{\rho}_0 + \frac{\bar{A}^2}{8}\right.$$

$$\left. + \frac{1}{2}\left(\bar{\rho}_2 + \frac{\bar{A}^2}{8}\right) - \left(d_0 - \frac{\bar{A}^2}{16}\right)\right] = \frac{\eta^2}{F}G_n \tag{3.36}$$

The results (3.32) - (3.35) can now be used in (3.36); for purposes of the present analysis, it is sufficient to employ the expanded versions. Thus, (3.36) becomes

$$[1-\Omega^2]\bar{A} - \bar{A}\frac{\Omega^2}{n^2}\left[1+\frac{\eta^2\Omega^2}{n^2F}+\cdots\right] + \eta^2\bar{A}\left\{-\frac{\bar{A}^2}{4}\Omega^2\left[1 + \frac{4\eta^2\Omega^2}{F}+\cdots\right] - \frac{\bar{A}^2}{32}\frac{\Omega^2}{n^2}\left[1+\frac{\eta^2\Omega^2}{n^2F}+\cdots\right]\right\} = G_n$$

Using $\eta^2 = \epsilon$, this may be regrouped to give

$$\left[1-\Omega^2\left(1+\frac{1}{n^2}\right) - \frac{\epsilon\Omega^4}{Fn^4}+\cdots\right]\bar{A}$$

$$- \frac{\epsilon\Omega^2\bar{A}^3}{4}\left[1+\frac{1}{8n^2}+\cdots\right] + O(\epsilon^2) = G_n \qquad (3.37)$$

where only terms up to $0(\epsilon)$ have been retained.

By comparison, applying the averaging method to the inextensional (3.4) or extensional (3.5) equations gives

$$[1-\Omega^2]\bar{A} - \frac{\epsilon\Omega^2\bar{A}^3}{4} + O(\epsilon^2) = G_n \qquad (3.38)$$

where the latter two cases differ in the $0(\epsilon^2)$ terms. The coefficient of $\bar{A}$ vanishes at $\Omega = 1$, which corresponds to resonance for linear vibrations. However, (3.38) indicates a resonant frequency of

$$\omega = \omega_n = \left[\frac{E}{\rho R^2}\frac{(n^2-1)^2h^2}{12(1-\nu^2)R^2}\right]^{1/2}$$

which does not agree with the classical result:

$$\omega_L = \left[\frac{E}{\rho R^2} \frac{n^2 (n^2-1)^2 k^2}{(n^2+1)\, 12 (1-\nu^2) R^2} \right]^{\frac{1}{2}} \tag{3.39}$$

Thus, it is of interest to see under what conditions the coefficient of $\bar{A}$ in (3.37) vanishes. Setting it equal to zero, and neglecting $\frac{\epsilon \Omega^4}{Fn^4}$ as small, one has*

$$1 - \frac{\Omega^2 (n^2+1)}{n^2} = 0$$

whence

$$\omega^2 = \frac{n^2}{(n^2+1)} \omega_M^2 = \frac{E}{\rho R^2} \frac{n^2 (n^2-1)^2 k^2}{(n^2+1)\, 12 (1-\nu^2) R^2}$$

in agreement with (3.39). With this information, (3.37) may be re-written as

$$\left[1 - \left(\frac{\omega}{\omega_L} \right)^2 \right] \bar{A} - \frac{\epsilon_i \left(\frac{\omega}{\omega_L} \right)^2}{4} \bar{A}^3 + O(\epsilon^2) = G_n \tag{3.40}$$

---

* Identical results are obtained (within $0(\epsilon^2)$) by putting

$$1 - \frac{\Omega^2 (n^2+1)}{n^2} + \frac{\epsilon \Omega^4}{F n^4} = 0$$

where

$$\epsilon_i = \frac{n^2}{n^2+1}\left[1 + \frac{1}{\beta n^2}\right]\epsilon \tag{3.41}$$

and $\frac{\epsilon\Omega^4}{Fn^4} \sim \frac{\epsilon}{12n^4} \sim \frac{h^2}{12R^2}$ has been neglected as small.

Comparing (3.38) and (3.40), one sees that they are identical in form. That is, (3.40) can be obtained from (3.38) by replacing Ω by $\frac{\omega}{\omega_L}$ and ϵ by ϵ_i. Furthermore, as n becomes large, $\omega_n \to \omega_L$ and $\epsilon \to \epsilon_i$, causing (3.38) and (3.40) to become equal within $0(\epsilon^2)$.

For free vibrations, $G_n = 0$. In this case, (3.38) gives

$$\Omega = \frac{\omega}{\omega_n} = 1 - \frac{\epsilon \bar{A}^2}{8} + O(\epsilon^2) \tag{3.42}$$

and (3.40) yields

$$\frac{\omega}{\omega_L} = 1 - \frac{\epsilon_i \bar{A}^2}{8} + O(\epsilon^2) \tag{3.43}$$

Again the results are identical in form and approach each other for large n. The perturbation calculations agree with (3.42); see (3.19).

Concerning the expressions for y, r_0, γ, and δ_0, one has

$$\begin{aligned}
y(\tau) &= \bar{A}\cos\Omega\tau \\
r_0(\tau) &= \eta r(\tau) = -\frac{\eta\bar{A}^2}{8}\left[1 + \left(1 + \frac{4\omega^2}{E/\rho R^2} + \cdots\right)\right]\cos 2\Omega\tau \\
\gamma(\tau) &= -\bar{A}\left[1 + \frac{\omega^2}{\frac{En^2}{\rho R^2}} + \cdots\right]\cos\Omega\tau \\
\delta_0(\tau) &= \eta\delta(\tau) = \frac{\eta\bar{A}^2}{16}\left[1 + \left(\frac{\omega^2}{\frac{En^2}{\rho R^2}} + 1 + \cdots\right)\right]\cos 2\Omega\tau
\end{aligned} \tag{3.44}$$

up to $0(\epsilon)$. These results include the effect of tangential inertia; they can be specialized to the extensional case by deleting the $\frac{\omega^2}{\frac{Em^2}{\rho R^2}}$ terms. By also removing the $\frac{4\omega^2}{E/\rho R^2}$ term, the inextensional results can be obtained. Thus, it is evident that all three cases are in agreement up to $0(\eta)$ when analyzed by the method of averaging. It will be noted that equations (3.44) also agree with the perturbation results to first order in η.

The preceding calculations demonstrate the similarity of the "inextensional", "extensional", and "tangential inertia" approximations. The results for ψ, r_o, γ, and δ_o are identical to $0(\eta)$. The relations between amplitude, frequency, and the forcing function vary slightly, but they are identical in form. By replacing Ω with $\frac{\omega}{\omega_L}$ and ϵ with ϵ_L, the inextensional results can be modified to account for extension and tangential inertia effects.

Comparing the results for the three cases, one sees that the basic non-linear behavior of the ring can be obtained by making the "inextensional" approximation. Including the effects of mid-plane extension and tangential inertia increase the complexity of the analysis without significantly modifying the outcome. In keeping with this fact, the remainder of this study will be restricted to inextensional vibrations.

2.3.3 The Effect of Damping on the Vibrations

Up to this point, the discussion has been restricted to undamped vibrations. Yet, in any experimental attempt to confirm the calculations, one must contend with damping. Thus it becomes

appropriate to consider how damping will affect the solutions. For purposes of simplicity, only damping of the linear, viscous type will be analyzed.

With linear damping included, the inextensional ring equation (3.4) becomes

$$\eta_{\tau\tau} + 2\beta\eta_\tau + \eta + \frac{\eta^2}{2}\eta\left[\eta\eta_{\tau\tau} + \eta_\tau^2\right] + \frac{\eta\eta}{2}G_o\cos\Omega\tau = G_n\cos\Omega\tau \tag{3.45}$$

where β is the familiar "per cent critical damping".

A perturbation solution to (3.45) outlined in Appendix B; when $G_o = G_n$, the results are

$$\begin{aligned}\eta &= \eta_0 + \eta\eta_1 + \eta^2\eta_2 + \cdots \\ &= \frac{G_n\cos(\Omega\tau+\phi_1)}{|Z(\Omega)|} - \frac{\eta G_n^2}{4|Z(\Omega)|}\left[\cos\phi_1 + \frac{\cos(2\Omega\tau+\phi_1+\phi_2)}{|Z(2\Omega)|}\right] + O(\eta^2)\end{aligned} \tag{3.46}$$

and

$$\begin{aligned}r &= -\frac{\eta^2}{4} = \rho_0 + \eta\rho_1 + \eta^2\rho_2 + \cdots \\ &= -\frac{G_n^2}{8|Z(\Omega)|^2}\left[1+\cos 2(\Omega\tau+\phi_1)\right] + O(\eta)\end{aligned} \tag{3.47}$$

where $|Z(\Omega)| = \left[(1-\Omega^2)^2 + (2\beta\Omega)^2\right]^{1/2}$

AND $$\phi_i(\Omega) = TAN^{-1}\left[\frac{2\beta\Omega}{1-\Omega^2}\right]$$

One is now in a position to compare the phase changes predicted by this anlysis with those found experimentally. The γ_0 and ρ_0 results compare favorably with the tests, but it was impossible to detect γ_1 and ρ_1.

Although the above results are useful for comparison purposes, they do not indicate the effect which damping has on the non-linear response curves. The main effect is to "round off" the response peak, as one might suspect. This result is conveniently demonstrated by applying the method of averaging to (3.45).

To do this, let

$$y(\tau) = A(\tau)\cos[\Omega\tau + \phi(\tau)] \tag{3.48}$$

where $A(\tau)$ and $\phi(\tau)$ are taken to be slowly varying. When (3.48) is used in (3.45) and the appropriate averages are carried out, one finds*

$$[1-\Omega^2]\bar{A} - \frac{\eta^2\Omega^2\bar{A}^3}{4} = G_m\cos\bar{\phi} \tag{3.49a}$$

and

$$-2\beta\Omega\bar{A} = G_m\sin\bar{\phi} \tag{3.49b}$$

---

* See Appendix B.

for steady-state vibrations. Here $\bar{A}$ and $\bar{\phi}$ are average values (over one period) of $A(\tau)$ and $\phi(\tau)$. Squaring and adding, (3.49) gives

$$\left\{ [1-\Omega^2]\bar{A} - \frac{\eta^2\Omega^2\bar{A}^3}{4} \right\}^2 + 4\beta^2\Omega^2\bar{A}^2 = G_n^2 \qquad (3.50)$$

For given values of G_n, β and η, $\bar{A}$ can be computed from (3.50). Then $\bar{\delta}$ may be determined from (3.49), and the approximate solution for y becomes

$$y(\tau) = \bar{A}\cos[\Omega\tau + \bar{\phi}] \qquad (3.51)$$

A typical response curve is shown in Fig. 3. As mentioned previously, the effect of the damping is to "round off" the peak response.

2.3.4 Stability of the Inextensional Solution

To consider the stability of the approximate solution $y = \bar{A}\cos[\Omega\tau + \bar{\phi}]$, let

$$y(\tau) = \bar{A}\cos[\Omega\tau + \bar{\phi}] + \xi(\tau) \qquad (3.52)$$

where ξ is a small perturbation or disturbance. Substituting (3.52) into (3.45) and retaining only the first order terms in ξ gives

$$\xi_{\tau\tau}\left[1+\frac{\eta^2\bar{A}^2}{2}\cos^2(\Omega\tau+\bar{\phi})\right]$$
$$+\xi_{\tau}\left[2\beta-\frac{\eta^2\bar{A}^2\Omega}{2}\sin 2(\Omega\tau+\bar{\phi})\right]$$
$$+\xi\left[1+\frac{\eta G_o}{2}\cos\Omega\tau+\frac{\eta^2\Omega^2\bar{A}^2}{2}\{\sin^2(\Omega\tau+\bar{\phi})\right. \tag{3.53}$$
$$\left.-2\cos^2(\Omega\tau+\bar{\phi})\}\right]=0$$

where the fact that (3.51) is an approximate solution of (3.45) has been used.

For simplicity, consider the case where $\beta = 0$ and $G_o = 0$. Then define

$$\lambda=\frac{\eta^2\bar{A}^2}{2}=\frac{\epsilon\bar{A}^2}{2},\quad z=(\Omega\tau+\bar{\phi}),\quad \eta^2=\epsilon$$

and let $\xi(z)=u(z)\,e^{-\int_0^z\frac{\lambda\sin 2z\,dz}{2[1+\lambda\cos^2 z]}}$

With these new variables, (3.53) becomes

$$\frac{d^2u}{dz^2}+\left\{\frac{1}{\Omega^2}+\lambda(\sin^2 z-2\cos^2 z)\right.$$
$$\left.+\frac{\lambda\cos 2z}{(1+\lambda\cos^2 z)}\right\}\left[1+\lambda\cos^2 z\right]^{-1}u=0 \tag{3.54}$$

Expanding this in powers of λ and letting

$$a=\frac{1}{\Omega^2}-\frac{\lambda}{2}\left(\frac{\Omega^2+1}{\Omega^2}\right)$$
$$16q=-\frac{\lambda}{2}\left(\frac{\Omega^2+1}{\Omega^2}\right) \tag{3.55}$$

gives a Mathieu equation

$$\frac{d^2u}{dz^2} + (a + 16q\cos 2z)u = 0 \qquad (3.56)$$

where only terms of $0(\lambda)$ have been retained. The boundaries of the first unstable region of the Mathieu equation are well approximated by

$$a = 1 - 8q$$
$$\text{AND} \quad a = 1 + 8q$$

as long as $q < .15$. (see Ref. 23).

When $a < 1$, stability requres $a < 1 + 8q$ (since $q < 0$). In terms of $\bar{A}, \Omega$, and ϵ, this becomes

$$1 - \frac{\epsilon\bar{A}^2}{8} + \frac{\epsilon^2\bar{A}^4}{64} + \cdots < \Omega \qquad (3.57)$$

This is very nearly the expression obtained previously for the "backbone curve", namely

$$\Omega = 1 - \frac{\epsilon\bar{A}^2}{8} + \frac{7\epsilon^2\bar{A}^4}{256} + \cdots \qquad (3.19)$$

The differences between (3.57) and (3.19) occur because terms of $0(\lambda^2)$ were dropped in deriving (3.56).

Similarly, when $a > 1$, stability requires that $a > 1 + 8q$, which becomes

$$1 - \frac{3\epsilon\bar{A}^2}{8} + \frac{9\epsilon^2\bar{A}^4}{64} + \cdots > \Omega \qquad (3.58)$$

When (3. 57) and (3. 58) are superimposed upon the single mode response curve, they delineate a region in which the solution $y = \bar{A} \cos(\Omega\tau + \bar{\psi})$ is unstable (in the absence of damping). When damping is included in the stability analysis, the unstable region is modified as shown in Fig. 4.

The second, third, and higher unstable regions of (3. 56) can be analyzed in a similar manner. This indicates that the solution (3. 51) becomes unstable in narrow regions centered about the lines

$$\Omega = \frac{1}{2}\left(1 - \frac{3\epsilon\bar{A}^2}{32} + \cdots\right)$$

$$\Omega = \frac{1}{3}\left(1 - \frac{11\epsilon\bar{A}^2}{72} + \cdots\right)$$

$$\Omega = \frac{1}{4}\left[1 + O(\epsilon) + \cdots\right]$$

and so on. Note that these instabilities occur at the same values of Ω where the perturbation solutions (Section 2. 3. 1b) break down. This is not a coincidence; both analyses point out that in the vicinity of $\Omega = \frac{1}{2}, \frac{1}{3}$, etc. the higher harmonic terms are no longer small with respect to $\cos \Omega\tau$. To provide adequate solutions in these regions, additional studies are required; such a result is discussed under the title of "Ultraharmonic Response", Section 2. 3. 5.

As regards the area bounded by

$$1 - \frac{\epsilon\bar{A}^2}{8} + O(\epsilon^2) < \Omega < 1 - \frac{3\epsilon\bar{A}^2}{8} + O(\epsilon^2) \qquad (3.59)$$

it does represent a region in which the response is truly unstable. That is, if one were to try to experimentally determine a response curve of the type shown in Fig. 4, he would find it impossible to obtain steady-state vibrations within the shaded region. The

boundaries of the unstable region (3.59) can be shown to coincide with the locus of vertical tangents to the response curves, where the well-known "jump phenomena" of forced non-linear vibrations occurs. For a detailed discussion of results of this type, the reader is referred to Stoker (Ref. 22).

Finally, it will be noted that when $G_o \neq 0$, (3.53) yields an additional instability, centered at $\Omega = 2$, which indicates the presence of a subharmonic.

2.3.5 Ultraharmonic Response

As noted previously, the approximation

$$\varphi(\tau) = \bar{A} \cos [\Omega\tau + \bar{\phi}]$$

is inadequate in the vicinity of $\Omega = \frac{1}{2}, \frac{1}{3}, \frac{1}{4}$, etc. Near these discrete values of Ω, an improved approximation for $\varphi(\tau)$ must be made. For example, to apply the method of averaging, one might try

$$\varphi(\tau) = A_1(\tau)\cos\Omega\tau + A_2(\tau)\cos 2\Omega\tau \qquad (3.60)$$

as an approximate solution to

$$\varphi_{\tau\tau} + \frac{\eta^2}{2}\varphi[\varphi\varphi_{\tau\tau} + \varphi_\tau^2] + \varphi + \frac{\eta\varphi}{2} G_o \cos\Omega\tau = G_m \cos\Omega\tau \qquad (3.4)$$

near $\Omega = \frac{1}{2}$. For simplicity, consider the case when $G_o = 0$, and put $\eta^2 = \epsilon$. Then, substituting (3.60) into (3.4) and taking the appropriate averages gives

$$[1-\Omega^2]\bar{A}_1 - \frac{\epsilon\Omega^2\bar{A}_1}{4}[\bar{A}_1^2 + 5\bar{A}_2^2] = G_m \tag{3.61a}$$

and

$$[1-4\Omega^2]\bar{A}_2 - \frac{\epsilon\Omega^2\bar{A}_2}{4}[5\bar{A}_1^2 + 4\bar{A}_2^2] = 0 \tag{3.61b}$$

When $\bar{A}_2 \neq 0$, (3.61b) yields

$$\bar{A}_2^2 = \frac{[1-4\Omega^2]}{\epsilon\Omega^2} - \frac{5\bar{A}_1^2}{4} \tag{3.62}$$

For real, non-zero $\bar{A}_2$, (3.62) requires that Ω satisfy

$$\Omega < \frac{1}{2}\left[1 - \frac{5\epsilon\bar{A}_1^2}{32} + \cdots\right] \tag{3.63}$$

If the above inequality is satisfied, (3.62) can be used in (3.61a), which becomes

$$\left[4\Omega^2 - \frac{1}{4}\right]\bar{A}_1 + \frac{21\epsilon\Omega^2\bar{A}_1^3}{16} = G_m \tag{3.64}$$

Recall that for $y = A(\tau)\cos\Omega\tau$, the previous results gave

$$[1-\Omega^2]\bar{A} - \frac{\epsilon\Omega^2\bar{A}^3}{4} = G_m \tag{3.38}$$

For comparison purposes, suppose $\Omega = 0.45$, $G_n = 1$, $\epsilon = \frac{1}{100}$. Inserting these values in the above equations gives

$$\bar{A} = 1.25 \qquad \text{(from 3.38)}$$

and

$$\bar{A}_1 = 1.79$$

$$\bar{A}_2 = 9.54 \qquad \text{(from 3.62 and 3.64)}$$

Thus, $\frac{A_2}{A_1} = 5.3 \not< 1$, and the importance of the $\cos 2\Omega\tau$ term in the vicinity of $\Omega = \frac{1}{2}$ is evident.

Similar analyses can be done to obtain the response near $\Omega = \frac{1}{3}, \frac{1}{4}$ etc. The effect of damping is to round off the response peaks and in some cases to eliminate them althogether. Several ultra-harmonic responses were detected experimentally for the ring, as were some subharmonics.

2.4. Ordinary Differential Equations which Result from "Multiple Bending Mode" Assumptions (Inextensional Case)

The preceding section demonstrated that when the vibration involves primarily a single bending mode, the basic non-linear behavior can be obtained from an inextensional analysis, providing $\omega^2 << \frac{E}{\rho R^2}$. Accordingly, in treating flexural vibrations involving more than one bending mode, it will be assumed that the ring vibrates inextensionally. One suspects that such solutions will again exhibit the main non-linear features of the problem; this is apparently correct.

The simplest case to analyze is that of two coupled bending modes. Both the theory and experiments suggest a deflection of the form

$$w(y,t) = A_n(t)\cos\frac{ny}{R} + B_n(t)\sin\frac{ny}{R} + A_o(t) \qquad (4.1)$$

where $A_o(t)$ is related to A_n and B_n by the inextensionality condition.

In a similar fashion, the more general deflection

$$w(y,t) = \sum_{n=2}^{\infty}\left[A_n\cos\frac{ny}{R} + B_n\sin\frac{ny}{R}\right] + A_o \qquad (2.1)$$

can also be investigated. Equations for these two cases are presented in this section; some approximate solutions and a discussion of them are presented in Section 2.5.

2.4.1 The Case of "Self-Coupled" Bending Modes

In analyzing two coupled bending modes, one might try

$$w(y,t) = A_n(t)\cos\frac{ny}{R} + A_m(t)\cos\frac{my}{R} + A_o(t)$$

or

$$w(y,t) = A_m(t)\cos\frac{my}{R} + B_m(t)\sin\frac{my}{R} + A_o(t)$$

However, a more realistic case is that of "self-coupled" bending modes, where $\cos\frac{ny}{R}$ is coupled with its "companion mode", $\sin\frac{ny}{R}$. Thus, one is led to consider deflections of the form (4.1).

Restricting the discussion to inextensional vibrations requires that

$$\varepsilon_{yy}\Big|_{z=0} = \frac{\partial v}{\partial y} + \frac{w}{R} + \frac{1}{2}\left(\frac{\partial w}{\partial y}\right)^2 = 0 \tag{2.7}$$

Solving for $\frac{\partial v}{\partial y}$ and substituting (4.1) into (2.7), one finds $\frac{\partial v}{\partial y} = -\frac{A_o}{R} - \frac{n^2}{4R^2}(A_n^2 + B_n^2)$ + terms periodic in y. Since $\frac{\partial v}{\partial y}$ can contain no terms which are functions of time alone, $A_o(t)$ is required to satisfy

$$-\frac{A_o(t)}{R} - \frac{n^2}{4R^2}(A_n^2 + B_n^2) = 0 \tag{4.2}$$

whence (4.1) becomes

$$w(y,t) = A_n(t)\cos\frac{ny}{R} + B_n(t)\sin\frac{ny}{R} - \frac{n^2}{4R}(A_n^2 + B_n^2) \tag{4.3}$$

As in the previous inextensional analysis, tangential inertia is neglected. Thus, the displacement equations of motion (1.5) read

$$\frac{\partial N_y}{\partial y} = 0$$

and

$$D\left(\frac{\partial^2}{\partial y^2} + \frac{1}{R^2}\right)\left(\frac{\partial^2 w}{\partial y^2} + \frac{w}{R^2}\right) - \frac{\partial}{\partial y}\left[N_y \frac{\partial w}{\partial y}\right] + \frac{N_y}{R} + \rho h \ddot{w} = q(y,t) \tag{4.4}$$

where $N_y = Eh\left[\frac{\partial v}{\partial y} + \frac{w}{R} + \frac{1}{2}\left(\frac{\partial w}{\partial y}\right)^2\right]$ has been used. The first of

(4.4) gives $N_y = E\,h\,f(t) = Eh\left[\frac{\partial v}{\partial y} + \frac{w}{R} + \frac{1}{2}\left(\frac{\partial w}{\partial y}\right)^2\right]$, but since inextensional vibrations are being considered, (2.7) gives $Eh\,f(t) = 0 = N_y$. Substituting $N_y = 0$ and expression (4.3) into the second of equations (4.4) results in

$$\frac{Eh^3(n^2-1)^2}{12(1-\nu^2)R^4}\left[A_n \cos\frac{ny}{R} + B_n \sin\frac{ny}{R}\right] + \rho h\left[\ddot{A}_n \cos\frac{ny}{R} + \ddot{B}_n \sin\frac{ny}{R} - \frac{n^2}{2R}\left(A_n\ddot{A}_n + \dot{A}_n^2 + B_n\ddot{B}_n + \dot{B}_n^2\right)\right] = q(y,t) \tag{4.5}$$

Applying Galerkin's method to this equation, using successively $\frac{\partial w}{\partial A_n}$ and $\frac{\partial w}{\partial B_n}$ as weighting functions, one obtains

$$\frac{Eh^3(n^2-1)^2}{12(1-\nu^2)R^4}A_n + \rho h\left[\ddot{A}_n + \frac{n^4}{2R^2}A_n\left(A_n\ddot{A}_n + \dot{A}_n^2 + B_n\ddot{B}_n + \dot{B}_n^2\right)\right] = \frac{C_n(t)}{\pi R} - \frac{n^2 A_n}{2R}\frac{Q_0(t)}{\pi R} \tag{4.6}$$

and

$$\frac{Eh^3(n^2-1)^2}{12(1-\nu^2)R^4}B_n + \rho h\left[\ddot{B}_n + \frac{n^4}{2R^2}B_n\left(B_n\ddot{B}_n + \dot{B}_n^2 + A_n\ddot{A}_n + \dot{A}_n^2\right)\right] = \frac{S_n(t)}{\pi R} - \frac{n^2 B_n}{2R}\frac{Q_0(t)}{\pi R} \tag{4.7}$$

where

$$C_n(t) = \int_0^{2\pi R} q(y,t)\cos\frac{ny}{R}\,dy, \quad Q_0(t) = \int_0^{2\pi R} q(y,t)\,dy,$$
$$S_n(t) = \int_0^{2\pi R} q(y,t)\sin\frac{ny}{R}\,dy \tag{4.8}$$

Defining

$$\mathcal{G}_c = \frac{A_n}{h} \qquad \mathcal{G}_s = \frac{B_n}{h} \qquad \eta = \frac{n^2 h}{R}$$
$$\omega_n^2 = \frac{E}{\rho R^2}\frac{(n^2-1)^2 h^2}{12(1-\nu^2)R^2}$$

and letting $\tau = \omega_n t$, (4.6) and (4.7) become

$$(\mathcal{G}_c)_{\tau\tau} + \frac{\eta^2 \mathcal{G}_c}{2}\left[\mathcal{G}_c(\mathcal{G}_c)_{\tau\tau} + (\mathcal{G}_c)_\tau^2 + \mathcal{G}_s(\mathcal{G}_s)_{\tau\tau} + (\mathcal{G}_s)_\tau^2\right] + \mathcal{G}_c + \frac{\eta \mathcal{G}_c}{2}\frac{Q_0(\tau)}{\pi R\rho h^2 \omega_n^2} = \frac{C_n(\tau)}{\pi R\rho h^2 \omega_n^2} \tag{4.9}$$

and

$$(\mathcal{G}_s)_{\tau\tau} + \frac{\eta^2 \mathcal{G}_s}{2}\left[\mathcal{G}_s(\mathcal{G}_s)_{\tau\tau} + (\mathcal{G}_s)_\tau^2 + \mathcal{G}_c(\mathcal{G}_c)_{\tau\tau} + (\mathcal{G}_c)_\tau^2\right] + \mathcal{G}_s + \frac{\eta \mathcal{G}_s}{2}\frac{Q_0(\tau)}{\pi R\rho h^2 \omega_n^2} = \frac{S_n(\tau)}{\pi R\rho h^2 \omega_n^2} \tag{4.10}$$

These equations are symmetric in η_c and η_s, as they must be. As in the previous cases, application of the energy method yields identical results. Had (1.4) been used in lieu of (1.5), ω_M^2 would have been replaced by ω_s^2. Putting $\eta_s = 0$ reduces (4.9) to the single bending mode equation, (2.15).

Defining $\quad r_o = \frac{A_o}{h} = \eta r$

and using the above dimensionless variables in (4.2) gives

$$k = -\frac{1}{4}(\eta_c^2 + \eta_s^2) \tag{4.11}$$

Approximate solutions to (4.9) and (4.10) are presented in Section 2.5, for the case $S_n = 0$, $C_n \neq 0$, and $Q_o \neq 0$. A possible solution (for this set of forces) is

$$\eta_c = \bar{A}\cos[\Omega\tau + \bar{\phi}]$$

$$\eta_s = 0$$

i.e., just a single bending mode is excited. By doing a stability analysis on this solution, one can show it to be unstable for $\bar{A} > A_{CR}$. In other words, the vibration will involve primarily a single bending mode as long as its amplitude is less than A_{CR}; above A_{CR}, two bending modes participate in the motion. Experimentally, this is found to be the case.

Before discussing the solutions, however, it is of interest to consider the "general" inextensional case".

2.4.2 The General Inextensional Case

In this case, the deflection is taken in the form

$$w(y,t) = \sum_{n=2}^{\infty} \left[A_n \cos \frac{ny}{R} + B_n \sin \frac{ny}{R} \right] + A_o \qquad (2.1)$$

For inextensional vibrations,

$$\epsilon_{yy}\Big|_{z=0} = \frac{\partial v}{\partial y} + \frac{w}{R} + \frac{1}{2}\left(\frac{\partial w}{\partial y}\right)^2 = 0 \qquad (2.7)$$

Substituting (2.1) into (2.7) and solving for $\frac{\partial v}{\partial y}$ gives

$$\frac{\partial v}{\partial y} = -\frac{A_o}{R} - \frac{1}{4R^2} \sum_{n=2}^{\infty}{}' n^2 \left[A_n^2 + B_n^2 \right] + \text{terms periodic in y,}$$

whence $A_o(t)$ is determined:

$$A_o(t) = -\frac{1}{4R} \sum_{n=2}^{\infty}{}' n^2 \left[A_n^2 + B_n^2 \right] \qquad (4.12)$$

In this case, (2.1) then becomes

$$w(y,t) = \sum_{n=2}^{\infty}{}' \left[A_n \cos \frac{ny}{R} + B_n \sin \frac{ny}{R} - n^2 \frac{(A_n^2 + B_n^2)}{4R} \right] \qquad (4.13)$$

Substituting (4.13) into the second of equations (4.4) and recalling that $N_y = 0$ for inextensional vibrations, one obtains

$$\sum_{m=2}^{\infty} \left\{ \frac{E h^3 (m^2-1)^2}{12(1-\nu^2) R^4} \left(A_m \cos\frac{my}{R} + B_m \sin\frac{my}{R}\right) + \rho h \left[\ddot{A}_m \cos\frac{my}{R} + \ddot{B}_m \sin\frac{my}{R} - \frac{m^2}{2R}\left(A_m \ddot{A}_m + \dot{A}_m^2 + B_m \ddot{B}_m + \dot{B}_m^2\right)\right]\right\} = q(y,t) \tag{4.14}$$

(The summation index has been changed, for convenience.)

Galerkin's method will be applied to (4.14), with

$$\frac{\partial w}{\partial A_n} = \cos\frac{ny}{R} - \frac{n^2 A_n}{2R} \tag{4.15}$$

and

$$\frac{\partial w}{\partial B_n} = \sin\frac{ny}{R} - \frac{n^2 B_n}{2R} \tag{4.16}$$

as weighting functions. Multiplying (4.14) by (4.15) and integrating from 0 to $2\pi R$ on y gives

$$\frac{E h^3 (n^2-1)^2}{12(1-\nu^2) R^4} A_n + \rho h \ddot{A}_n + \rho h \frac{n^2 A_n}{2R^2} \sum_{m=2}^{\infty} m^2 \left[A_m \ddot{A}_m + \dot{A}_m^2 + B_m \ddot{B}_m + \dot{B}_m^2\right] = \frac{C_n(t)}{\pi R} - \frac{n^2 A_n}{2R} \frac{Q_o(t)}{\pi R} \tag{4.17}$$

$$n = 2, 3, 4, \ldots$$

where $C_n(t) = \int_0^{2\pi R} q(y,t) \cos \frac{ny}{R}\, dy$, etc. as defined in (4.8), and the orthogonality of the trigonometric functions has been employed.

In a similar manner, taking (4.16) through (4.14) gives

$$\frac{E h^3 (n^2-1)^2}{12(1-\nu^2) R^4} B_n + \rho h \ddot{B}_n + \rho h \frac{n^2 B_n^2}{2R^2} \sum_{m=2}^{\infty} m^2 \left[A_m \ddot{A}_m + \dot{A}_m^2 + B_m \ddot{B}_m + \dot{B}_m^2 \right] = \frac{S_n(t)}{\pi R} - \frac{n^2 B_n}{2R} \frac{Q_0(t)}{\pi R} \qquad (4.18)$$

$$n = 2, 3, 4, \cdots$$

where $S_n(t) = \int_0^{2\pi R} q(y,t) \sin \frac{ny}{R}\, dy$, AND

$$Q_0(t) = \int_0^{2\pi R} q(y,t)\, dy$$

Define

$$\mathcal{J}_{cn} = \frac{A_n}{h} \qquad \mathcal{J}_{sn} = \frac{B_n}{h} \qquad \eta_n = \frac{n^2 h}{R}$$

$$\omega_{Mn}^2 = \frac{E}{\rho R^2} \frac{(n^2-1)^2 h^2}{12(1-\nu^2) R^2}$$

Then (4.17) and (4.18) can be re-written as

$$\ddot{\mathcal{J}}_{cn} + \omega_{Mn}^2 \mathcal{J}_{cn} + \frac{\eta_n}{2} \mathcal{J}_{cn} \sum_{k=2}^{\infty} \eta_k \left[\mathcal{J}_{ck} \ddot{\mathcal{J}}_{ck} + \dot{\mathcal{J}}_{ck}^2 + \mathcal{J}_{sk} \ddot{\mathcal{J}}_{sk} + \dot{\mathcal{J}}_{sk}^2 \right] + \frac{\eta_n \mathcal{J}_{cn}}{2} \frac{Q_0(t)}{\pi R \rho h^2} = \frac{C_n(t)}{\pi R \rho h^2} \qquad (4.19)$$

$$\ddot{\mathcal{J}}_{sn} + \omega_{nn}^2 \mathcal{J}_{sn} + \frac{\eta_n \mathcal{J}_{sn}}{2} \sum_{k=2}^{\infty} \eta_k \left[\mathcal{J}_{ck} \ddot{\mathcal{J}}_{ck} + \dot{\mathcal{J}}_{ck}^2 + \mathcal{J}_{sk} \ddot{\mathcal{J}}_{sk} + \dot{\mathcal{J}}_{sk}^2 \right] + \frac{\mathcal{J}_{sn} \eta_n}{2} \frac{Q_o(t)}{\pi R \rho h^2} = \frac{S_n(t)}{\pi R \rho h^2} \qquad (4.20)$$

where n = 2, 3, 4, ...

In the same notation, the expression for $r_o(t)$ becomes

$$\eta_o(t) = \frac{A_o}{h} = -\frac{1}{4} \sum_{k=2}^{\infty} \eta_k \left[A_k^2 + B_k^2 \right] \qquad (4.21)$$

Equations (4.19) and (4.20) could also have been derived directly by energy methods. They form a doubly infinite set of non-linear differential equations; the general solution is not presented in Appendix B! It is possible to obtain solutions to (4.19) and (4.20) for particular forcing functions; a discussion of the equations and their solutions for two special cases is presented in the next section.

2.5. Discussion and Approximate Solutions of the "Multiple Bending Mode" Approaches

Having found the differential equations which govern the (inextensional) vibrations of more than one bending mode, one is now in a position to answer several interesting questions.

For example, when does the "single bending mode" assumption cease to be valid? An answer to this question for some important

forcing functions is given in this section. When $C_n(t) = F_n \cos\omega t$ and $S_n(t) = 0$, it is shown that for

$$|y_c|_{MAX} < A_{CRITICAL}$$

the "self-coupled" bending mode problem reduces to the single mode case discussed previously. Conversely, when $|y_c|_{MAX} > A_{CR}$ the "companion mode" becomes unstable and the vibration thereafter involves two bending modes. Approximate solutions for the case of "self-coupled" bending modes are given in this section, and the stability of the solutions is discussed.

The "general inextensional case" is considered for two important sets of forces. One is

$$S_m(t) = 0 \quad \text{FOR ALL } m, \; m = 2, 3, 4, \cdots$$

$$C_m(t) = \begin{cases} F_m \cos\omega t & \text{FOR ONE } m \text{ VALUE} \\ 0 & \text{FOR ALL OTHER VALUES} \end{cases}$$

$$Q_0(t) = 0$$

which corresponds to the forcing function $q(y,t) = \pi R F_n \cos\omega t \cos \frac{ny}{R}$. The other is

$$S_m(t) = 0 \quad \text{FOR ALL } m$$

$$C_m(t) = F\cos\omega t \quad \text{FOR ALL } m$$

$$Q_0(t) = F\cos\omega t$$

corresponding to $q(y,t) = \delta(y) F \cos\omega t$.

In both cases, it can be shown that under relatively minor restrictions the solutions to the general case reduce very nearly to

those for the self-coupled bending modes. By examining the stability of these solutions, one can show that normally $\cos \frac{ny}{R}$ will couple with $\sin \frac{ny}{R}$ before it couples with any other mode ($\cos \frac{my}{R}$, $\sin \frac{my}{R}$, $m \neq n$). As a further consequence of the stability analyses, it appears that (for most cases) modes other than $\cos \frac{ny}{R}$ and $\sin \frac{ny}{R}$ will remain virtually quiescent until the vibration amplitudes become very large.

2.5.1 Self-Coupled Bending Modes: Approximate Solutions and their Stability

As in the one mode analyses, the discussion will be restricted to loadings of the form $q(y,t) = Y(y) \cos \omega t$. Thus, the forcing functions become (see 4.8)

$$C_n(t) = \cos \omega t \int_0^{2\pi R} Y(y) \cos \frac{ny}{R} dy = F_n \cos \omega t$$

$$Q_0(t) = \cos \omega t \int_0^{2\pi R} Y(y) dy = F_0 \cos \omega t \qquad (5.1)$$

$$S_n(t) = \cos \omega t \int_0^{2\pi R} Y(y) \sin \frac{ny}{R} dy = E_n \cos \omega t$$

where $F_n = \int_0^{2\pi R} Y(y) \cos \frac{ny}{R} dy$, ETC.

As a further restriction, only symmetric loadings will be considered; that is, loadings for which $E_n = \int_0^{2\pi R} Y(y) \sin \frac{ny}{R} dy = 0$. Then, let $\Omega = \frac{\omega}{\omega_n}$ and define

$$G_n = \frac{F_n}{\pi R \rho h^2 \omega_n^2}, \qquad G_o = \frac{F_o}{\pi R \rho h^2 \omega_n^2} \tag{5.2}$$

as in (3.3).

Then, with the addition of damping, (4.9) and (4.10) give

$$(\mathcal{Y}_c)_{\tau\tau} + 2\beta_c (\mathcal{Y}_c)_\tau + \mathcal{Y}_c + \frac{\eta^2}{2} \mathcal{Y}_c \left[\mathcal{Y}_c (\mathcal{Y}_c)_{\tau\tau} (\mathcal{Y}_c)_\tau^2 + \mathcal{Y}_s (\mathcal{Y}_s)_{\tau\tau} + (\mathcal{Y}_s)_\tau^2 \right] + \frac{\eta}{2} \mathcal{Y}_c G_o \cos \Omega\tau = G_n \cos \Omega\tau \tag{5.3a}$$

and

$$(\mathcal{Y}_s)_{\tau\tau} + 2\beta_s (\mathcal{Y}_s)_\tau + \mathcal{Y}_s + \frac{\eta^2}{2} \mathcal{Y}_s \left[\mathcal{Y}_c (\mathcal{Y}_c)_{\tau\tau} + (\mathcal{Y}_c)_\tau^2 + \mathcal{Y}_s (\mathcal{Y}_s)_{\tau\tau} + (\mathcal{Y}_s)_\tau^2 \right] + \frac{\eta}{2} \mathcal{Y}_s G_o \cos \Omega\tau = 0 \tag{5.3b}$$

where β_c and β_s are the "per cent critical damping" in the $\cos \frac{ny}{R}$ and $\sin \frac{ny}{R}$ modes, respectively.

(a) Stability of the Solution where only One Mode is Excited

A possible solution to (5.3) is $\mathcal{Y}_s = 0$, and $\mathcal{Y}_c$ satisfying

$$(\mathcal{Y}_c)_{\tau\tau} + 2\beta_c (\mathcal{Y}_c)_\tau + \mathcal{Y}_c + \frac{\eta^2}{2} \mathcal{Y}_c \left[\mathcal{Y}_c (\mathcal{Y}_c)_{\tau\tau} + (\mathcal{Y}_c)_\tau^2 \right] + \frac{\eta}{2} \mathcal{Y}_c G_o \cos \Omega\tau = G_n \cos \Omega\tau \tag{3.45}$$

i. e., only one bending mode ($\cos \frac{ny}{R}$) is excited. Recall that an approximate solution to (3.45) was given previously; it is (see Section 2.3.3)

$$\mathcal{Y}_c(\tau) = \bar{A} \cos [\Omega \tau + \bar{\phi}] \tag{3.51}$$

To analyze the stability of the solution

$$\begin{aligned} \mathcal{Y}_c(\tau) &= \bar{A} \cos [\Omega \tau + \bar{\phi}] \\ \mathcal{Y}_s(\tau) &= 0 \end{aligned} \tag{5.4}$$

both $\mathcal{Y}_c$ and $\mathcal{Y}_s$ are perturbed:

$$\begin{aligned} \mathcal{Y}_c(\tau) &= \bar{A} \cos [\Omega \tau + \bar{\phi}] + \xi(\tau) \\ \mathcal{Y}_s(\tau) &= 0 + x(\tau) \end{aligned} \tag{5.5}$$

Substituting (5.5) into (5.3) and retaining only first order terms in the perturbations gives

$$\begin{aligned} &\xi_{\tau\tau} \left[1 + \frac{\eta^2 \bar{A}^2}{2} \cos^2(\Omega \tau + \bar{\phi})\right] + \xi_\tau \left[2\beta_c \right. \\ &\left. - \frac{\eta^2 \bar{A}^2 \Omega}{2} \sin 2(\Omega \tau + \bar{\phi})\right] + \xi \left[1 + \frac{\eta G_0}{2} \cos \Omega \tau \right. \\ &\left. + \frac{\eta^2 \bar{A}^2 \Omega^2}{2} \{\sin^2(\Omega \tau + \bar{\phi}) - 2\cos^2(\Omega \tau + \bar{\phi})\}\right] = 0 \end{aligned} \tag{5.6a}$$

and

$$\begin{aligned} &x_{\tau\tau} + 2\beta_s x_\tau + x + \frac{\eta^2 x}{2} \left[-\Omega^2 \bar{A}^2 \cos 2(\Omega \tau + \bar{\phi})\right] \\ &+ \frac{\eta x}{2} G_0 \cos \Omega \tau = 0 \end{aligned} \tag{5.6b}$$

Equation (5. 6a) is identical with (3. 53), which was discussed previously (Section 3. 4) in connection with the stability of the single mode solution. In studying (5. 6b), first consider the case in which $G_o = 0$ and $\beta_s = 0$. Then (5. 6b) may be transformed to the familiar Mathieu equation

$$\frac{d^2x}{dz^2} + (a + 16q\cos 2z)x = 0 \qquad (5.7)$$

where $z = (\Omega\tau + \bar{\phi})$ $\quad a = \frac{1}{\Omega^2}$ $\quad \eta^2 = \epsilon$

and $16q = -\frac{\epsilon\bar{A}^2}{2}$

Near the first unstable region of (5. 7), when $a \leq 1$ (i. e., $\Omega \geq 1$) stability requires

$$a < 1 + 8q$$

which means that $\bar{A}$ must be such that

$$\bar{A}^2 < \frac{4(\Omega^2 - 1)}{\epsilon\Omega^2} \qquad (5.8b)$$

Similar analyses can be done for the other unstable regions as well; it is of interest to note that these instabilities are located at

$$\Omega = \frac{1}{2}, \frac{1}{3}, \frac{1}{4}, \ldots\ldots$$

which are the very areas that (3. 53 and 5. 6a) exhibit instabilities.

When G_o and β_s are non-zero, let

$$x(\tau) = u(\tau)\, e^{-\beta_s \tau}, \qquad \tau = \frac{2z}{\Omega}$$

$$\theta_0 = \frac{4}{\Omega^2}(1-\beta_s^2)$$

$$2\theta_1 = \frac{2}{\Omega^2}\eta G_0 \qquad \epsilon_1 = 0 \tag{5.9}$$

$$2\theta_2 = -2\eta^2\bar{A}^2 \qquad \epsilon_2 = \bar{\phi}$$

Then (5.6b) reduces to the standard form of Hill's equation:

$$\frac{d^2u}{dz^2} + \left[\theta_0 + 2\sum_{n=1}^{2}\theta_n \cos(2nz+\epsilon_n)\right]u = 0 \tag{5.10}$$

The stability boundaries of (5.10) may be approximated by employing Whittaker's method. When this is done, one obtains

$$4n^2\theta_0 + \theta_n^2 < \left[(\theta_0+n^2) + \frac{4\beta_s^2}{\Omega^2}\right]^2 \tag{5.11}$$

as the condition for stability near the nth unstable region*. Substituting from (5.9), stability near the first unstable region requires

$$\eta^2 G_0^2 < \left[4-\Omega^2\right]^2 + 16\Omega^2\beta_s^2 \tag{5.12}$$

which reduces to $\eta G_0 < 8\beta_s$ at $\Omega = 2$.

Similarly, near the second unstable region, (5.11) yields

$$\frac{\eta^4\Omega^4\bar{A}^4}{16} < 4\beta_s^2\Omega^2 + \left[\Omega^2-1\right]^2 \tag{5.13}$$

---

* See Appendix C.

For $\beta_s = 0$, (5.13) yields (5.8), in agreement with the preceding Mathieu analysis. At $\Omega = 1$, (5.13) gives

$$\bar{A} < \frac{\sqrt{8\beta_s}}{\eta}$$

as the requirement for stability.

The higher unstable regions are located at $\Omega = \frac{2}{3}, \frac{1}{2}, \frac{2}{5}, \ldots \frac{2}{n}$ but for $\beta_s > 0$, (5.11) is always satisfied in these cases.

For $\beta_s > 0$, then, the solution

$$\eta_c = \bar{A}\cos[\Omega\tau + \bar{\phi}]$$

$$\eta_s = 0 \qquad (5.4)$$

is stable with respect to perturbations of η_s as long as the inequalities (5.12) and (5.13) are satisfied. Similarly, from the results of Section 2.3.4, one knows that (5.4) is stable with respect to perturbations of η_c as long as the inequality

$$1 - \frac{\epsilon\bar{A}^2}{8} + O(\epsilon^2) < \Omega < 1 - \frac{3\epsilon\bar{A}^2}{8} + O(\epsilon^2) \qquad (3.59)$$

is satisfied and Ω is not in the vicinity of $\frac{1}{2}, \frac{1}{3}, \ldots$ etc.

When (5.12) is not satisfied, a subharmonic response is indicated. However, (5.6a) itself indicates an instability in the same area, which makes the solution $\eta_c = A\cos[\Omega\tau + \bar{\phi}]$ questionable there.

A more interesting result occurs when the inequality (5.13) is not met. In that case, η_s goes unstable as $e^{\mu\tau}\sin(\Omega\tau - \sigma)$

and one must consider vibrations in which both η_s and η_c are non-zero; this led directly to the topic of the next section.

(b) Steady State Vibration with Both "Self-Coupled" Bending Modes Excited

The method of averaging will be used to obtain approximate solutions to (5.3) as follows. Let*

$$\eta_c(\tau) = A(\tau)\cos[\Omega\tau + \phi(\tau)] = A(\tau)\cos\chi_1$$
$$\eta_s(\tau) = B(\tau)\sin[\Omega\tau + \psi(\tau)] = B(\tau)\sin\chi_2 \qquad (5.14)$$

where $\chi_1 = [\Omega\tau + \phi]$ etc., and A, B, ϕ, and ψ are slowly varying. Using (5.14) in (5.3) and averaging over one period, one obtains

$$[1-\Omega^2]\bar{A} - 2\Omega\bar{A}\bar{\phi}_\tau - \frac{\gamma^2\bar{A}}{4}\left[\Omega^2\bar{A}^2 + \frac{3\Omega\bar{A}^2\bar{\phi}_\tau}{2} - \Omega^2\bar{B}^2\cos 2\bar{\Delta} - \frac{1}{2}\Omega\bar{B}_\tau\bar{B}\sin 2\bar{\Delta} + \Omega\bar{B}^2\bar{\psi}_\tau\left(1 - \frac{\cos 2\bar{\Delta}}{2}\right)\right] = G_n\cos\bar{\phi} \qquad (5.15a)$$

$$-2\Omega\bar{A}_\tau - 2\Omega\beta_c\bar{A}_\tau - \frac{\gamma^2\bar{A}}{4}\left[\frac{\Omega\bar{A}_\tau\bar{A}}{2} + \Omega^2\bar{B}^2\sin 2\bar{\Delta} - \frac{\Omega\bar{B}_\tau\bar{B}}{2}\cos 2\bar{\Delta} + \frac{\Omega\bar{B}^2\bar{\psi}_\tau}{2}\sin 2\bar{\Delta}\right] = G_n\sin\bar{\phi} \qquad (5.15b)$$

---

* The choice of $\eta_c = A\cos(\Omega\tau+\phi_1)$, $\eta_s = B\cos(\Omega\tau+\phi_2)$ gives similar results; however, for the undamped case the "in-phase" solution $\eta_c \sim \cos\Omega\tau$, $\eta_s \sim \cos\Omega\tau$ will not satisfy (5.3) whereas $\eta_c \sim \cos\Omega\tau$, $\eta_s \sim \sin\Omega\tau$ will; hence the choice (5.14) above.

$$[1-\Omega^2]\bar{B} - 2\Omega\bar{B}\bar{\psi}_\tau - \frac{\eta^2\bar{B}}{4}\left[-\Omega^2\bar{A}^2\cos 2\bar{\Delta} + \Omega\bar{A}^2\bar{\phi}_\tau\left(1-\frac{\cos 2\bar{\Delta}}{2}\right) + \frac{\Omega\bar{A}_\tau\bar{A}}{2}\sin 2\bar{\Delta} + \Omega^2\bar{B}^2 + \frac{3\Omega\bar{B}^2\bar{\psi}_\tau}{2}\right] = 0 \tag{5.15c}$$

$$2\Omega\bar{B}_\tau + 2\beta_s\Omega\bar{B} - \frac{\eta^2\bar{B}}{4}\left[\Omega^2\bar{A}^2\sin 2\bar{\Delta} + \frac{\Omega\bar{A}_\tau\bar{A}}{2}\cos 2\bar{\Delta} + \frac{\Omega\bar{A}^2\bar{\phi}_\tau}{2}\sin 2\bar{\Delta} - \frac{\Omega\bar{B}\bar{B}_\tau}{2}\right] = 0 \tag{5.15d}$$

where $A(\tau)$, etc. has been replaced by its average value over one cycle, denoted by $\bar{A}$, etc. The symbol $\bar{\Delta}$ is an average phase difference

$$\bar{\Delta} = \bar{\psi} - \bar{\phi} \tag{5.16}$$

For steady-state vibrations, $\bar{A}_\tau$, $\bar{B}_\tau$, $\bar{\phi}_\tau$, and $\bar{\psi}_\tau$ are all zero. In this case, (5.15) reduces to

$$[1-\Omega^2]\bar{A} - \frac{\epsilon\Omega^2\bar{A}}{4}\left[\bar{A}^2 - \bar{B}^2\cos 2\bar{\Delta}\right] = G_m\cos\bar{\phi} \tag{5.17a}$$

$$-2\beta_c\Omega\bar{A} - \frac{\epsilon\Omega^2\bar{A}}{4}\bar{B}^2\sin 2\bar{\Delta} = G_m\sin\bar{\phi} \tag{5.17b}$$

$$[1-\Omega^2]\bar{B} - \frac{\epsilon\Omega^2\bar{B}}{4}\left[\bar{B}^2 - \bar{A}^2\cos 2\bar{\Delta}\right] = 0 \tag{5.17c}$$

$$2\beta_s\Omega\bar{B} - \frac{\epsilon\Omega^2\bar{B}}{4}\bar{A}^2\sin 2\bar{\Delta} = 0 \tag{5.17d}$$

When $\bar{A} \neq 0$ and $\bar{B} \neq 0$, the latter two equations give

$$\cos 2\bar{\Delta} = \frac{4[\Omega^2-1]}{\epsilon\Omega^2\bar{A}^2} + \frac{\bar{B}^2}{\bar{A}^2} \tag{5.18a}$$

and

$$\sin 2\bar{\Delta} = \frac{\delta\beta_s\Omega}{\epsilon\Omega^2\bar{A}^2} \tag{5.18b}$$

respectively. Since $|\cos 2\bar{\Delta}| \leq 1$ and $|\sin 2\bar{\Delta}| \leq 1$, these equations require

$$\frac{4[1-\Omega^2]}{\epsilon\Omega^2} \leq \bar{A}^2 + \bar{B}^2 \qquad \bar{B}^2 + \frac{4[\Omega^2-1]}{\epsilon\Omega^2} \leq \bar{A}^2$$

$$\frac{\delta\beta_s}{\Omega\epsilon} \leq \bar{A}^2 \tag{5.19}$$

In the limit as $\bar{B} \to 0$, (5.19) can be shown to be equivalent to (5.13) of the stability analysis.

Using $\sin^2 2\bar{\Delta} + \cos^2 2\bar{\Delta} = 1$, (5.18) yields a quadratic equation for $\bar{B}^2$, which may be solved to obtain*

$$\bar{B}^2 = \frac{4[1-\Omega^2]}{\epsilon\Omega^2} + \frac{1}{\epsilon\Omega^2}\left[(\epsilon\Omega^2\bar{A}^2)^2 - (\delta\beta_s\Omega)^2\right]^{1/2} \tag{5.20}$$

Substituting this result in (5.18a) yields

$$\cos 2\bar{\Delta} = \frac{\left[(\epsilon\Omega^2\bar{A}^2)^2 - (\delta\beta_s\Omega)^2\right]^{1/2}}{\epsilon\Omega^2\bar{A}^2} \tag{5.21}$$

---

* The solution $\bar{B}_2^2 \sim [\,] - [\,]^{1/2}$ corresponds to the "in-phase" solution for the undamped case. In the absence of damping, such a solution will not satisfy (5.3), and $\bar{B}_2^2$ is thus discarded as an extraneous root.

When (5.17a), (5.20) and (5.21) are solved simultaneously, the solution

$$\mathcal{J}_c(\tau) = \bar{A} \cos [\Omega\tau + \bar{\phi}]$$
$$\mathcal{J}_s(\tau) = \bar{B} \sin [\Omega\tau + \bar{\Psi}] \qquad (5.22a)$$

results. For example, (5.18b), (5.20), and (5.21) can be inserted in (5.17a) and (5.17b), which then combine to give

$$G_m^2 (\sin^2\bar{\phi} + \cos^2\bar{\phi}) = G_m^2 = f(\bar{A}, \Omega, \epsilon, \beta_c, \beta_s) \qquad (5.22b)$$

Because of the complexity of (5.22b), it is desirable to examine some special cases of (5.17) in the case of "light damping" - i.e., β_s, $\beta_c << 1$.

Then, when $\bar{A} \neq 0$, $\bar{B} \neq 0$, and $\Omega \neq 1$, (5.17b) and (5.17d) are well approximated by

$$-\frac{\epsilon\Omega^2\bar{A}\bar{B}^2}{4} \sin 2\bar{\Delta} = G_m \sin\bar{\phi} \qquad (5.23a)$$

and

$$-\frac{\epsilon\Omega^2\bar{B}}{4} \bar{A}^2 \sin 2\bar{\Delta} = 0 \qquad (5.23b)$$

Combining these yields the results $\bar{\phi} = 0, \pm\pi$, $2\bar{\Delta} = 0, \pm\pi, \pm 2\pi$.

Making use of (5.23b), (5.17a) may be combined with (5.17c) to give

$$\bar{A} = \frac{G_m \cos\bar{\phi}}{[1-\Omega^2][1+\cos 2\bar{\Delta}]}$$

Notice that if $2\bar{\Delta} = \pm \pi$, $\bar{A}$ becomes unbounded, which is unlikely for all $\Omega = 1$; hence the possibility $2\bar{\Delta} = \pm \pi$ is excluded.

For $\Omega < 1$, the above results become

$$\bar{\phi} = 0, \quad \bar{\Delta} = 0, \pm \pi, \quad \bar{\Psi} = 0, \pm \pi$$

$$\bar{A} = \frac{G_n}{2[1-\Omega^2]}, \qquad \bar{B}^2 - \bar{A}^2 = \frac{4[1-\Omega^2]}{\epsilon \Omega^2} \tag{5.24a}$$

and for $\Omega > 1$, they are

$$\bar{\phi} = -\pi, \quad \bar{\Delta} = 0, \pm \pi, \quad \bar{\Psi} = 0, -\pi, -2\pi$$

$$\bar{A} = \frac{G_n}{2[-1+\Omega^2]}, \qquad \bar{A}^2 - \bar{B}^2 = \frac{4[-\Omega^2-1]}{\epsilon \Omega^2} \tag{5.24b}$$

Finally, suppose $\bar{\phi} = -\frac{\pi}{2}$. Then (5.17) can be manipulated to give

$$\bar{A} = \frac{G_n}{2\Omega[\beta_s + \beta_c]}, \qquad \bar{B}^2 = \bar{A}^2 \tag{5.25}$$

$$\text{and} \qquad -\frac{\pi}{2} \leq \bar{\Psi} < 0$$

$$\text{or} \qquad \frac{\pi}{2} \leq \bar{\Psi} < \pi$$

Although the preceding special cases give some insight in the problem, a complete analysis must include a discussion of (5.22b). For this purpose, a small computer program was set up to calculate G_n, $\bar{\varphi}$, $\bar{B}$, and $\bar{\Psi}$ for given values of $\bar{A}, \Omega, \epsilon, \beta_s$, and β_c. By cross-plotting the results, it was possible to obtain curves of $\bar{A}$ vs. Ω, $\bar{B}$ vs Ω, etc. for constant values of G_n, ϵ, β_s, and β_c. These curves are shown in Fig. 5.

One of the surprising features of the two mode response was the appearance of a "gap" or discontinuity in the solution. Slightly to the left of the resonance peak, the computer results indicated that

solutions of the form (5.22b) did not exist for $G_n = 0.1$. (Note that the curves of Figs. 3, 5, and 6 are all drawn for constant values of the forcing function, etc.). Subsequent results of the stability analysis (Section 2.5.1c) showed that the gap in the response coincides with a narrow region in which both the one mode solution (5.4) and the two mode solution are unstable. The experiments suggest that a "beating" response exists in this area, with the ring vibrating first in one mode, then two, then back to one, etc.

The computer program was used to obtain the response curves for the single bending mode case by simply putting $\beta_s >> 1$, (i.e., damping the $\sin \frac{ny}{R}$ mode heavily) which makes $\bar{B} = 0$ and causes (5.17) to revert to (3.49). A comparison of the one and two mode responses is given in Fig. 6.

Finally, it will be noted from Fig. 5 and from (5.24a) that for $\Omega < 1$, it is possible to have the companion mode $(\sin \frac{ny}{R})$ vibrate to larger amplitudes than the mode which is being directly driven $(\cos \frac{ny}{R})$. Responses of this type were detected experimentally.

Having found the steady-state response when both self-coupled modes are excited, one is then concerned with the stability of the solution, which is discussed below.

(c) Stability of the Solutions when both Self-Coupled Bending Modes are Excited

One way to investigate the stability of (5.22a) is to perturb the solution by putting

$$\eta_c(\tau) = \bar{A}\cos[\Omega\tau + \bar{\phi}] + \xi(\tau)$$

$$\eta_s(\tau) = \bar{B}\sin[\Omega\tau + \bar{\psi}] + x(\tau)$$

into (5.3) and then examine the resulting variational equations for ξ and x. The equations governing these perturbations are given and discussed in Section 2.5.2 (a).

A less general but much simpler means of stability analysis can be done via the method of averaging. To apply this technique, let

$$\begin{aligned} \bar{A} &= \bar{A}_0 + a(\tau) & \bar{\phi} &= \bar{\phi}_0 + \varphi(\tau) \\ \bar{B} &= \bar{B}_0 + b(\tau) & \bar{\Psi} &= \bar{\Psi}_0 + \psi(\tau) \end{aligned} \tag{5.26}$$

where the steady-state solution has been redesignated by

$$\begin{aligned} y_c(\tau) &= \bar{A}_0 \cos[\Omega\tau + \bar{\phi}_0] \\ y_s(\tau) &= \bar{B}_0 \sin[\Omega\tau + \bar{\Psi}_0] \end{aligned} \tag{5.27}$$

a, b, φ, and ψ are perturbations in the amplitudes and phases of the steady-state solution.

Recall that (5.15) governs the non-steady behavior of (5.3) when the latter are analyzed by the averaging method with (5.14) as possible solutions. By substituting (5.26) into (5.15) and retaining only first order terms in the perturbations, the equations governing a, b, φ, and ψ can be obtained. They are of the form*

$$\begin{aligned} &c_{1j}\, a + c_{2j} \frac{da}{d\tau} + c_{3j}\, b + c_{4j} \frac{db}{d\tau} \\ &+ c_{5j}\, \varphi + c_{6j} \frac{d\varphi}{d\tau} + c_{7j}\, \psi + c_{8j} \frac{d\psi}{d\tau} = 0 \end{aligned} \tag{5.28}$$

where the C_{ij} depend on $\bar{A}_0$, $\bar{B}_0$, $\bar{\phi}_0$, $\bar{\Psi}_0$, β_s, β_c, Ω, ϵ, and G_n but not on τ. Thus, for any steady-state values of $\bar{A}_0$, $\bar{B}_0$, $\bar{\phi}_0$, etc.,

---

* For details, see Appendix C.

the C_{ij} are constant, and (5.28) is just a system of linear equations with constant coefficients. This is in direct contrast with the more general approach (Section 2.5.2 (a)), where every coefficient is a periodic function of time.

To solve (5.28), one inserts

$$a(\tau) = a_1 e^{\lambda\tau} \quad , \quad b = b_1 e^{\lambda\tau}$$
$$\varphi(\tau) = \varphi_1 e^{\lambda\tau} \quad , \quad \psi = \psi_1 e^{\lambda\tau} \tag{5.29}$$

and requires a non-trivial solution. This results in an eigenvalue problem

$$|D - \lambda E| = 0 \tag{5.30}$$

for the λ. D and E are real, non-symmetric matrices, and complex values of λ result.

If $\mathrm{Re}(\lambda) > 0$ for any λ, then the perturbations increase with time, and the original steady-state solution at that point ($\bar{A}_o$, $\bar{B}_o$, Ω, etc.) is unstable. Conversely, if all $\mathrm{Re}(\lambda) < 0$ for a particular combination of $\bar{A}_o$, $\bar{B}_o$, etc., the solution (5.27) is stable there.

For example, consider the following (special) case:

$$\beta_s = 0, \quad \beta_c = 0 \qquad \text{(undamped)}$$

Then (5.30) becomes

$$0 = \begin{vmatrix} (\beta^2 - 2\alpha^2) & \alpha\beta & \lambda(2\Omega + \frac{3\alpha^2}{4\Omega}) & \frac{\alpha\beta\lambda}{4\Omega} \\ \alpha\beta & -\beta^2 & \frac{\alpha\beta\lambda}{4\Omega} & \lambda(2\Omega + \frac{3\beta^2}{4\Omega}) \\ -\lambda(2\Omega + \frac{\alpha^2}{4\Omega}) & \frac{\alpha\beta\lambda}{4\Omega} & -\alpha^2 & \alpha\beta \\ \frac{\alpha\beta\lambda}{4\Omega} & -\lambda(2\Omega + \frac{\beta^2}{4\Omega}) & \alpha\beta & -\alpha^2 \end{vmatrix} \tag{5.31}$$

where $\alpha^2 = \frac{\epsilon\Omega^2\bar{A}_0^2}{2}$, $\beta^2 = \frac{\epsilon\Omega^2\bar{B}_0^2}{2}$, $\alpha\beta = \frac{\epsilon\Omega^2\bar{A}_0\bar{B}_0}{2}$ and (5.17a), (5.17c) have been used. Expanding (5.31) and putting $z = 2\Omega\lambda$ gives

$$z^4 + 2\alpha^2(\alpha^2+\beta^2)z^2 + \alpha^2\beta^2(\alpha^2-\beta^2)^2 = 0 \tag{5.32}$$

For the roots of (5.32) to have negative real parts, the discriminant must be non-negative:

$$4\alpha^4(\alpha^2+\beta^2)^2 - 4\alpha^2\beta^2(\alpha^2-\beta^2)^2 \geq 0$$

$$4\alpha^8\left[1 + \left(\frac{\beta}{\alpha}\right)^2 + 3\left(\frac{\beta}{\alpha}\right)^4 - \left(\frac{\beta}{\alpha}\right)^6\right] \geq 0 \tag{5.33}$$

Solving $(\frac{\beta}{\alpha})^6 - 3(\frac{\beta}{\alpha})^4 - (\frac{\beta}{\alpha})^2 - 1 = 0$, one finds that (5.33) will be satisfied if

$$\left(\frac{\beta}{\alpha}\right)^2 \leq 3.38, \quad \text{i.e.,} \quad \bar{B}_0^2 \leq 3.38\bar{A}_0^2 \tag{5.34}$$

Using (5.34) with (5.17c), it can be shown that (5.33) requires

$$1 - \frac{2.38\epsilon\bar{A}_0^2}{8} + O(\epsilon^2) \leq \Omega \tag{5.35}$$

On the other hand, in the absence of damping (5.17c) shows that real values of $\bar{B}$ will exist only if

$$\Omega \leq 1 + \frac{\epsilon \bar{A}^2}{8} + O(\epsilon^2) \tag{5.36}$$

Combining the above results, one sees that the solution (5.27) is real-valued and stable (in the absence of damping) within the region

$$1 - \frac{2.38\,\epsilon \bar{A}^2}{8} + O(\epsilon^2) \leq \Omega \leq 1 + \frac{\epsilon \bar{A}^2}{8} + O(\epsilon^2) \tag{5.37}$$

The results of the stability analyses are summarized in Fig. 7. In connection with (5.35), it was noted that the results of the computer solution to (5.17) became discontinuous near the curve $1 - \frac{2.38\,\epsilon \bar{A}^2}{8} = \Omega$. (See Fig. 6).

2.5.2 The General Inextensional Case: Approximate Solutions and their Stability

As noted previously, this case will be considered for two sets of forces: $q(y,t) = \frac{F_m}{\pi R} \cos \frac{my}{R} \cos\omega t$ and $q(y,t) = \delta(y)\, F \cos\omega t$. The first of these drives only one mode ($\cos \frac{my}{R}$) directly, and for linear vibrations would excite only that mode. The other case is one which is approximated by the experiments. Under the restrictions that

(a) ω is in the vicinity of the natural frequency of the mth bending mode,

(b) ω is not in the vicinity of a sub-multiple or multiple of the natural frequency of the nth bending mode, and

(c) the damping is very small and is the same order of magnitude for all the modes,

it can be shown that the solutions of the general case approach those obtained previously for the self-coupled bending modes.

(a) The General Inextensional Case, with $q(y,t) = \frac{F_m}{\pi R} \cos \frac{my}{R} \cos \omega t$

With $q(y,t)$ as specified and with the addition of viscous damping, equations (4.19) and (4.20) become

$$\ddot{\varphi}_{cn} + 2\beta_{cn}\omega_{nn}\dot{\varphi}_{cn} + \omega_{nn}^2\varphi_{cn} + \frac{\eta_n}{2}\varphi_{cn}\sum_{k=2}^{\infty}\eta_k\left[\dot{\varphi}_{ck}^2 + \varphi_{ck}\ddot{\varphi}_{ck} + \varphi_{sk}\ddot{\varphi}_{sk} + \dot{\varphi}_{sk}^2\right] = \begin{cases} 0 & \text{FOR } n \neq m \\ \omega_{nm}^2 G_m \cos\omega t & \text{FOR } n = m \end{cases} \quad (5.38a)$$

and

$$\ddot{\varphi}_{sn} + 2\beta_{sn}\omega_{nn}\dot{\varphi}_{sn} + \omega_{nn}^2\varphi_{sn} + \frac{\eta_n}{2}\varphi_{sn}\sum_{k=2}^{\infty}\eta_k\left[\dot{\varphi}_{ck}^2 + \varphi_{ck}\ddot{\varphi}_{ck} + \varphi_{sk}\ddot{\varphi}_{sk} + \dot{\varphi}_{sk}^2\right] = 0 \quad \text{FOR ALL } n \quad (5.38b)$$

where

$\omega_{nn}^2 G_m = \frac{F_m}{\pi R \rho h^2}$; and β_{sn}, β_{cn} are the "per cent critical damping" in the modes $\sin \frac{ny}{R}$, $\cos \frac{ny}{R}$ respectively.

Excitation of a Single Bending Mode; Stability of the Solution

Inspection of (5.38) reveals that a possible solution is

$$\varphi_{sn} = 0 \text{ FOR ALL } n, \quad \varphi_{cn} = 0 \text{ FOR } n \neq m \quad (5.39)$$

and $\varphi_{cm} \neq 0$,

where φ_{cm} satisfies

$$\ddot{\eta}_{cm} + 2\beta_{cm}\omega_{nm}\dot{\eta}_{cm} + \omega_{nm}^2\eta_{cm} + \frac{\eta_m^2}{2}\eta_{cm}\left[\eta_{cm}\ddot{\eta}_{cm} + \dot{\eta}_{cm}^2\right] = \omega_{nm}^2 G_m \cos\omega t \tag{5.40}$$

That is, for q(y,t) as specified, a possible solution is that only a single bending mode becomes excited! From the single mode analysis, Section 2.3.3, an approximate solution to (5.40) is

$$\eta_{cm}(t) = \bar{A}\cos\left[\omega t + \bar{\phi}\right] \tag{5.41}$$

where $\bar{A}$ and $\bar{\phi}$ satisfy (3.49) with $\Omega = \frac{\omega}{\omega_{nm}}$ and $\beta = \beta_{cm}$.

With (5.39) and (5.41) as a possible solution to the system, one then asks if it is a stable solution. To do this, the entire system must be perturbed. Let

$$\begin{aligned}\eta_{cn} &= 0 + \xi_n(t) \quad \text{FOR } n \neq m\\ \eta_{cm} &= \bar{A}\cos\left[\omega t + \bar{\phi}\right] + \xi_m(t)\\ \eta_{sn} &= 0 + x_n(t)\end{aligned} \tag{5.42}$$

and substitute these into (5.38). Retaining only the linear terms in the perturbations, one has

$$\ddot{\xi}_n + 2\beta_{cn}\omega_{nn}\dot{\xi}_{cn} + \left[\omega_{nn}^2 - \frac{\eta_n\eta_m\omega^2\bar{A}^2}{2}\cos 2(\omega t + \bar{\phi})\right]\xi_n = 0, \quad n \neq m \tag{5.43a}$$

$$\ddot{\xi}_m\left[1 + \frac{\eta_m^2}{2}\bar{A}^2\cos^2(\omega t + \bar{\phi})\right] + \dot{\xi}_m\left[2\beta_{cm}\omega_{nm} - \frac{\eta_m^2\omega\bar{A}^2}{2}\sin 2(\omega t + \bar{\phi})\right] + \xi_m\left\{\omega_{nm}^2 + \frac{\eta_m^2\omega^2\bar{A}^2}{2}\left[\sin^2(\omega t + \bar{\phi}) - 2\cos^2(\omega t + \bar{\phi})\right]\right\} = 0 \tag{5.43b}$$

and

$$\ddot{x}_n + 2\beta_{sn}\omega_{nn}\dot{x}_n + \left[\omega_{nn}^2 - \frac{\eta_n\eta_m}{2}\omega^2\bar{A}^2\cos 2(\omega t + \bar{\phi})\right]x_n = 0 \tag{5.43c}$$

$$n = 2, 3, 4, \cdots$$

Putting $\Omega = \frac{\omega}{\omega_{nm}}$ and $\beta = \beta_{cm}$, (5.43b) becomes identical with (3.53), which was discussed in Section 2.3.4. Equations (5.43a) and (5.43c) can be studied simultaneously, since they are identical in form.

Letting $y_n = \xi_n$ or x_n, $z = (\omega t + \bar{\phi})$

$$a_n = \frac{\omega_{nn}^2}{\omega^2}, \quad 16q_n = -\frac{\eta_n \eta_m \bar{A}^2}{2}$$

and considering the undamped case first, equations (5.43a) or (5.43c) take on the standard form of Mathieu's equation:

$$\frac{d^2 y_n}{dz^2} + [a_n + 16q_n \cos 2z] y_n = 0 \qquad (5.44)$$

$$n = 2, 3, 4, \cdots$$

Near the first unstable region, (5.44) indicates that y_n becomes unstable when

$$\bar{A}^2 > \frac{4\left[1 - \frac{\omega_{nn}^2}{\omega^2}\right]}{\eta_n \eta_m} \qquad (5.45a)$$

FOR $\omega_{nn} \leq \omega$

and when

$$\bar{A}^2 > \frac{4\left[\frac{\omega_{nn}^2}{\omega^2} - 1\right]}{\eta_m \eta_n} \qquad (5.45b)$$

FOR $\omega \leq \omega_{nn}$

Now imagine that the $\cos\frac{my}{R}$ mode (i.e., the mode which is being forced by $q(y,t)$ is excited in the vicinity of its resonant frequency. In other words, consider what happens when $\omega = \omega_{nn}$. In that case, (5.45) gives

$$\bar{A}^2 > \frac{4\left|1 - \frac{\omega_{nn}^2}{\omega_{nm}^2}\right|}{\eta_n \eta_m} \quad \text{FOR } n \neq m \tag{5.46a}$$

and

$$\bar{A}^2 > 0 \quad \text{FOR } n = m \tag{5.46b}$$

where (5.46b) occurs only for one mode, namely $\sin \frac{my}{R}$. Thus, for the undamped case, the theory indicates that when $\omega = \omega_{nm}$, any positive value of $\bar{A}$ will cause $\sin \frac{my}{R}$ to become unstable. Note that for all <u>other</u> modes (i.e., $n \neq m$), a greater value of $\bar{A}$ is required for instability. In other words, at $\omega = \omega_{nm}$,

$$\bar{A}^2_{\text{critical for mode n}} > \bar{A}^2_{\text{critical for mode } \sin \frac{my}{R}}$$

If one allows m to become very large, both $\omega_{n(m-1)}$ and $\omega_{n(m+1)}$ approach ω_{nm}, which causes the critical amplitudes of the $(m \pm 1)$ modes to become very small. Recall, however, that the present analysis neglects shear deformation and rotary inertia, which restricts the range of m; see Section 2.6.2.

With the addition of damping, an analysis similar to that outlined in Section 2.5.1 (a) shows that at $\omega = \omega_{nm}$, (5.45) is replaced by

$$\bar{A}^4 > \frac{64\beta_n \mu^{-2} + [\mu^2 - 1]^2}{\eta_n^2 \eta_m^2} \qquad n = 2, 3, 4, \ldots$$

where $\mu = \frac{\omega_{nn}}{\omega_{nm}}$ and $\beta_n = \beta_{sn}$ or β_{cn}. For $n = m$, this reduces

to $\bar{A}^2 > \frac{\beta_{sm}}{\eta_m^2}$. Assuming for the moment that $\beta_{cm} \cong \beta_{sm} \cong \beta_{cn} \cong \beta_{sn}$ (i. e., equal damping in all the modes), it is apparent that

$$\bar{A}^2_{CR \text{ FOR MODES WITH } m \neq n} > \bar{A}^2_{CR \text{ FOR } \sin \frac{my}{R}} = \frac{\beta_{sm}}{\eta_m^2}$$

as in the undamped case, and $\sin \frac{my}{R}$ will participate in the motion prior to the advent of any other bending mode.

On the other hand, if $\beta_{sm} >> \beta_{s(m-1)}$ and if ω is near enough to $\omega_{m(m-1)}$, then it is possible that $\sin \frac{(m-1)y}{R}$ or $\cos \frac{(m-1)y}{R}$ might begin to vibrate before $\sin \frac{my}{R}$. Such a situation seems highly unlikely, however.

Finally, it will be noted that if $\cos \frac{my}{R}$ is driven at the resonant frequency of some other mode (i. e., if $\omega = \omega_{mn}$) that mode can be parametrically unstable and may participate in the motion. Similarly, the higher unstable regions of (5.44) point out that the nth mode can be excited by driving at sub-multiples of its natural frequency ($\frac{\omega_{mn}}{2}$, $\frac{\omega_{mn}}{3}$, etc.). In the event that ω_{mn} is near a sub-multiple of ω_{mn}, there exists the possibility of exciting $\cos \frac{my}{R}$ (directly) and $\cos \frac{ny}{R}$ (ultraharmonic response) simultaneously. The presence of damping lessens the probability of this occurring; however, such responses were detected experimentally.

Coupled bending mode vibrations of the type just mentioned can be analyzed, but they are of less interest than the "self-coupled" case and will not be discussed further.

With the restrictions that

(a) ω is in the vicinity of ω_{nm}

(b) ω is not in the vicinity of $\frac{\omega_{nm}}{2}$, $\frac{\omega_{nm}}{3}$, etc. and (5.47)

(c) the damping in the various modes is of the same order of magnitude,

one concludes that the solution

$$\eta_{cm} = \bar{A}\cos[\omega t + \bar{\phi}], \quad \eta_{sm} = 0$$
$$\eta_{cn} = 0, \quad \eta_{sn} = 0 \quad \text{FOR ALL } n \neq m \tag{5.39}$$

is stable for $\bar{A} < A_{CR}$, where A_{CR} is approximated by

$$A_{CR}^4 = \frac{64\beta_{sm}^2\left(\frac{\omega}{\omega_{nm}}\right)^2 + \left[\frac{\omega_{nm}^2}{\omega^2} - 1\right]^2}{\eta_m^4} \tag{5.48}$$

For $\bar{A} > A_{CR}$, this solution ceases to be valid, and one must consider vibrations in which $\cos\frac{my}{R}$ and $\sin\frac{my}{R}$ both participate.

Excitation of the "Self-Coupled" Bending Modes; Stability of the Solution

For $\bar{A} > A_{CR}$, a possible solution to (5.38) is

$$\eta_{cn} = 0, \quad \eta_{sn} = 0 \quad \text{FOR } n \neq m$$
$$\eta_{cm} \neq 0, \quad \eta_{sm} \neq 0 \tag{5.49}$$

where η_{cm} and η_{sm} satisfy

$$\ddot{\eta}_{cm} + 2\beta_{cm}\omega_{nm}\dot{\eta}_{cm} + \omega_{nm}^2\eta_{cm} + \frac{\eta_m^2}{2}\eta_{cm}\left[\eta_{cm}\ddot{\eta}_{cm} + \dot{\eta}_{cm}^2 + \eta_{sm}\ddot{\eta}_{sm} + \dot{\eta}_{sm}^2\right] = \omega_{nm}^2 G_m \cos\omega t \tag{5.50a}$$

and

$$\ddot{\eta}_{sm} + 2\beta_{sm}\omega_{nm}\dot{\eta}_{sm} + \omega_{nm}^2\eta_{sm} + \frac{\eta_m^2}{2}\eta_{sm}[\dot{\eta}_{cm}^2 + \eta_{cm}\ddot{\eta}_{cm} + \eta_{sm}\ddot{\eta}_{sm} + \dot{\eta}_{sm}^2] = 0 \tag{5.50b}$$

which are the equations for "self-coupled" bending modes. This case was analyzed previously; approximate solutions to these equations are

$$\eta_{cm}(t) = \bar{A}\cos[\omega t + \bar{\phi}]$$
$$\eta_{sm}(t) = \bar{B}\sin[\omega t + \bar{\psi}] \tag{5.51}$$

where $\bar{A}$, $\bar{B}$, etc. satisfy equations (5.17) with

$$\Omega = \frac{\omega}{\omega_{nm}}, \quad \beta_c = \beta_{cm}, \quad \beta_s = \beta_{sm}, \quad \text{AND} \quad \bar{\Delta} = \bar{\psi} - \bar{\phi}.$$

Having (5.49) and (5.51) as a possible solution for the system, one must determine its stability. Perturbing the entire system, one puts

$$\eta_{cm} = \bar{A}\cos[\omega t + \bar{\phi}] + \xi_m$$
$$\eta_{sm} = \bar{B}\sin[\omega t + \bar{\psi}] + \chi_m \tag{5.52}$$

and $\eta_{cm} = 0 + \xi_m$, $\eta_{sm} = 0 + \chi_m$ FOR $n \neq m$

Substituting (5.52) into (5.38) and retaining first order terms in the perturbations gives

$$\ddot{\gamma}_n + 2\beta\omega_{nm}\dot{\gamma}_n + \left\{\omega_{nm}^2 - \frac{\eta_n\eta_m\omega^2}{2}[\bar{A}^2\cos 2(\omega t + \bar{\phi}) - \bar{B}^2\cos 2(\omega t + \bar{\psi})]\right\}\gamma_n = 0 \tag{5.53}$$

FOR $n = 2, 3, 4, \ldots$
$n \neq m$

where $\gamma_n = \xi_n$ OR χ_n, AND $\beta = \beta_{cm}$ OR β_{sm}

and

$$\ddot{\zeta}_m\left[1+\frac{\eta_m^2\bar{A}^2}{2}\cos^2 X\right]+\dot{\zeta}_m\left[2\beta_{cm}\omega_{nm}-\frac{\eta_m^2\bar{A}^2\omega}{2}\sin 2X\right]+\zeta_m\left\{\omega_{nm}^2+\frac{\omega^2\eta_m^2}{2}\left[\bar{A}^2(\sin^2 X-2\cos^2 X)+\bar{B}^2\cos 2(X+\bar{\Delta})\right]\right\}+\frac{\eta_m^2\bar{A}\bar{B}}{2}\cos X\left[\ddot{x}_m\sin(X+\bar{\Delta})+2\omega\dot{x}_m\cos(X+\bar{\Delta})-\omega^2 x_m\sin(X+\bar{\Delta})\right]=0 \tag{5.54a}$$

$$\ddot{x}_m\left[1+\frac{\eta_m^2\bar{B}^2}{2}\sin^2(X+\bar{\Delta})\right]+\dot{x}_m\left[2\beta_{sm}\omega_{nm}+\frac{\eta_m\bar{B}^2\omega}{2}\sin 2(X+\bar{\Delta})\right]+x_m\left\{\omega_{nm}^2+\frac{\eta_m^2\omega^2}{2}\left[\bar{B}^2\cos^2(X+\bar{\Delta})-2\bar{B}^2\sin^2(X+\bar{\Delta})-\bar{A}^2\cos 2X\right]\right\}+\frac{\eta_m^2\bar{A}\bar{B}}{2}\sin(X+\bar{\Delta})\left[\ddot{\zeta}_m\cos X-2\omega\dot{\zeta}_m\sin X-\omega^2\zeta_m\cos X\right]=0 \tag{5.54b}$$

for the perturbations ζ_m and x_m, where $X=\omega t+\bar{\phi}$ and $\bar{\Delta}=\bar{\psi}-\bar{\phi}$.

Equation (5.53) may be analyzed in the same manner as (5.43a) and (5.43c). Such a study yields the result that $\cos\frac{ny}{R}$ and $\sin\frac{ny}{R}$ do not participate in the motion as long as the conditions (5.47) are met.

The equations for ζ_m and x_m, (5.50), form a system of coupled equations with each coefficient a periodic function of time. Because of the manner in which $\ddot{\zeta}_m$, $\dot{\zeta}_m$, $\ddot{x}_m$, and $\dot{x}_m$ appear in these equations, it is unlikely that they can be reduced to coupled Hill's equations or some other recognizable equations whose stability

is known. Approximate solutions to (5. 50) can be obtained by the method of averaging; when this is done, one obtains a stability determinant which is equivalent to (5. 30). Since the stability of the two mode steady-state solution was discussed previously (Section 2. 5. 1c), the results of that analysis can be applied here.

Thus, one has that the solution (5. 49) and (5. 51) is stable and real-valued as long as ω lies in the region

$$1 - \frac{2.38\,\epsilon \bar{A}^2}{\beta} \leq \frac{\omega}{\omega_{nm}} \leq 1 + \frac{\epsilon \bar{A}^2}{\beta} \qquad (5.55)$$

and the conditions (5. 47) are met.

For the loading $q(y,t) = \frac{F_m}{\pi R} \cos\frac{my}{R} \cos\omega t$, and with the restrictions on ω and on the damping, one sees that the solutions to the general inextensional case are identical to the one and two mode solutions presented previously. This is only approximately true for the loading $q(y,t) = \delta(y)\, F \cos\omega t$.

(b) <u>The General Inextensional Case with $q(y,t) = \delta(y) F \cos\omega t$</u>

With the addition of viscous damping, and with $q(y,t)$ as specified, equations (4. 19) and (4. 20) become

$$\ddot{\mathcal{J}}_{cn} + 2\beta_{cn}\omega_{nm}\dot{\mathcal{J}}_{cn} + \omega_{nm}^2 \mathcal{J}_{cn} + \frac{\eta_n}{2}\mathcal{J}_{cn}\sum_{k=2}^{\infty}\eta_k\left[\mathcal{J}_{ck}\ddot{\mathcal{J}}_{ck} + \dot{\mathcal{J}}_{ck}^2 + \mathcal{J}_{sk}\ddot{\mathcal{J}}_{sk} + \dot{\mathcal{J}}_{sk}^2\right] + \frac{\eta_n \mathcal{J}_{cn}}{2} G\cos\omega t = G\cos\omega t \qquad (5.56a)$$

and

$$\ddot{\mathcal{J}}_{sn} + 2\beta_{sn}\omega_{nn}\dot{\mathcal{J}}_{sn} + \omega_{nn}^2\mathcal{J}_{sn} + \frac{\eta_n \mathcal{J}_{sn}}{2}\sum_{k=2}^{\infty}\eta_k\left[\dot{\mathcal{J}}_{ck}^2 + \mathcal{J}_{ck}\ddot{\mathcal{J}}_{ck} + \mathcal{J}_{sk}\ddot{\mathcal{J}}_{sk} + \dot{\mathcal{J}}_{sk}^2\right] \qquad (5.56b)$$

$$+ \frac{\eta_n \mathcal{J}_{sn}}{2} G\cos\omega t = 0$$

where $G = \frac{F}{\pi R\rho h^2}$. $\qquad n = 2, 3, 4, \cdots$

For ω near ω_{nn}, not near $\frac{\omega_{nn}}{2}$, $\frac{\omega_{nn}}{3}$, etc., and with "light damping", an approximate solution to (5.56) is

$$\mathcal{J}_{sn} = 0 \quad \text{FOR ALL } n$$

$$\mathcal{J}_{cn} = \frac{G\cos\omega t}{\omega_{nn}^2 - \omega^2} \quad \text{FOR } n \neq m \qquad (5.57)$$

$$\mathcal{J}_{cm} = \bar{A}\cos(\omega t + \bar{\phi})$$

where $\mathcal{J}_{cm}$ satisfies (5.55a) with n = m.

In general, one can show that

$$\left|\frac{\mathcal{J}_{cn}}{\mathcal{J}_{cm}}\right| << 1 \quad \text{AND} \quad |\mathcal{J}_{cn}| \to 0 \quad \text{AS } n \to \infty$$

Thus, the sum $\sum_k \eta_k\left[\dot{\mathcal{J}}_{ck}^2 + \cdots + \dot{\mathcal{J}}_{sk}^2\right]$ is dominated by the k = m term. In this case, (5.56) is very nearly equal to (3.45), which governs the vibration of a single bending mode! Similarly, the deflection

$$\frac{w(y,t)}{h} = \sum_{n=2}^{\infty}\left[\mathcal{J}_{cn}\cos\frac{ny}{R} + \mathcal{J}_{sn}\sin\frac{ny}{R} - \frac{\eta_n}{4}\left(\mathcal{J}_{cn}^2 + \mathcal{J}_{sn}^2\right)\right]$$

is dominated by $\mathcal{J}_{cm}$, and $\frac{w}{h} \cong \mathcal{J}_{cm}\cos\frac{my}{R} - \frac{\eta_m}{4}\mathcal{J}_{cm}^2$, which demonstrates that an approximate solution to (5.56) is the excitation of primarily a single bending mode.

If the stability of (5.57) is examined, the analysis closely parallels that of the preceding case, Section 2.5.2a. For (5.57) to be stable, the conditions (5.47) must be met and in addition (a) ω must not be near $2\omega_{mn}$, and (b) $\bar{A}$ must be less than A_{CR}, where the latter is given by (5.48).

When $\bar{A} > A_{CR}$, (5.57) is no longer stable, and $\sin \frac{my}{R}$ participates in the motion. In this case, an approximate solution to (5.56) is

$$\eta_{sn} = 0, \quad \eta_{cn} = \frac{G \cos \omega t}{\omega_{mn}^2 - \omega^2} \qquad n \neq m$$

$$\eta_{cm} = \bar{A} \cos(\omega t + \bar{\phi}) \tag{5.58}$$

$$\eta_{sm} = \bar{B} \sin(\omega t + \bar{\psi})$$

where η_{sm} and η_{cm} satisfy (5.56) with n = m.

With only slight modifications, the stability analysis of this "primarily two mode" solution parallels that of the previous case. When ω is not in the vicinity of $2\omega_{mn}$ and the conditions (5.47) and (5.55) are met, the solution (5.58) is stable.

2.6 Additional Non-Linearities and Other Effects

The preceding analyses have several features in common, one of them being the omission of some minor non-linear terms and of shear deformation and rotary inertia. The conditions under which these effects are negligible are pointed out in this section.

By examining the non-linear strain-displacement relations, one can improve the analysis. Shear and rotary inertia effects have been

investigated previously (Ref. 4), and the results of that study will be outlined.

2.6.1 The Inclusion of some Additional Non-Linearities

For vibrations involving primarily one bending mode, the theory indicates

$$w(y,t) \cong A \cos\omega t \cos\frac{ny}{R} + A_o(t) \qquad (2.3)$$

where

$$A_o(t) \cong -\frac{n^2A^2}{8R}(1+\cos 2\omega t) \quad \text{(Cf. 3.44)}$$

Experimentally, it was possible to independently measure the maximum amplitude (A) of $\cos\frac{ny}{R}$ and the amplitude of the second harmonic term* in $A_o(t)$. When the experimental values of $(A)^2$ were plotted against $(A_o)_{2\omega}$, a linear relationship was indicated. According to the theory, such a line should have a slope of $\frac{n^2}{8R}$; preliminary experiments indicated a lesser slope, suggesting that the coefficient $\frac{n^2}{8R}$ might be in error.

Since the theoretical results (3.44) for the deflections are basically unchanged by including the effects of extension or tangential inertia, one suspects a discrepancy in the inextensionality condition itself. This leads to an examination of the strain-displacement relation. For thin rings, the general form is (See reference 24)

$$\epsilon_{yy}\Big|_{z=0} = \frac{\partial v}{\partial y} + \frac{w}{R} + \frac{1}{2}\left[\left(\frac{\partial w}{\partial y} - \frac{v}{R}\right)^2 + \left(\frac{w}{R} + \frac{\partial v}{\partial y}\right)^2\right] \qquad (6.1)$$

---

* Designated by $(A_o)_{2\omega}$

Up to this point, only a first approximation to (6. 1) has been used, namely

$$\varepsilon_{yy}\Big|_{z=0} = \frac{\partial v}{\partial y} + \frac{w}{R} + \frac{1}{2}\left(\frac{\partial w}{\partial y}\right)^2 \tag{1.2}$$

Taking w(y, t) in the form

$$w_1(y,t) = A(t)\cos\frac{ny}{R} + [A_0(t)]_1 \tag{6.2}$$

and using it together with (1. 2) in the inextensionality condition gives

$$\varepsilon_{yy}\Big|_{z=0} = \frac{\partial v_1}{\partial y} + \frac{(A_0)_1}{R} + \frac{A}{R}\cos\frac{ny}{R} + \frac{1}{2}\left(\frac{nA}{R}\sin\frac{ny}{R}\right)^2$$

whence

$$(A_0)_1 = -\frac{n^2A^2}{4R} \tag{6.3a}$$

and

$$v_1(y,t) = -\frac{A}{n}\sin\frac{ny}{R} + \frac{nA^2}{8R}\sin\frac{2ny}{R} \tag{6.3b}$$

To improve these results, (6. 1) will be employed, with v_1 and w_1 used to compute the non-linear terms. Let the second approximation be

$$w_2(y,t) = A(t)\cos\frac{ny}{R} + [A_0(t)]_2 \tag{6.4}$$

From (6. 2) and (6. 3), one has

$$\left(\frac{\partial w_2}{\partial y} - \frac{v_1}{R}\right)^2 = \left[\frac{n^2\left(1-\frac{1}{n^2}\right)^2A^2}{2R^2}\left(1-\cos\frac{2ny}{R}\right)\right] + O\left(\frac{A}{R}\right)^3 \tag{6.5a}$$

and

$$\left(\frac{\partial v_2}{\partial y} + \frac{w_2}{R}\right)^2 = O\left(\frac{A}{R}\right)^4 \tag{6.5b}$$

Using (6.4) and (6.5) in (6.1), the inextensionality condition is again applied:

$$\epsilon_{yy}\Big|_{z=0} = \frac{\partial v_2}{\partial y} + \frac{A}{R}\cos\frac{ny}{R} + \frac{(A_0)_2}{R}$$

$$+ \frac{1}{2}\left[\frac{n^2\left(1-\frac{1}{n^2}\right)^2 A^2}{2R^2}\left(1-\cos\frac{2ny}{R}\right)\right] + O\left(\frac{A}{R}\right)^3$$

This results in

$$[A_0(t)]_2 = -\frac{n^2\left(1-\frac{1}{n^2}\right)^2 A^2}{4R} \tag{6.6a}$$

and

$$v_2(y,t) = -\frac{A}{n}\sin\frac{ny}{R} + \frac{nA^2}{8R}\left(1-\frac{1}{n^2}\right)^2\sin\frac{2ny}{R} \tag{6.6b}$$

Repeating this process with w_2 and v_2 yields the third approximation,

$$w_3(y,t) = A(t)\cos\frac{ny}{R} - \frac{n^2\left(1-\frac{1}{n^2}\right)^2 A^2}{4R} \tag{6.7a}$$

$$v_3(y,t) = -\frac{A}{n}\sin\frac{ny}{R} + \frac{nA^2\left(1-\frac{1}{n^2}\right)^2}{8R}\sin\frac{2ny}{R} + O\left(\frac{A}{R}\right)^3 \tag{6.7b}$$

which differs from the second only in the higher order terms. Subsequent iterations will likewise differ in the $0(\frac{A}{R})^3$ terms; for present purposes, it is sufficient to stop at this point.

Note that (6. 7a) is in the same form as (2. 3). Thus, the results of all the previous analyses can be easily modified to better approximate the full strain-displacement relation, (6. 1). For example, (2. 3) becomes

$$w(y,t) \cong A\cos\omega t \cos\frac{ny}{R} + A_o(t) \qquad (6.8a)$$

where

$$A_o(t) \cong -\frac{n^2(1-\frac{1}{n^2})^2}{8R} A^2(1+\cos 2\omega t) \qquad (6.8b)$$

from (3. 44) and (6. 7a). Equation (6. 8b) indicates a linear variation of $(A_o)_{2\omega}$ vs. A^2, with slope $\frac{n^2(1-\frac{1}{n^2})^2}{8R}$. This improved the agreement with the preliminary experiments on $(A_o)_{2\omega}$, but such was not the case in later tests. (See Fig. 17f and the related discussion in Section 3. 2.).

Recall that the inextensional analyses can be corrected for the effect of tangential inertia by replacing $\frac{\omega}{\omega_M}$ by $\frac{\omega}{\omega_L}$ and ϵ by ϵ_i. (See Section 2. 3. 2). Similarly, the results of the present section can be employed by substituting ϵ_c for ϵ_i where

$$\epsilon_c = \left(1-\frac{1}{n^2}\right)^4 \epsilon_i = \left(1-\frac{1}{n^2}\right)^4 \left(\frac{n^2}{n^2+1}\right)\left(1+\frac{1}{8n^2}\right)\epsilon \qquad (6.9)$$

These combined corrections lead to a significant improvement in the theory; the calculated curves shown in Figs. 17a-e all employ ϵ_c in place of ϵ . Similar corrections apply to the multiple bending mode analyses.

2.6.2 Shear Deformation and Rotary Inertia

An extensive analysis of shear and rotary inertia effects was done by Buckens, reference 4. His results can be put in the form

$$\omega = \omega_L \left[1 + C\left(\frac{h}{R}\right)^2 + O\left(\frac{h}{R}\right)^4 \right]$$

where ω_L is the classical expression for the natural frequency of a ring (3.39),

ω is the natural frequency where shear and rotary inertia are included, and

C is a correction factor.

The largest term in C arises from shear deformation. For rectangular cross-sections, both shear and rotary inertia effects can be neglected if

$$\frac{n^2 h^2}{3R^2} << 1 \qquad (6.10)$$

Or, with $\lambda = \frac{\pi R}{n}$ = the half-wave length of $\cos \frac{ny}{R}$, (6.10) becomes

$$\frac{\pi h}{\sqrt{3}} << \lambda \qquad (6.11)$$

This is agreement with the analogous result for beams, namely that shear effects can be neglected if the ratio $\frac{\text{depth}}{\text{length}}$ is much less than unity. Considering a section of the ring as a curved beam with length λ and depth h, one sees the similarity of the two statements. For

complete details, the reader is referred to Buckens' original work, (Ref. 4).

Conditions such as the above (6.11) are derived from linear analyses. When (6.11) is met, the effect of shear deformation and rotary inertia on the linear vibrations of a ring are negligible. It is assumed that these effects remain negligible for the non-linear vibrations, as long as (6.10) holds. Examination of this assumption is left to another report.

2.7 Comparison with Other Results

In order to better understand the present work, it will be compared with some similar results. A few studies on the non-linear vibrations of rings have been done; they are not concerned with the forced vibration problem. (See Refs. 6 - 8). Some of these contain certain inconsistencies, and none discuss the phenomenon of self-coupled bending modes.

The forced non-linear vibrations of a ring have several features in common with the analogous problems for a thin circular cylindrical shell and a thin cylindrical membrane. Many other systems which possess axial symmetry behave in a qualitatively similar fashion. A few systems such as these and the results of previous investigators are discussed in this section.

2.7.1 The Free Non-Linear Vibrations of a Ring

Federhofer (Ref. 6) examined this problem by an iteration scheme. First, equations are derived which include tangential inertia,

mid-plane extension, and the major quadratic terms in the strain-displacement relations. The "thin ring assumption" ($\frac{h^2}{R^2} \ll 1$) is not made. After several manipulations, the problem is reduced to a single non-linear partial differential equation

$$L(w) = S(w) \tag{7.1}$$

where L is a linear operator and S is a non-linear relation that depends on w. To obtain an approximate solution, Federhofer solves

$$L(w_o) = 0$$

which gives

$$w_o = A \cos\omega t \cos \frac{ny}{R}$$

Then he puts $w = w_o + w_1$ into (7.1) and has

$$L(w_o + w_1) = S(w_o + w_1) \tag{7.2}$$

Since L is a linear operator, and since w_1 is a correction that is assumed to be small, (7.2) is replaced by

$$L(w_o) + L(w_1) \cong S(w_o) \tag{7.3}$$

But $L(w_o) = 0$; thus one can solve

$$L(w_1) = S(w_o) \tag{7.4}$$

to obtain the correction term, w_1.

In the notation of the present work, reference 6 gives

$$\frac{w(y,t)}{h} = \frac{A}{h} \cos\omega t \cos\frac{ny}{R} + \left(\frac{A}{h}\right)^2 \frac{h}{R} \left[b_1(n,\alpha) \cos 2\omega t + b_2(n,\alpha) \cos\frac{2ny}{R} + b_3(n,\alpha) \cos 2\omega t \cos\frac{2ny}{R}\right] \tag{7.5}$$

where $b_i(n, \alpha)$ depend on the mode number, n, and the ring parameter, α ($\alpha = \frac{h^2}{12R^2}$). In the limit as $\alpha \to 0$, (7.5) reduces to

$$\frac{w(y,t)}{h} = \frac{A}{h} \cos\omega t \cos\frac{ny}{R} + \left(\frac{A}{h}\right)^2 \frac{n^2 h}{8R}\left(1-\frac{1}{n^2}\right)^2 \cos 2\omega t \tag{7.6}$$

where $b_3(n, 0) \cong 0$ and $b_2 \sim 0(10^{-3})$. The present solution (when corrected for the additional non-linearities) gives

$$w(y,t) = \frac{A}{h} \cos\omega t \cos\frac{ny}{R} + \left(\frac{A}{h}\right)^2 \frac{n^2 h}{8R}\left(1-\frac{1}{n^2}\right)^2 (1+\cos 2\omega t) \tag{6.8}$$

which is identical with (7.6) except for the term which is constant in time. Reference 6 tabulates $b_i(n, \alpha)$ for $n = 2, 3, 4$ and $\alpha = 0, \frac{1}{1000}$, and $\frac{1}{300}$. When $\alpha = \frac{1}{1000}$, the b_2 correction becomes relatively large. In fact, for

$$\alpha = \alpha_R = \frac{(n^2+1)(\alpha_R n^2+1)}{4n^2(n^2-1)^2} = \frac{(n^2+1)}{n^2(4n^4-9n^2+3)} \tag{7.7}$$

the correction term becomes <u>infinite,</u> and the solution breaks down. At the value of α given by (7.7), $S(w_o)$ causes a resonance in equation (7.4) and the corresponding w_1 becomes unbounded. Clearly, the approximation made in going from (7.2) to (7.3), namely

$$S(\omega_1 + \omega_0) \cong S(\omega_0) \tag{7.8}$$

is not valid when the magnitude of w_1 exceeds that of w_o. Even when the maximum amplitude of w_1 is less than that of w_o, (7.8) may be questionable. For example, when $\alpha > \alpha_R$, (7.5) indicates that the ring expands (instead of contracting) as it vibrates. On physical grounds, this would seem to be incorrect.

As regards the constant term, $(\frac{A}{h})^2 \quad \frac{n^2 h}{8R}(1 - \frac{1}{n^2})^2$, one might note that it is impossible to satisfy (6.1) up to $0(\frac{A^2}{R^2})$ without including it. This suggests that Federhofer has neglected a quadratic term in his analysis. Comparing the results for $v(y,t)$ confirms this. Finally, the method of solution used in reference 6 does not provide any information about changes in frequency as the ring vibrates to large amplitudes - i.e., one cannot plot A vs. ω. Nevertheless, the solution does exhibit the $\cos 2\omega t$ contraction at the nodes of $\cos \frac{ny}{R}$.

Shkenev, (Ref. 7), studied both free vibrations and parametric excitation of a ring. He apparently neglects tangential inertia, and the ring is assumed to vibrate inextensionally:

$$\varepsilon_{yy}\Big|_{z=0} = \frac{\partial v}{\partial y} + \frac{w}{R} + \frac{1}{2}\left(\frac{\partial w}{\partial y}\right)^2 = 0 \tag{2.7}$$

Both w and v are assumed; in the notation of the present work, they are

$$w(y,t) = A_n(t)\cos\frac{ny}{R} \tag{7.9}$$

$$v(y,t) = -\frac{A_n}{n}\sin\frac{ny}{R} + \frac{nA_n^2}{8R}\sin\frac{2ny}{R} \qquad (7.10)$$

Note, however that (7.9) and (7.10) are incompatible with (2.7); (see Section 2.2.1a). For free vibrations, reference 7 gives

$$\ddot{A}_n + \omega^2 A_n + cA_n^3 + aA_n(A_n\ddot{A}_n + \dot{A}_n^2) = 0 \qquad (7.11)$$

which is similar to

$$\ddot{A}_n + \omega_n^2 A_n + \frac{\epsilon}{2}A_n(A_n\ddot{A}_n + \dot{A}_n^2) = 0 \qquad (7.12)$$

of the present work (inextensional, one bending mode), where

$$w(y,t) = A_n(t)\cos\frac{ny}{R} - \frac{n^2A_n^2}{4R} \qquad (2.8)$$

Since (7.9) does not allow the ring to contract as it vibrates, (7.11) is in error. Consequently, one finds

$$\frac{a}{\epsilon/2} = \frac{1}{16(n^2+1)} << 1$$

McIvor and Goodier (Ref. 8) study the response of a ring that is subjected to a uniform radial impulse. The "thin ring" assumption ($\frac{h^2}{R^2} << 1$) is made, and tangential inertia is included. By comparing some inextensional and extensional linear vibration problems, they observe the results to be nearly equal when the inequality

$$\frac{n^2h^2}{12R^2} << 1$$

is met. This leads them to consider the non-linear response problem in which the flexural modes vibrate inextensionally. However, these modes are required to satisfy a linear inextensionality condition

$$\frac{\partial v}{\partial y} + \frac{w}{R} = 0$$

rather than the non-linear one:

$$\frac{\partial v}{\partial y} + \frac{w}{R} + \frac{1}{2}\left(\frac{\partial w}{\partial y}\right)^2 = 0 \qquad (2.7)$$

This discrepancy does not invalidate the dynamic stability analysis of reference 7 (since it is done for small amplitudes), but the "long term equations" are in error.

2.7.2 Some Comments on the Non-Linear Vibration of Axisymmetric Systems

The non-linear vibrations of many axisymmetric systems (such as a ring) possess several features in common. With the assumption that the motion involves primarily one or two vibration modes, it is possible to reduce the problem to one involving non-linear ordinary differential equations. In the event that only one mode is vibrating (near its linear resonant frequency), one can show that above a certain critical amplitude the companion mode begins to participate in the motion. The companion mode is excited parametrically, via the non-linear coupling terms. This phenomenon is not restricted to axisymmetric systems, but it occurs in such cases since the natural frequencies of the driven mode and its companion are identical. In the following paragraphs, a few such examples are discussed.

One of the simplest systems to exhibit this behavior is a string. Let the vertical deflection be given by

$$v(x,t) = A(t) \sin \frac{m\pi x}{L}$$

and the horizontal by $h(x,t) = B(t) \sin \frac{m\pi x}{L}$. After various approximations and non-dimensionalizing, the string equations become

$$\ddot{A} + A + \epsilon A(A^2 + B^2) = F \cos \Omega \tau \tag{7.13a}$$

and

$$\ddot{B} + B + \epsilon B(A^2 + B^2) = 0 \tag{7.13b}$$

where ϵ is the non-linearity parameter, and the vertical motion is being forced harmonically. A possible solution to (7.13) is

$$\begin{aligned} A(\tau) &= \bar{A} \cos \Omega \tau \\ B(\tau) &= 0 \end{aligned} \tag{7.14}$$

When the stability of this solution is analyzed, one finds it to be unstable if $\bar{A} > A_{CR}(\Omega, \epsilon)$, where the critical amplitude depends on Ω and ϵ. For $\bar{A} > A_{CR}$, a solution of the form

$$\begin{aligned} A(\tau) &= \bar{A} \cos \Omega \tau \\ B(\tau) &= \begin{Bmatrix} \bar{B} \sin \Omega \tau \\ \bar{B} \cos \Omega \tau \end{Bmatrix} \end{aligned} \tag{7.15}$$

is suggested. As in the case of the ring, the "in-phase" solution

$$\begin{aligned} A(\tau) &= \bar{A} \cos \Omega \tau \\ B(\tau) &= \bar{B} \cos \Omega \tau \end{aligned}$$

will not satisfy the differential equations of the problem: (7.13). Thus, one has

$$A(\tau) = \bar{A} \cos \Omega\tau$$
$$B(\tau) = \bar{B} \sin \Omega\tau \qquad (7.16)$$

as the solution, and the string "whirls". This is analogous to the appearance of travelling waves for the ring.

Equations similar to (7.13) result for the non-linear vibration of circular rods that are constrained longitudinally. The problem of a string (or a circular rod) with a concentrated mass on the end and having constant applied tension gives

$$\ddot{A} + A + \epsilon A(A\ddot{A} + \dot{A}^2 + B\ddot{B} + \dot{B}^2) = F\cos\Omega\tau \qquad (7.17a)$$

$$\ddot{B} + B + \epsilon B(B\ddot{B} + \dot{B}^2 + A\ddot{A} + \dot{A}^2) = 0 \qquad (7.17b)$$

which are identical in form to the equations for a ring! The non-linear vibration of a long, pressurized cylindrical membrane (no axial variation) also results in (7.17), where the deflection of the membrane is

$$w(\theta,t) = A_m(t)\cos m\theta + B_m(t)\sin m\theta - \frac{m^2}{4R}(A_m^2 + B_m^2)$$

For thin cylindrical shells, a deflection of the form

$$w(x,y,t) = A_m(t)\cos\frac{ny}{R}\sin\frac{m\pi x}{L}$$
$$+ B_m(t)\sin\frac{ny}{R}\sin\frac{m\pi x}{L} - \frac{m^2}{4R}(A_m^2+B_m^2)\sin^2\frac{m\pi x}{L} \qquad (7.18)$$

seems appropriate, and the following equations result*:

---

* See reference 25.

$$\ddot{A}_n + A_n + \frac{3\eta^2}{8} A_n (A_n \ddot{A}_n + \dot{A}_n^2 + B_n \ddot{B}_n + \dot{B}_n^2)$$

$$+ \alpha_1 A_n (A_n^2 + B_n^2) + \alpha_2 A_n (A_n^2 + B_n^2)^2 \qquad (7.19a)$$

$$= F \cos \omega t$$

$$\ddot{B}_n + B_n + \frac{3\eta^2}{8} B_n (B_n \ddot{B}_n + \dot{B}_n^2 + A_n \ddot{A}_n \qquad (7.19b)$$

$$+ \dot{A}_n^2) + \alpha_1 B_n (A_n^2 + B_n^2) + \alpha_2 B_n (A_n^2 + B_n^2)^2 = 0$$

Here, $\eta = \frac{n^2 h}{R}$, and α_1 and α_2 depend on ξ, where $\xi = (\frac{m\pi/L}{n/R})$. As $L \to \infty$, $\xi \to 0$ and α_1, $\alpha_2 \to 0$. Thus, (7.19) then becomes similar to the inextensional ring equations, but with $\frac{3\eta^2}{8}$ in place of $\frac{\eta^2}{2}$.

Many other axisymmetric systems exist; in general, any axisymmetric elastic body can exhibit similar behavior. The non-linear vibration of circular discs (studied extensively by Tobias, Refs. 26 and 27) is a very good example. The forced oscillations of a spherical pendulum (Ref. 29) and sloshing of a liquid in a circular tank (Ref. 30) are others.

The present analysis seems to fit nicely within the general results common to non-linear vibrations of axisymmetric systems. Previous studies (Refs. 6 - 8) on the non-linear vibration of rings appear to contain certain shortcomings which cause them to disagree with both the theory and experiments presented herein.

III. THE EXPERIMENTAL PROBLEM

Many aspects of the preceding analysis should be readily observable experimentally. If these salient features are not detected, both theory and experiment must be reexamined.

Preliminary tests indicated (a) the jump phenomena and a slight non-linearity of the "softening" type, (b) the presence of the double frequency term at the nodes of $\cos \frac{ny}{R}$, (c) several ultra-harmonic responses, and (d) at certain combinations of amplitude and frequency, the "single bending mode" approximation was inadequate. The latter observation prompted a study of the "self-coupled bending modes", which successfully explained the experimental results.

The initial tests were followed by a more refined experimental program. It had two main objectives, namely (1) to determine the extent to which the theory and experiments agreed quantitatively, and (2) to measure the actual deflection shape of the vibrating ring. These experiments led to analytical consideration of the "additional non-linearities" and a subsequent improvement in the results. Measurement of the actual vibration form demonstrated the validity of the mode shapes which were assumed in the analysis.

The calculated response and the measured values were generally found to be in good agreement. In retrospect, it seems that the main benefit derived from the experiments was that they served as an independent check on the analysis and motivated significant improvements in it.

3.1. Description of the Experimental Set-Up

The ring used for these experiments was formed by an electroplating process in the same manner as the thin cylinders of reference 31. It was 8 inches in diameter, had an average thickness of 5.14×10^{-3} inches, and an average length of 0.988 inches. Based upon tests which were done in connection with cylinder specimens, the material properties of the copper were taken to be

E = Young's modulus = 16×10^6 lb/in^2

ρg = weight density = 0.322 lb/in^3

ν = Poisson's ratio = 0.3

The ring was suspended by four very thin threads, equally spaced around the circumference, as shown in Fig. 8.

Two inductance-type pickups were operated in a push-pull arrangement to measure the deflections. They were supported on a fixture with a large bearing that permitted them to travel circumferentially around the ring. (see Figs. 9 and 10). The signal from each pickup was fed through a carrier amplifier and into one side of a differential amplifier; its output was in turn sent through a band-pass filter to a cathode ray oscilloscope. (A block diagram is given in Fig. 11). This arrangement resulted in an anti-symmetric operating characteristic for the system, which was highly desirable.

For instance, if one were to represent a characteristic such as Fig. 12 in a power series, he would have

$$V = a_1 \delta + a_2 \delta^2 + a_3 \delta^3 + \cdots \qquad (8.1)$$

where V is the output voltage, δ is the displacement seen by the system, and a_i are the coefficients of the power series. If the displacement is sinusoidal in time, the output voltage will contain higher harmonics, due to the non-linearity of the system. That is, for $\delta = \delta_1 \sin\omega t$, the voltage is

$$V(t) = (a_1\delta_1 + \frac{3}{4}a_3\delta_1^3)\sin\omega t + \frac{a_2\delta_1^2}{2}(1 - \cos 2\omega t) - \frac{a_3\delta_1^3}{4}\sin 3\omega t + \cdots$$

Thus, if one attempts to measure a non-linear displacement such as $\delta = \delta_1 \cos\omega t + \delta_2 \cos 2\omega t + \delta_3 \cos 3\omega t$, he will find it difficult to determine the magnitude of δ_2 and δ_3. (In general, $a_1\delta_1 >> a_2\delta_1^2$, $a_3\delta_1^3$ etc., and δ_1 can be found fairly accurately.) To eliminate such "harmonic distortion" altogether, one needs a perfectly <u>linear</u> pickup system, which is difficult to obtain. On the other hand, it <u>is</u> possible (theoretically) to eliminate the even order harmonics with a system having an anti-symmetric characteristic; this led to the pickup arrangement used herein.

Vibrations of the ring were excited by oscillating a fine tungsten wire (0.001" dia.) that was attached to it, as shown in Figs. 8 and 10. A standard electrodynamic shaker was used to drive the wire, with the latter serving as a soft coupling spring between the shaker and the ring. The shaker amplitude and frequency were controlled by a standard oscillator-amplifier arrangement. (see Fig. 11). By recording the displacement of the shaker and knowing the spring constant of the wire, it was possible to compute the force acting on the ring.

For example, consider a simple model of the ring-spring system,

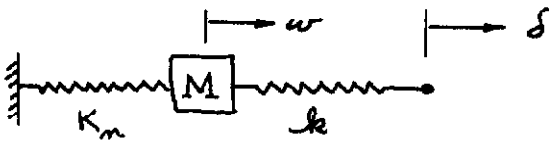

in which M = $\rho\pi Rhb$ = one-half the mass of the ring,

K_n = $M\omega_{mn}^2$ = the stiffness of the ring when vibrating in the nth mode

k = the stiffness of the spring that couples the ring to the shaker

δ = the displacement of the shaker

w = the small amplitude radial displacement of the ring.

The equation of motion of the system is

$$M\ddot{w} + M\omega_{mn}^2 w = F(t) = k(\delta - w) \tag{8.2}$$

where the force exerted by the coupling spring is approximated by

$$F(t) = k(\delta - w) \tag{8.3}$$

With the shaker displacement $\delta = \delta_o \cos\omega t$, (8.2) can be rearranged to read

$$\ddot{w} + (\omega_{mn}^2 + \frac{k}{M})w = \frac{k\delta_o}{M}\cos\omega t = F(t) \tag{8.4}$$

Thus, it is apparent that the force input to the ring can be determined by knowing k, δ_o, and M. It is also evident that the coupling spring

constrains the ring and will affect the natural frequency of the system. Finally, (8. 3) is valid only for a spring which (a) is perfectly linear, and (b) has a high resonant frequency.

To avoid exerting a large constraint on the ring, one requires

$$\frac{k/M}{\omega_{mn}^2} << 1 \tag{8. 5}$$

which means using a very soft coupling spring. But, to neglect the inertia of the spring itself in writing (8. 3) necessitates

$$\omega^2 << \frac{k}{M_{SP}} \tag{8. 6}$$

where M_{SP} is the effective mass of the spring in its first vibration mode and ω is the frequency of the motion which is being transmitted to the ring. Unfortunately, the preceding requirements tend to conflict with one another; i. e., soft springs tend to have low resonant frequencies.

To get around this problem, the tungsten drive wire was devised. The wire that was used in the experiments gave k = 0. 035 lb/in and had a first resonant frequency of 300 cps; this resulted in

$$\frac{k/M}{\omega_{mn}^2} = 0.008 \quad \text{AND} \quad \frac{\omega^2}{k/M_{SP}} = 0.01$$

for the mode which was studied in detail. To make the coupling spring as linear as possible, the system was designed such that (a) the deflections of the wire were much less than its length, and (b) the initial tension applied to the wire was very high.

The analysis of the ring was carried out with the assumption of a "monochromatic" forcing function - $F(t) = F \cos \omega t$. However, the force which was experimentally applied to the ring actually contained several frequencies. This harmonic distortion of the input arose from two main sources:

(1) the output displacement of the shaker itself contained higher harmonics as well as $\cos \omega t$, and

(2) the drive wire introduced harmonics, since it was a non-linear spring.

It was possible to determine the distortion in the shaker output by using a harmonic analyzer to examine the output voltage of the signal generating coil*. The shaker displacement was found to be

$$\delta = \delta_1 [\cos \omega t + 0.03 \cos 2\omega t + 0.01 \cos 3\omega t] \quad (8.7)$$

for $\delta_{max} = 0.2$ inches (the maximum employed). The harmonics introduced by the non-linear drive wire can be estimated from its static calibration curve, Fig. 13. The force generated by the wire was approximately

$$F(t) = \frac{k \delta_1}{2} [\cos \omega t + 0.02 \cos 3\omega t]$$

(k is the spring constant, and the geometry of Fig. 13 has been used)

---

* The shaker was equipped with a signal generating coil which produced a voltage proportional to the velocity of the armature.

for a pure harmonic displacement $\delta = \delta_1 \cos\omega t$ and $\delta_1 = 0.15$ inches. Combining these effects, the force exerted on the ring by the wire may be expressed as

$$F(t) = \frac{k\delta_0}{2}\left[\cos\omega t + b_2 \cos 2\omega t + b_3 \cos 3\omega t + \cdots\right]$$

where b_2 and b_3 depend non-linearly on δ_0, and $|b_2|_{max} \cong 0.033$, $|b_3|_{max} \cong 0.030$ for the experiments described herein. Note $|b_2|, |b_3| << 1$, which means that the input forcing function was quite "clean".

Both the displacement pickup and the forcing function are a source of extraneous non-linearities; such effects must be examined if the data to be obtained on non-linear ring vibrations is to have much significance. In addition, one must consider the non-linearities which arise from the manner in which the ring was constrained by the drive wire and suspension system.

When the equation analogous to (8.2) is written down for large displacements of the ring, one has

$$\begin{aligned} &y_{\tau\tau} + (1+K_1)\,y + \frac{\eta^2}{2}\,y\,(y\,y_{\tau\tau} + y_\tau^2) \\ &+ \frac{\eta y}{2} K_1 \left(\frac{\delta_0}{2h}\right)\cos\Omega\tau + \underline{\frac{\mu\eta}{2}\,(y\,y_{\tau\tau} + y_\tau^2)} \\ &\underline{-\frac{3\eta K_c}{4}\,y^2} + \underline{\frac{K_c\eta^2}{8}\,y^3} = K\left(\frac{\delta_0}{2h}\right)\cos\Omega\tau \end{aligned} \tag{8.8}$$

where the deflection has been taken as

$$w(y,t) = A_m(t)\cos\frac{my}{R} - \frac{m^2 A_m^2}{4R}$$

the shaker displacement as $\delta = \delta_0 \cos\omega t$, the effect of the

constraints has been included, and the following non-dimensional parameters have been used*:

$$\tau = \omega_{nn} t \qquad \Omega = \frac{\omega}{\omega_{nn}} \qquad \gamma = \frac{A_n}{h}$$

$$K_1 = \frac{k_2/M}{\omega_{nn}^2} = \frac{k_2}{(\pi R \rho h b)\omega_{nn}^2} \qquad K_2 = \frac{k_s/M}{\omega_{nn}^2}$$

$$K_c = K_1 + K_2 \qquad \mu = \frac{m_s}{M}$$

Putting

$$K_1\left(\frac{\delta_0}{2h}\right) = G = \frac{F}{(\pi R \rho h b) h \omega_{nn}^2}, \quad \text{i.e.} \quad \frac{k\delta_0}{2} = F$$

and recalling that $K_1 << 1$, one sees that (8.8) is equivalent to (3.4) (one mode, inextensional) except for the terms which are underlined. Nevertheless, an analysis of (8.8) demonstrates that its solution is practically identical to that of (3.4). For example, using the method of averaging on (8.8) with $\gamma(\tau) = A(\tau)\cos\Omega\tau + C_0(\tau)$ gives $\bar{C}_0 \cong \frac{3\eta K_c}{8}\bar{A}^2$ and a "backbone curve" of

$$\Omega = 1 - \frac{\eta^2 \bar{A}^2}{8}\left[1 - \frac{3K_c}{8} + \frac{9K_c^2}{4}\right] + O(\eta^4) \qquad (8.9)$$

vs. $\Omega = 1 - \frac{\eta^2 A^2}{8} + O(\eta^4)$ for (3.4). Since $K_C \leq 0.012$, it is apparent that the effect of the additional non-linear terms in (8.8) is very small, at least in the vicinity of resonance. Their presence is felt mainly near $\Omega = \frac{1}{2}$, but even then the effect is slight.

---

* (k_s, m_s are the stiffness and mass associated with the suspension system).

Similarly, one can show that the stability of the solutions is virtually unaffected by such terms.

The preceding paragraphs demonstrate that the experimental arrangement corresponded quite closely to the theoretical problem analyzed in Section 2. 5. 2b. This agreement was borne out throughout the experimental program, which is outlined in the next section.

3. 2. Steady-State Response

Preliminary tests were conducted with the ring suspended from the ceiling on long threads and with a soft coil spring in place of the tungsten drive wire. These tests demonstrated the basic features of the response, including the appearance of the "self-coupled" bending modes. Their presence was detected by the use of Lissajous figures, as follows.

The voltage proportional to the radial deflection of the ring was fed into the vertical axis of the oscilloscope, with the horizontal axis being driven from the oscillator which controlled the shaker. The resulting Lissajous figure indicated the amplitude and the phase (relative to the input force) of the vibration at that point on the ring. By moving the pickup around the circumference of the ring and noting the Lissajous figures, it was possible to detect which modes were present.

For example, when primarily a single bending mode responded (near resonance) one saw the Lissajous patterns shown in the top half of Fig. 14. The open vertical ellipses indicate a response that is $\pm 90^{\circ}$ out of phase with the forcing function (resonance) and the

horizontal figure eights demonstrate the double frequency contraction at the nodes of $\cos \frac{ny}{R}$. The amplitude of A was measured at the antinode and the amplitude of $(A_o)_{2\omega}$ at the "nodes" of $\cos \frac{ny}{R}$.

The appearance of the companion mode ($\sin \frac{ny}{R}$) occurred near resonance of $\cos \frac{ny}{R}$ and resulted in the lower pattern in Fig. 14. The vertical ellipses at the antinodes of $\cos \frac{ny}{R}$ indicate that it is $\pm 90^{\circ}$ out of phase with the input. The lines at the antinodes of $\sin \frac{ny}{R}$ demonstrate that it is directly in (or out) of phase with the input, which means that $\sin \frac{ny}{R}$ is $\pm 90^{\circ}$ out of phase with its companion mode. A pattern such as Fig. 14 (b) can be produced by a deflection of the form*

$$w(y,t) = \bar{A}\cos(\omega t + \bar{\phi})\cos\frac{ny}{R} + \bar{B}\sin(\omega t + \bar{\psi})\sin\frac{ny}{R} \quad (8.10)$$

Other combinations of modes are at variance with the experimental results. The amplitude A was measured at the antinodes of $\cos \frac{ny}{R}$, and the amplitude of B at the nodes of $\cos \frac{ny}{R}$. As further evidence that a deflection of the form (8.10) was correct, travelling waves were detected with the aid of a strobotach when Lissajous patterns such as Fig. 14 (b) were observed.

The exploratory tests were concluded after noting the linear (small amplitude) vibration frequencies and many ultra- and sub-harmonic responses of the ring; (see Table I). The forcing frequency in these tests was determined by an electronic counter which monitored the output frequency of the oscillator.

---

* The contraction term, $\frac{n^2}{4R}(\bar{A}^2 + \bar{B}^2)$, has been omitted from (8.10) since it has little effect on the Lissajous figures when the coupled modes are present.

When the preliminary set-up was replaced with the improved arrangement of Fig. 9, it was possible to obtain response curves which could be compared with the analysis. The apparatus was designed to investigate the $n = 4$ mode in particular; thus the drive wire and suspension threads were arranged such that the former was at an antinode and the latter at four nodes of $\cos \frac{4y}{R}$.

Typical response curves for this set-up are shown in Fig. 15. The A values were measured at one antinode of $\cos \frac{ny}{R}$, and the $(A_o)_{2\omega}$ and B values at an adjacent node. The amplitude of the input force was held constant for the response curves of Fig. 15; this was accomplished by maintaining a known, constant peak-to-peak displacement ($2\delta_o$) of the shaker throughout each run. The force itself was calculated from $F = \frac{k\delta_o}{2}$. An electronic counter was used to measure the frequency of the forcing function at each data point; these values were then non-dimensionalized on the linear frequency, which was known from prior tests.

Having measured $(\frac{\omega}{\omega_L})$ and F, and knowing η, M, and β^*, one can compute the theoretical response, using (3. 50) and (6. 9). The calculated values are shown in Fig. 15 by the solid lines.

A notable discrepancy between the response curves of Fig. 15 and the preliminary experiments was immediately apparent: the improved set-up had altered the "jump" phenomena! Now the ring

---

* The damping was determined from amplitude decay measurements; see Section 3. 3, "Some Transient Responses".

jumped from one mode ($\cos \frac{ny}{R}$, low amplitude) to two modes ($\sin \frac{ny}{R}$, $\cos \frac{ny}{R}$); previously it had remained in one mode when it jumped. The cause of this behavior was found to be the drive wire.

By constraining the $\cos \frac{ny}{R}$ mode but not $\sin \frac{ny}{R}$, it had raised the effective natural frequency of the former and left the latter unchanged. This creates an overlapping of two instability regions (see Fig. 16) and leads to the observed results. It was possible to obtain the "standard" jumps found previously, by (a) adding concentrated viscous damping in the $\sin \frac{ny}{R}$ mode, thus modifying its instability region, or (b) adding a small, concentrated mass to an antinode of $\cos \frac{ny}{R}$, which lowered its natural frequency and separated the unstable regions (see Fig. 16).

Adding the mass had another beneficial effect, as it greatly reduced the tendency of the nodes to "drift" circumferentially. Such shifting of the nodes can be explained by considering small imperfections in the ring (variations in thickness, material properties, etc.) as was pointed out by Tobias (Ref. 28). The added mass was a short piece of solder, (it weighed 0.26 grams, vs. 18.62 grams for the entire ring) and it was glued to the ring directly alongside the drive wire. This arrangement fixed the two "preferential modes" of the ring (see Ref. 28) while simultaneously insuring that the forcing function would directly drive only one of them.

Four response curves were run on the $n = 4$ mode with the added mass; the results are shown in Fig. 17. (Again, the solid lines represent the theoretical results, where ϵ_c has been used; see (6.9)). A, B, and $(A_o)_{2\omega}$ were measured as in the previous tests.

The phase of the signal at the antinode was measured with a standard phase meter. The electronic counter was set up to measure the period of the input signal (rather than the frequency) in these tests. This enabled $\frac{\omega}{\omega_L}$ to be determined more accurately than previously*.

As seen from Fig. 17 a-e, the calculated results agree fairly well with the measured values. On a frequency basis, Fig. 17 e shows a difference of less than 1 per cent between theory and experiment, and the "backbone curves" of Fig. 17 a-d also show good correlation. The results seem to agree less well for the higher amplitudes; this may be due to the non-linearity of the displacement pickup. (The voltage measurements of A, B. etc. were converted to displacements by using the linear gain factor of Fig. 12).

Figure 17 f shows qualitative agreement with the theory, but the experimental data differ by 30 per cent from the improved analysis (which includes the "additional non-linearities"). However, it should be noted that 10 units on the vertical scale of Fig. 17 f represent a displacement of 0.001". An error of 0.001" in the measurement of $(A_o)_{2\omega}$ could account for the 30 per cent discrepancy noted above. Since 2ω for the $n = 4$ mode is equivalent to 66 cps, a possible source of error might have been the 60 cycle "noise" present in the electronics.

---

* For example, the counter would give the period of the wave as 0.030280 + 0.000010, with drift in the electronics accounting for the slight variations in period.

An approximate determination of the instability boundaries for the companion mode can be made by extrapolating the steepest part of the B/h vs. $\frac{\omega}{\omega_L}$ curves onto the horizontal axis. This gives an estimate of the $\frac{\omega}{\omega_L}$ value at which the companion mode goes unstable; the corresponding amplitude of the driven mode can then be found from A vs. $\frac{\omega}{\omega_L}$. The resulting instability boundaries are shown in Fig. 18; attempts to determine these boundaries directly by experiment were unsuccessful. The other instability region - bounded by the locus of vertical tangents - is also given in Fig. 18.

Similar responses, jumps, and instabilities were noted in other modes as well as n = 4; some results for the n = 3 mode are given in Fig. 19.

The mode shapes were measured by exciting one mode (n = 4) and recording the amplitude at known positions along a half-wave length. Measurements were made at several amplitudes, on two half-waves; the results are shown in Fig. 20, where the solid lines are the assumed deflection shape.

The response voltage from the pickup system can be represented as a Fourier series in time

$$V(y,t) = f_1(y)\cos\omega t + f_2(y)\cos 2\omega t + f_3(y)\cos 3\omega t + \cdots$$

with coefficients that vary around the circumference of the ring. The coefficients, $f_1(y)$, $f_2(y)$, etc. contain the spatial variation of the deflection shape combined with the harmonics introduced by the pickup system. As shown by Fig. 20, $f_1(y)$ is very nearly $A \cos \frac{ny}{R}$. By passing the deflection signal through the harmonic analyzer and using

a narrow (2 cps band width) filter, it was possible to determine the circumferential variation of the first, second and third harmonics in the signal. The results are given in Fig. 21; the higher harmonics contain the influence of non-linearities in the displacement pickup, despite efforts to avoid them.

It was thus impossible to determine the true spatial variation of the $\cos 2\omega t$ term of the deflection, but Fig. 21 does suggest a major component that is constant in space. Furthermore, Figs. 20 and 21 indicate that (6.8) is a good approximation to the deflection, which would account for the presence of just such a uniform second harmonic component. The perturbation calculations suggest that $A_n(t)$ itself contains some double frequency terms (which would vary as $\cos \frac{ny}{R}$ in space) but their presence could not be confirmed experimentally.

The close agreement shown in Fig. 20 indicates that the main motion of the ring (when vibrating in a single mode) was of the form $A \cos \frac{ny}{R} \cos \omega t$. This conclusion is supported by Fig. 21, which also suggests that the bulk of the third harmonic in the response signal was generated by non-linearity in the displacement pickup.

In addition to the close examination of particular half-waves of the vibration mode, the root-mean-square response was plotted for three-fourths of the ring's circumference. Results were obtained for four different amplitudes; Fig. 22 is typical. Some non-uniformity in the mode shape was apparent, with two antinode peaks varying 10 - 15 per cent from the mean antinode response. Anomalies of this type

might be the result of circumferential variations in thickness, material properties, pickup spacing, etc.

3. 3. Some Transient Responses

Although the bulk of the experimental work was concerned with the steady-state response of the ring, some transient motions were also of interest. For example, it was possible to observe the growth of the companion mode as it went unstable or the decay of the vibrations due to damping.

To accomplish the former, the excitation was adjusted such that the long time (steady-state) response would involve the vibration of both $\cos \frac{ny}{R}$ and $\sin \frac{ny}{R}$. Then a switch box was inserted in the system, allowing one to simultaneously turn on the excitation to the ring and trigger the sweep of the oscilloscope. To obtain the transient response of the $\sin \frac{ny}{R}$ mode, the pickup was fixed at a node of $\cos \frac{ny}{R}$. When the excitation was suddenly switched on, the oscilloscope recorded the amplitude of the former, showing that it grew rapidly at first and then levelled off to the steady-state value. The initial growth was much like an exponential increase, as is predicted by stability theory; for large amplitudes, the non-linearity of the ring (and the damping) limit the response.

In a similar fashion, the transient response of $\cos \frac{ny}{R}$ and of the shaker (velocity) were obtained, for the same excitation setting. Typical results are shown in Fig. 23, which points out that the shaker and the $\cos \frac{ny}{R}$ mode responded rapidly to the excitation. As $\sin \frac{ny}{R}$ began to vibrate, it took energy from its companion mode, which

caused the amplitude of $\cos \frac{ny}{R}$ to dip slightly. (see Fig. 23). The low frequency ripples in the amplitudes occurred because the rigid body mode of the system was excited by the shaker start-up.

Using a similar arrangement, but triggering the scope as the excitation was switched off, damping traces for the $n = 3$ and $n = 4$ modes were obtained. Some typical traces are shown in Fig. 24, which points out that the damping is amplitude dependent - i. e., non-linear. Damping in the $n = 3$ mode ranged from $\beta = 0.008$ to $\beta = 0.003$ in going from high to low amplitudes; similarly, β for $n = 4$ ranged from 0. 002 to 0. 001. Note that these values contain the damping effects exerted on the ring by the drive and suspension system. The slight beating in Fig. 24 is again due to excitation of the rigid body mode.

3. 4. Other Results of Interest

The $n = 4$ mode was investigated in detail for reasons of experimental convenience. The response of several other modes and combinations of modes was also observed, as shown in Table I. It will be noted that in addition to the "standard" ultraharmonic responses where a single mode is excited, Table I contains coupled responses where one mode vibrates at the driving frequency and another mode at some multiple thereof. Such motions were readily detected by use of the harmonic analyzer; the analysis indicated these responses might occur. (see Section 2. 5. 2).

Finally, since this work originated with a study of non-linear cylindrical shell vibrations, it is of interest to report that recent

experiments on cylinders (Ref. 32) have demonstrated many of the phenomena noted here. In particular, the softening type non-linearity and the double frequency contraction at the nodes have been detected.

IV. CONCLUDING REMARKS

The similarity of the analytical results for a single bending mode suggests that the main features of the non-linear flexural vibrations of thin rings can be obtained by using an "inextensional" theory. This information can be applied to greatly simplify the analysis of vibrations in which several bending modes participate. For example, an inextensional study of the "self-coupled" bending modes demonstrates that the single mode solution is valid only for certain combinations of amplitude and frequency. Thus, when the single (driven) mode exceeds a "critical amplitude", its companion mode becomes excited and participates in the motion.

Examination of the "general inextensional case" (involving an infinite number of modes) shows that possible solutions are (a) vibration of primarily a single bending mode, and (b) vibration of primarily the "self-coupled" modes. Furthermore, a stability analysis of these solutions indicates that when certain restrictions are met, all other bending modes play only a minor role in the vibrations.

Significant improvement in the analysis is obtained by including the effect of "additional non-linearities" in the strain-displacement relations. Retaining the effect of tangential inertia also improves the calculations, but to a lesser extent. Both these modifications lose their importance as the mode number increases; however, they combine to decrease the non-linearity parameter (ϵ) by more than 25 per cent for the $n = 4$ mode.

The experiments are in generally good agreement with the analysis, both qualitatively and quantatively. Early tests exhibited the jump phenomena, a non-linearity of the "softening" type, double frequency contraction at the nodes, ultraharmonic responses, and the appearance of the companion mode. Subsequent improved experiments showed the measured responses to be in good agreement with the calculated values. Similarly, measurements of the mode shape (for a single mode) and of the contraction at the nodes indicate the appropriateness of the assumed deflection form. Experimental damping traces point out that the damping is amplitude dependent; this is substantiated by the steady-state response curves. Consequently, to calculate response curves that agree with the measured values, (including the maximum amplitude) one must know the damping which is appropriate for that amplitude.

In conclusion, it seems that the basic approach presented here is applicable to the non-linear vibration of thin cylindrical shells, as well as many other axi-symmetric systems. First, the system is assumed to vibrate in primarily a single mode, and its behavior is examined. Then, the vibration of "self-coupled" modes must be considered, since the non-linear coupling tends to excite the companion mode. If possible, the vibration of an infinite number of modes should be studied and a stability analysis done to determine the validity of the one and two-mode solutions. Finally, as the theoretical results become available, their main features should be subjected to experimental confirmation.

In some cases, it will become apparent that these restricted analyses are useful only for relatively small amplitudes and that an adequate study must involve additional modes. On the other hand, the study of primarily one and two modes is sufficient to explain a great deal about the non-linear vibrations of rings, and similar analyses will undoubtedly prove worthwhile in many related problems.

REFERENCES

1. Hoppe, R., Vibrationen eines Ringes in seiner Ebene, J. Math. (Crelle) Vol. 73, (1871).
2. Strutt, J. W., The Theory of Sound, Second Edition, (1945) Dover, New York.
3. Philipson, L. L., On the Role of Extension in the Flexural Vibrations of Rings, J. Applied Mech., Vol. 23, (September 1956), pp. 364-366.
4. Buckens, F., Influence of the Relative Radial Thickness of a Ring on its Natural Frequencies, J. Acoust. Soc., Vol. 22, No. 4, (July 1950), pp. 437-443.
5. Federhofer, K., Biegungsschwingungen eines Kriesringes bei konstantem Aussen-oder Innendrucke, Ing. - Archiv, Vol. 4, (1933), pp. 110-120.
6. Federhofer, K., Nicht-lineare Biegungsschwingungen des Kreisringes, Ing.- Archiv, Vol. 28, (1959), pp. 53-58.
7. Shkenev, Yu. S., Non-Linear Vibrations of Circular Rings, Inzhener Sbornik, Vol. 28, (1960), Akad Nauk SSSR, pp. 82-86 (In Russian).
8. McIvor, I. K., and Goodier, J. N., Dynamic Stability and Non-Linear Oscillations of Cylindrical Shells (Plane Strain) Subjected to Impulsive Pressure, Stanford Univ. Tech. Rept. No. 132, Division of Eng. Mech. (June 1962).
9. Kaiser, E. R., Acoustical Vibration of Rings, J. Acoust. Soc., Vol. 25, No. 4, (July 1953), pp. 617-623.

10. Lang, T. E., Vibration of Thin Circular Rings, Tech. Rept. No. 32-261, Jet Prop. Lab., Calif. Inst. of Tech., Pasadena, Calif. (July 1962).

11. Reissner, E., Non-Linear Effects in the Vibration of Cylindrical Shells, Aeromechanics Rept. No. 5-6, Ramo-Wooldridge Corp. (September 1955).

12. Chu, H., Influence of Large Amplitudes on Flexural Vibrations of a Thin Circular Cylindrical Shell, J. Aero-Space Sci., Vol. 28, No. 8, (August 1961), pp. 602-609.

13. Cummings, B. E., Some Non-Linear Vibration and Response Problems of Cylindrical Panels and Shells, Doctoral Thesis, California Institute of Technology (1962).

14. Evensen, D. A., Some Observations on the Non-Linear Vibration of Thin Cylindrical Shells, AIAA Journal, Vol. 1, No. 12, (December 1963), pp. 2857-2858.

15. Morley, L. S. D., An Improvement on Donnell's Approximation for Thin-Walled Circular Cylinders, Quart. J. Mech. and Applied Math., Vol XII, Pt. 1, (1959), pp. 89-99.

16. Singer, J., On the Equivalence of the Galerkin and Rayleigh-Ritz Methods, J. of the Royal Aero., Soc., Vol. 66, (Sept. 1962), p. 592.

17. Houghton, D. S., and Johns, D. J., A Comparison of the Characteristic Equations in the Theory of Circular Cylindrical Shells, The Aeronautical Quarterly, Vol. 12, (August 1961), pp. 228-236.

18. Oplinger, D. W., Frequency Response of a Nonlinear Stretched String, J. Acoust. Soc., Vol. 32, No. 12, (December 1960), pp. 1529-1538.

19. Woinowsky-Krieger, S., The Effect of an Axial Force on the Vibration of Hinged Bars, J. Applied Mech. (March 1950), Trans. ASME, Vol. 72, p. 35-36.

20. Chu, H., and Hermann, G., Influence of Large Amplitudes on Free Flexural Vibrations of Rectangular Elastic Plates, J. Applied Mech., Vol. 23 (December 1956), pp. 532-540.

21. Burgreen, D., Free Vibrations of a Pin-Ended Column with Constant Distance between Pin Ends, J. Applied Mech., Vol. 18 (June 1951).

22. Stoker, J. J., Nonlinear Vibrations, Interscience, New York, (1950).

23. McLaghlan, N. W., Ordinary Non-Linear Differential Equations, Second Edition, (1958), Oxford Univ. Press, London.

24. Herrmann, G. and Armenakas, A. E., Dynamic Behavior of Cylindrical Shells under Initial Stress, AFOSR TN 60-425, Columbia Univ., Institute of Flight Structures, (April 1960).

25. Evensen, D. A., The Forced Non-Linear Flexural Vibrations of Thin Circular Cylindrical Shells, (in preparation).

26. Tobias, S. A., Free Undamped Non-Linear Vibrations of Imperfect Circular Disks, Proc. Inst. of Mech. Eng., Vol. 171, (1957), pp. 691-715.

27. Tobias, S. A., Non-Linear Forced Vibrations of Circular Discs, Engineering, Vol. 179, (July 1958), pp. 51-56.

28. Tobias, S. A., A Theory of Imperfection for the Vibration of Elastic Bodies of Revolution, Engineering, Vol. 172, (Sept. 1951), pp. 409-411.

29. Miles, J. W., Stability of Forced Oscillations of a Spherical Pendulum, Quart. Applied Math., Vol 20, (April 1962), pp. 21-32.

30. Hutton, R. E., An Investigation of Resonant, Non-Linear, Non-Planar Free Surface Oscillations of a Fluid, NASA TN D-1870, (May 1963).

31. Babcock, C. D., and Sechler, E. E., The Effect of Initial Imperfections on the Buckling Stress of Cylindrical Shells, NASA TN D-2005 (July 1963).

32. Olson, M. D., (Private Communication), Graduate Aeronautical Laboratories, California Institute of Technology, Pasadena, California.

33. Novozhilov, V. V., Foundations of the Nonlinear Theory of Elasticity, Graylock Press, Rochester, N. Y., (1953).

34. Fung, Y. C., and Wittrick, W. H., A Boundary Layer Phenomenon in the Large Deflexion of Thin Plates, Quart. Journ. Mech. and Applied Math., Vol VIII, Pt. 2, (1955), pp. 191-210.

APPENDIX A

A more exact set of ring equations can be obtained by retaining the assumption $(\frac{\partial w}{\partial y})^2 << 1$ but not assuming that $\frac{1}{n^2} << 1$. The derivation itself is readily carried out by the application of Hamilton's Principle, which involves the elastic strain energy, the kinetic energy, and the potential energy of the applied forces.

The Strain Energy

The strain energy density (per unit volume) is $dW = \frac{1}{2}\sigma_{ij}\epsilon_{ij}$ in general. For simplicity, the following assumptions will be made:

(a) $\sigma_{zz} = 0$

(b) $\sigma_{xx} = 0$, $\sigma_{xy} = 0$ ("plane stress" assumptions)

(c) $\epsilon_{xz} = 0$

(d) $\epsilon_{yz} = 0$ (shearing strains are neglected)

Then, dW becomes simply $dW = \frac{1}{2}\sigma_{yy}\epsilon_{yy}$

or $dW = \frac{E}{2}[\epsilon_{yy}]^2$ upon using Hooke's Law.

Since we eventually want to write dW in terms of the displacements of the ring, it is necessary to consider the strain-displacement relations. The Lagrangian form of the pertinent strain-displacement relation is given (Ref. 24) by

$$\epsilon_{yy} = \epsilon_{\theta\theta} = \frac{1}{(R+z)}\left(u_z + \frac{\partial u_\theta}{\partial \theta}\right) + \frac{1}{2(R+z)^2}\left[\left(\frac{\partial u_z}{\partial \theta} - u_\theta\right)^2 + \left(u_z + \frac{\partial u_\theta}{\partial \theta}\right)^2\right] \tag{A.1}$$

in the notation of reference 24.

The displacements $u_z(\theta, z, t)$ and $u_\theta(\theta, z, t)$ are taken to be related to the displacements of the mid-surface of the ring, as follows:

$$\begin{aligned} u_z &= w \\ u_\theta &= v + z\,\psi_\theta \end{aligned} \tag{A. 2}$$

Here,

$$\psi_\theta = -\frac{1}{R}\left(\frac{\partial w}{\partial \theta} - v\right) + \frac{1}{R^2}\left(\frac{\partial w}{\partial \theta} - v\right)\left(w + \frac{\partial v}{\partial \theta}\right) \tag{A. 3}$$

and w and v are the radial and tangential displacements of the mid-surface (see Fig. 1).

For present purposes, it is sufficient to approximate (A. 3) by

$$\psi_\theta = -\frac{1}{R}\left(\frac{\partial w}{\partial \theta} - v\right)\left[1 - \left(w + \frac{\partial v}{\partial \theta}\right)\right] \cong -\frac{1}{R}\left(\frac{\partial w}{\partial \theta} - v\right) \tag{A. 4}$$

i. e., by assuming $\left|w + \frac{\partial v}{\partial \theta}\right| << 1$.

After several manipulations, one can show that the assumption

$$\left|w + \frac{\partial v}{\partial \theta}\right| << 1$$

is equivalent to

$$\left[\frac{1}{R}\left(\frac{\partial w}{\partial \theta} - v\right)\right]^2 << 1 \tag{A. 5}$$

which is similar to $\left(\frac{\partial w}{\partial x}\right)^2 << 1$ for the shallow shell equations.

Similarly, employing the assumption (A. 5) allows (A. 1) to be approximated by

$$\epsilon_{yy} = \epsilon_{\theta\theta} = \frac{\left(u_z + \frac{\partial u_\theta}{\partial \theta}\right)}{R+z} + \frac{1}{2(R+z)^2}\left(\frac{\partial u_z}{\partial \theta} - u_\theta\right)^2 \qquad \text{(A. 6)}$$

Substituting (A. 2) and (A. 4) into (A. 6) gives

$$\epsilon_{\theta\theta} = \frac{(\alpha_1 + z\phi_\theta)}{R+z} + \frac{1}{2(R+z)^2}(\alpha_2 - z\phi)^2 \qquad \text{(A. 7)}$$

where the following notation has been used

$$\begin{aligned} \alpha_1 &= w + \frac{\partial v}{\partial \theta} \qquad \alpha_2 = \frac{\partial w}{\partial \theta} - v \\ \phi &= -\frac{1}{R}\left(\frac{\partial w}{\partial \theta} - v\right) = -\frac{\alpha_2}{R} \\ \phi_\theta &= \frac{\partial \phi}{\partial \theta} = -\frac{1}{R}\frac{\partial \alpha_2}{\partial \theta} \end{aligned} \qquad \text{(A. 8)}$$

Finaly then, the strain energy in a ring of unit width is approximated by

$$W = \frac{E}{2}\int_0^{2\pi} d\theta \int_{-\frac{h}{2}}^{\frac{h}{2}} [\epsilon_{\theta\theta}]^2 (R+z)\, dz$$

$$W = \frac{E}{2}\int_0^{2\pi} d\theta \int_{-h/2}^{h/2} \left\{ \frac{(\alpha_1 + z\phi_\theta)}{R+z} + \frac{(\alpha_2 - z\phi)^2}{2(R+z)^2} \right\}^2 (R+z)\, dz \qquad \text{(A. 9)}$$

The z integration can be done approximately by expanding $\frac{1}{(R+z)}$ and $\frac{1}{(R+z)^2}$ in powers of $(\frac{z}{R})$. When this is done and the inequalities

$$\left[\frac{1}{R}\left(\frac{\partial w}{\partial \theta} - v\right)\right]^2 << 1$$

$$\left(\frac{h}{R}\right)^2 << 1$$

$$\left|\frac{w}{h}\right|_{MAX} >> \frac{h}{R} \qquad \text{(A. 10)}$$

are used, (A. 9) gives

$$W = \frac{Eh}{2}\int_0^{2\pi}\left\{\left[\frac{\alpha_1^2}{R} - \frac{2\alpha_1\phi_0 h^2}{12R^2} + \frac{\phi_0^2 h^2}{12R}\right] + \frac{\alpha_1\alpha_2^2}{R^2} + \frac{\alpha_2^4}{4R^3}\right\} d\theta \qquad \text{(A. 11)}$$

The inequality $\left|\frac{w}{h}\right|_{max} >> \frac{h}{R}$ insures that the non-linear stretching terms in (A. 9) exceed the non-linear bending terms. The former have $\frac{Eh}{R}$ as a coefficient, while the latter go as $\frac{Eh^3}{12R^4}$.

First Variation of the Strain Energy

To apply Hamilton's Principle, it is necessary to compute the first variation of the strain energy, the kinetic energy, and the virtual work of the applied forces. Applying the standard techniques of variational calculus to (A. 11) gives

$$\delta W = \frac{Eh}{R}\int_0^{2\pi}\left[\alpha_1\delta\alpha_1 - \frac{\alpha_1 h^2}{12R}\delta\phi_0 - \frac{\phi_0 h^2}{12R}\delta\alpha_1 + \frac{h^2\phi_0}{12R}\delta\phi_0 + \frac{\alpha_2^2}{2R}\delta\alpha_1 + \frac{\alpha_1\alpha_2}{R}\delta\alpha_2 + \frac{\alpha_2^3}{2R^2}\delta\alpha_2\right] d\theta \qquad \text{(A. 12)}$$

where

$$\alpha_1 = w + \frac{\partial v}{\partial \theta}, \qquad \alpha_2 = \frac{\partial w}{\partial \theta} - v$$
$$\text{AND} \quad \phi_\theta = \frac{-1}{R}\left(\frac{\partial^2 w}{\partial \theta^2} - \frac{\partial v}{\partial \theta}\right) \tag{A.8}$$

To derive the equations of motion in the radial and tangential directions, one computes the variation of the strain energy with respect to w and v respectively. Variations with respect to a particular variable will be denoted by a bar, as follows:

$\delta\alpha_1\big|_w$ = The first variation of α_1 with respect to w, etc.

Using the definitions of α_1, α_2, and ϕ_θ, one finds

$$\delta\alpha_1\big|_w = \delta w \qquad \delta\alpha_1\big|_v = \frac{\partial}{\partial\theta}(\delta v)$$

$$\delta\alpha_2\big|_w = \frac{\partial}{\partial\theta}(\delta w) \qquad \delta\alpha_2\big|_v = -\delta v \tag{A.13}$$

$$\delta\phi_\theta\big|_w = -\frac{1}{R^2}\frac{\partial^2}{\partial\theta^2}(\delta w)$$

$$\delta\phi_\theta\big|_v = \frac{1}{R}\frac{\partial}{\partial\theta}(\delta v)$$

When (A. 13) are substituted in (A. 12) and various integrations by parts are performed, the required variations of W are obtained. They are

$$\delta W|_w = -\left[\frac{\partial}{\partial\theta}(\delta w)\frac{1}{R}\left(\phi_\theta - \frac{\alpha_1}{R}\right)\right]_0^{2\pi}\left(\frac{Eh^3}{12R^2}\right)$$

$$+\left[\frac{1}{R}\frac{\partial}{\partial\theta}\left(\phi_\theta - \frac{\alpha_1}{R}\right)(\delta w)\right]_0^{2\pi}\left(\frac{Eh^3}{12R^2}\right)$$

$$+\frac{Eh}{R}\left[\frac{\alpha_2}{R}\left(\alpha_1 + \frac{\alpha_2^2}{2R}\right)\delta w\right]_0^{2\pi} \qquad \text{(A. 14a)}$$

$$+\frac{Eh}{R}\int_0^{2\pi}\left\{\left(\alpha_1 - \frac{\phi_\theta h^2}{12R} + \frac{\alpha_2^2}{2R}\right) - \frac{1}{R}\frac{\partial^2}{\partial\theta^2}\left(\phi_\theta - \frac{\alpha_1}{R}\right)\right.$$

$$\left.-\frac{1}{R}\frac{\partial}{\partial\theta}\left[\alpha_2\left(\alpha_1 + \frac{\alpha_2^2}{2R}\right)\right]\right\}\delta w\, d\theta$$

and

$$\delta W|_v = \frac{Eh}{R}\left[\alpha_1\,\delta v\right]_0^{2\pi}$$

$$-\frac{Eh}{R}\int_0^{2\pi}\left\{\frac{\partial}{\partial\theta}\left[\alpha_1 - \frac{\phi_\theta h^2}{12R} + \frac{\alpha_2^2}{2R}\right]\right. \qquad \text{(A. 14b)}$$

$$\left.+\frac{h^2}{12R}\frac{\partial}{\partial\theta}\left(\phi_\theta - \frac{\alpha_1}{R}\right) + \frac{\alpha_2}{R}\left(\alpha_1 + \frac{\alpha_2^2}{2R}\right)\right\}\delta v\, d\theta$$

The Kinetic Energy

The kinetic energy of the ring (for unit width) is approximated by

$$T = \frac{\rho h R}{2} \int_0^{2\pi} [(\dot{w})^2 + (\dot{v})^2] d\theta \qquad \text{(A.15)}$$

where the ring is assumed to have a constant density (before deformation) and the kinetic energy of rotation has been neglected. (See Section 2.6.2 for a discussion of rotary inertia effects).

The Potential Energy of the Applied Forces

The potential energy of the applied loading (for a ring of unit width) is given by

$$A = - \int_0^{2\pi} q(\theta, t)\, w\, R\, d\theta \qquad \text{(A.16)}$$

where the pressure $q(\theta, t)$ is assumed to act only in the radial direction and is defined as positive outward (in the same manner as w).

Application of Hamilton's Principle

Hamilton's Principle can be formulated as the stationary variation of a certain time integral:

$$\delta \int_{t_1}^{t_2} (T - V)\, dt = 0 \qquad \text{(A.17)}$$

where T is the kinetic energy of the system

V is the potential energy of the internal and external (applied) forces

and t_1 and t_2 are fixed times.

In the present problem, T is given by (A.15), and

$$V = (W + A) \tag{A.18}$$

where W and A are approximated by (A.11) and (A.16) respectively.

From (A.17) and (A.18), one has

$$\int_{t_1}^{t_2} (\delta T - \delta W - \delta A) dt = 0 \tag{A.19}$$

Employing (A.8) and (A.14 - A.16) in (A.19), integrating by parts, and performing the variation first with respect to w, then with respect to v gives equations of the form

$$\int_{t_1}^{t_2} \left\{ \left[f_1(w, v, \delta w) \right]_0^{2\pi} + \int_0^{2\pi} f_2(w, v)\, \delta w\, d\theta \right\} dt = 0 \tag{A.20a}$$

and

$$\int_{t_1}^{t_2} \left\{ \left[f_3(w, v, \delta v) \right]_0^{2\pi} + \int_0^{2\pi} f_4(w, v)\, \delta v\, d\theta \right\} dt = 0 \tag{A.20b}$$

The variations δw and δv are not completely arbitrary, since physical considerations require w and v to be continuous and single-valued. Thus, δw and δv must satisfy this constraint; in particular, $\delta w(\theta = 0)$ must be identical with $\delta w(\theta = 2\pi)$, etc. Using this, and applying the standard arguments of variational calculus to (A. 20) yields the differential equations of motion and the associated boundary conditions.

From (A. 20a), one obtains

$$\rho h \ddot{w} + \frac{Eh}{R^2}\left\{\left(w + \frac{\partial v}{\partial \theta}\right) + \frac{h^2}{12R^2}\left(\frac{\partial^4 w}{\partial \theta^4} + 2\frac{\partial^2 w}{\partial \theta^2} - \frac{\partial v}{\partial \theta}\right) - \frac{1}{R}\left[\left(\frac{\partial^2 w}{\partial \theta^2} - \frac{\partial v}{\partial \theta}\right)\left(w + \frac{\partial v}{\partial \theta}\right) - \frac{v^2}{2} + \frac{1}{2}\left(\frac{\partial w}{\partial \theta}\right)^2 + \frac{\partial^2 w}{\partial \theta^2}\left(\frac{\partial w}{\partial \theta} - v\right)\right] - \frac{3}{2R^2}\left(\frac{\partial^2 w}{\partial \theta^2} - \frac{\partial v}{\partial \theta}\right)\left[\left(\frac{\partial w}{\partial \theta}\right)^2 - 2v\frac{\partial w}{\partial \theta} + v^2\right]\right\} = q(\theta, t) \tag{A.21a}$$

and boundary conditions of the form

$$-\frac{Eh^3}{12R^2}\left(\frac{\partial^2 w}{\partial \theta^2} + w\right)\Bigg|_{\theta=0} = -\frac{Eh^3}{12R^2}\left(\frac{\partial^2 w}{\partial \theta^2} + w\right)\Bigg|_{\theta=2\pi}$$

etc.

Equation (A. 20b) gives

$$\rho h \ddot{w} - \frac{Eh}{R}\left\{\frac{\partial w}{\partial \theta} + \frac{\partial^2 v}{\partial \theta^2} + \frac{1}{R}\left(\frac{\partial w}{\partial \theta} - v\right)\left[w\right.\right.$$

$$\left.\left.\frac{\partial^2 w}{\partial \theta^2} + \frac{1}{2R}\left(\frac{\partial w}{\partial \theta} - v\right)^2\right]\right\} = 0 \qquad \text{(A.21b)}$$

and the boundary condition

$$\frac{Eh}{R}\left(w + \frac{\partial v}{\partial \theta}\right)\Big|_{\theta=0} = \frac{Eh}{R}\left(w + \frac{\partial v}{\partial \theta}\right)\Big|_{\theta=2\pi}$$

By using the transformation $y = R\theta$ and manipulating the various terms, (A.21) can be put in the form of (1.6). In writing (1.6), D has been used to replace $\frac{Eh^3}{12}$ in (A.21a).

APPENDIX B

It is the purpose of this Appendix to demonstrate the approximate techniques which were used to obtain the solutions presented in Sections 2.3 and 2.5. Some representative examples from Section 2.3 are examined in detail, and the reader will have no difficulty verifying the other solutions which are discussed in the body of the thesis.

The Perturbation Method: Vibrations near Resonance

For simplicity, consider (3.4) in the case when $G_o = 0$. Then (3.4) contains η^2 as the non-linearity parameter. Defining $\eta^2 = \epsilon$, $G_n = \epsilon P_n$ and $\theta = \Omega\tau$, (3.4) becomes

$$\Omega^2 y_{\theta\theta} + \frac{\epsilon\Omega^2}{2} y\left[y y_{\theta\theta} + y_\theta^2\right] + y = \epsilon P_n \cos\theta \tag{B.1}$$

where $y(\theta)$ is required to satisfy the conditions

$$y(\theta) = y(\theta + 2\pi)$$
$$y(0) = A$$
$$y_\theta(0) = 0$$

since periodic, steady-state solutions are being sought.

To apply the perturbation method, both y and Ω are expanded in powers of the non-linearity parameter:

$$y = y_0 + \epsilon y_1 + \epsilon^2 y_2 + \epsilon^3 y_3 + \cdots \tag{B.2a}$$

$$\Omega = 1 + \epsilon\omega_1 + \epsilon^2\omega_2 + \epsilon^3\omega_3 + \cdots \tag{B.2b}$$

Substituting (B. 2) into (B. 1) gives

$$[1 + 2\epsilon\omega_1 + \epsilon^2(\omega_1^2 + 2\omega_2) + \cdots]\{\ddot{\varphi}_0 + \epsilon\ddot{\varphi}_1 + \epsilon^2\ddot{\varphi}_2 + \cdots$$
$$+ \frac{\epsilon}{2}[\varphi_0 + \epsilon\varphi_1 + \cdots][\varphi_0\ddot{\varphi}_0 + \epsilon(\varphi_0\ddot{\varphi}_1 + \varphi_1\ddot{\varphi}_0) + \cdots$$
$$+ \dot{\varphi}_0^2 + 2\epsilon\dot{\varphi}_1\dot{\varphi}_0 + \cdots]\} + \varphi_0 + \epsilon\varphi_1 + \epsilon^2\varphi_2 + \cdots$$
$$= \epsilon P_m \cos\theta$$

where $\frac{d(\,)}{d\theta}$ has been replaced by $(\dot{})$ for simplicity.

In keeping with the perturbation method, the equation and the subsidiary conditions are satisfied for terms having like powers of ϵ. Thus, one has

$$O(\epsilon^0): \qquad \ddot{\varphi}_0 + \varphi_0 = 0$$
$$O(\epsilon^1): \quad \ddot{\varphi}_1 + \varphi_1 + 2\omega_1\ddot{\varphi}_0 + \frac{\varphi_0}{2}[\varphi_0\ddot{\varphi}_0 + \dot{\varphi}_0^2] = P_m\cos\theta$$
$$O(\epsilon^2): \quad \ddot{\varphi}_2 + \varphi_2 + (\omega_1^2 + 2\omega_2)\ddot{\varphi}_0 + 2\omega_1\ddot{\varphi}_1$$
$$+ \omega_1\varphi_0[\varphi_0\ddot{\varphi}_0 + \dot{\varphi}_0^2] + \frac{\varphi_1}{2}[\varphi_0\ddot{\varphi}_1 + \varphi_1\ddot{\varphi}_0$$
$$+ 2\dot{\varphi}_1\dot{\varphi}_0] + \frac{\varphi_1}{2}[\varphi_0\ddot{\varphi}_0 + \dot{\varphi}_0^2] = 0$$

etc., with the conditions

$$\varphi_i(\theta) = \varphi_i(\theta + 2\pi) \quad \text{FOR ALL } i$$
$$\left.\begin{aligned} \varphi_0(0) &= A & \varphi_i(0) &= 0 \\ \dot{\varphi}_0(0) &= 0 & \dot{\varphi}_i(0) &= 0 \end{aligned}\right\} \; i > 0 \qquad \text{(B. 3)}$$

Solving these linear equations in succession gives

$$O(\epsilon^0): \qquad \varphi_0 = A\cos\theta = A\cos\Omega\tau$$
$$O(\epsilon^1): \quad \ddot{\varphi}_1 + \varphi_1 = [P_m + 2\omega_1 A + \frac{A^3}{4}]\cos\theta + \frac{A^3}{4}\cos 3\theta$$

To avoid secular terms, (since a periodic solution is desired) one puts

$$P_m + 2\omega_1 A + \frac{A^3}{4} = 0 \qquad \text{(B. 4)}$$

Then $\varphi_1 = a\cos\theta + b\sin\theta - \frac{A^3}{32}\cos 3\theta$

and to satisfy (B. 3) it is clear that b = 0 and a = $\frac{A^3}{32}$. Thus,

$$\varphi_1 = \frac{A^3}{32}(\cos\theta - \cos 3\theta)$$

From $0(\epsilon^2)$, one has (using φ_0 and φ_1)

$$\ddot{\varphi}_2 + \varphi_2 = \left[(\omega_1^2 + 2\omega_2)A + \frac{\omega_1 A^3}{16} + \frac{\omega_1 A^3}{2}\right]\cos\theta$$
$$- \left[\frac{\omega_1 A^3}{16} + \frac{A^5}{16} + \frac{A^5}{128}\right]\cos 3\theta$$
$$- \left[\frac{A^5}{16} - \frac{A^5}{128}\right]\cos 5\theta$$

Again, to avoid secular terms, one requires

$$\left[(\omega_1^2 + 2\omega_2)A + \frac{9\omega_1 A^3}{16}\right] = 0 \qquad \text{(B. 5)}$$

Then φ_2 can be found, and the method can be continued; for present purposes, it is sufficient to stop at this point. The result for φ is

$$\varphi(\tau) = A\cos\Omega\tau + \frac{\epsilon A^3}{32}(\cos\Omega\tau - \cos 3\Omega\tau) + \cdots$$

Similarly, ω_1 and ω_2 are related to A by (B. 4) and (B. 5), giving

$$\Omega = 1 + \epsilon\omega_1(A, P_m) + \epsilon^2\omega_2(A, P_m) + \cdots \qquad \text{(B. 6)}$$

Equation (B. 6) results in the response curves and the "backbone curve" as well. The latter is obtained by putting $P_m = 0$ and considering the case of free vibrations. In this case, (B. 4) gives

$$2\omega_1 A + \frac{A^3}{4} = 0, \qquad i.e., \quad \omega_1 = -\frac{A^2}{8}$$

whence (B. 5) yields $\omega_2 = \frac{7A^4}{256}$. Hence, for free vibrations, the inextensional ring results give

$$\Omega = 1 - \frac{\epsilon A^2}{8} + \frac{7\epsilon A^4}{256} + \cdots$$

which is plotted in Fig. 2.

Finally, to complete the calculation, r must be determined from $r = -\frac{\gamma^2}{4}$. Substituting the result for γ gives

$$r(\tau) = -\frac{A^2}{8}(1+\cos 2\Omega\tau) - \frac{\epsilon A^4}{64}(1-\cos 4\Omega\tau) + \cdots$$

up to $0(\epsilon)$.

The Perturbation Method: Vibrations Away from Resonance

A simple perturbation scheme is used when vibrations away from the resonant frequency are examined. For example, consider the equations for the "extensional" case:

$$\begin{aligned} \gamma_{\tau\tau} + \gamma + F\gamma\left[r + \frac{\gamma^2}{4}\right] &= G_m \cos\Omega\tau \\ \eta^2 r_{\tau\tau} + F\left[r + \frac{\gamma^2}{4}\right] &= \frac{\eta G_0}{2}\cos\Omega\tau \end{aligned} \tag{3.5}$$

With $\theta = \Omega\tau$, and $\frac{d(\,)}{d\theta} = (\,)'$, these become

$$\begin{aligned} \Omega^2\gamma'' + \gamma + F\gamma\left[r + \frac{\gamma^2}{4}\right] &= G_m\cos\theta \\ \eta^2\Omega^2 r'' + F\left[r + \frac{\gamma^2}{4}\right] &= \frac{\eta G_0}{2}\cos\theta \end{aligned} \tag{B. 7}$$

For vibrations away from resonance, φ and r must satisfy

$$\varphi(\theta) = \varphi(\theta + 2\pi) \qquad r(\theta) = r(\theta + 2\pi)$$

Expanding φ and r in powers of the non-linearity parameter, (in this case, η) one has

$$\varphi = \varphi_0 + \eta\varphi_1 + \eta^2\varphi_2 + \cdots$$

$$r = \rho_0 + \eta\rho_1 + \eta^2\rho_2 + \cdots$$

which are then substituted into (B. 7) to yield

$$\Omega^2[\ddot{\varphi}_0 + \eta\ddot{\varphi}_1 + \cdots] + [\varphi_0 + \eta\varphi_1 + \eta^2\varphi_2 + \cdots] + F[\varphi_0 + \eta\varphi_1 + \cdots]\left\{\rho_0 + \eta\rho_1 + \cdots + \frac{\varphi_0^2 + 2\eta\varphi_0\varphi_1 + \cdots}{4}\right\} = G_m\cos\theta$$

$$\eta^2\Omega^2[\ddot{\rho}_0 + \eta\ddot{\rho}_1 + \cdots] + F\left[\rho_0 + \eta\rho_1 + \cdots \frac{\varphi_0^2 + 2\eta\varphi_1\varphi_0 + \cdots}{4}\right] = \frac{\eta G_0}{2}\cos\theta$$

Equating the terms having like powers of η and solving, one has

$$O(\eta^0): \quad \Omega^2\ddot{\varphi}_0 + \varphi_0 = G_m\cos\theta$$

$$\varphi_0 = \frac{G_m}{1-\Omega^2}\cos\theta$$

and

$$\rho_0 = -\frac{\varphi_0^2}{4} = -\frac{G_m^2}{(1-\Omega^2)^2}(1+\cos 2\theta)$$

$$O(\eta^1): \quad \Omega^2\ddot{\varphi}_1 + \varphi_1 = -\frac{G_0 G_m}{4(1-\Omega^2)}(1+\cos 2\theta)$$

and

$$F\left[\rho_1 + \frac{2\varphi_0\varphi_1}{4}\right] = \frac{G_0}{2}\cos\theta$$

whence

$$\mathcal{G}_1 = -\frac{G_0 G_n}{4(1-\Omega^2)}\left[1 + \frac{\cos 2\theta}{1-4\Omega^2}\right]$$

$$\rho_1 = \frac{G_0}{2F}\cos\theta - \frac{\mathcal{G}_0 \mathcal{G}_1}{2}$$

$$= \left[\frac{G_0}{2F} + \frac{G_0 G_n^2}{8(1-\Omega^2)^2} + \frac{G_0 G_n^2}{8(1-\Omega^2)^2(1-4\Omega^2)}\right]\cos\theta$$

$$+ \frac{G_0 G_n^2 \cos 3\theta}{8(1-\Omega^2)^2(1-4\Omega^2)}$$

etc. Up to $0(\eta)$, one has

$$\mathcal{G} = \frac{G_n \cos\Omega\tau}{1-\Omega^2} - \frac{\eta G_n^2}{4(1-\Omega^2)}\left[1 + \frac{\cos 2\Omega\tau}{1-4\Omega^2}\right] + O(\eta^2)$$

$$\rho = -\frac{G_n^2}{8(1-\Omega^2)^2}(1+\cos 2\Omega\tau) + \eta\left\{\frac{G_n^3}{8(1-\Omega^2)^2}\left[\cos\Omega\tau\right.\right.$$

$$\left.\left. + \frac{\cos 3\Omega\tau + \cos\Omega\tau}{(1-4\Omega^2)}\right] + \frac{G_n \cos\Omega\tau}{2F}\right\} + O(\eta^2)$$

for $G_o = G_n$, and analogous results for $G_o = 0$.

The Method of Averaging

As a straightforward example, consider the inextensional equations with linear viscous damping:

$$\eta_{\tau\tau} + 2\beta\eta_\tau + \eta + \frac{\gamma^2\eta}{2}\left[\eta\eta_{\tau\tau} + \eta_\tau^2\right] + \frac{\gamma G_0 \eta}{2}\cos\Omega\tau = G_m\cos\Omega\tau \tag{3.45}$$

To apply the method of averaging, let

$$\eta(\tau) = A(\tau)\cos\left[\Omega\tau + \phi(\tau)\right] = A\cos\chi$$

where $A(\tau)$ and $\phi(\tau)$ are taken to be slowly varying. Differentiating, one has

$$\eta_\tau = -\Omega A\sin\chi + \underline{A_\tau\cos\chi - \phi_\tau A\sin\chi}$$

In keeping with the averaging method, the underlined terms are set equal to zero; thus,

$$A_\tau\cos\chi - \phi_\tau A\sin\chi = 0 \tag{B.8}$$

and

$$\eta_\tau = -\Omega A\sin\chi$$

Differentiating once more gives

$$\eta_{\tau\tau} = -\Omega^2 A\cos\chi - \Omega A_\tau\sin\chi - \Omega A\phi_\tau\cos\chi$$

When the expressions for η, η_τ, and $\eta_{\tau\tau}$ are substituted into (3.45), one finds

$$\begin{aligned}&\left[1-\Omega^2\right]A\cos\chi - \Omega\left[A_\tau\sin\chi + A\phi_\tau\cos\chi\right] \\ &- 2\beta\Omega A\sin\chi - \frac{\gamma^2}{2}\left\{\Omega^2A^3\cos\chi\cos 2\chi\right. \\ &\left. + \Omega A^2A_\tau\sin\chi\cos^2\chi + \Omega A^3\phi_\tau\cos^3\chi\right\} \\ &+ \frac{\gamma}{2}AG_0\cos\chi\cos(\chi-\phi) = G_m\cos(\chi-\phi)\end{aligned} \tag{B.9}$$

Multiplying (B. 8) by $\Omega \sin\chi$ and (B. 9) by $\cos\chi$ and adding gives

$$[1-\Omega^2]A\cos^2\chi - 2\beta\Omega A \sin\chi\cos\chi - \Omega A\phi_\tau$$
$$-\frac{\eta^2}{2}\left[\frac{\Omega^2 A^3}{2}(\cos^2\chi + \cos\chi\cos 3\chi) + \Omega A^2 A_\tau \sin\chi\cos^3\chi\right.$$
$$\left.+\frac{\Omega A^3\phi_\tau}{4}(\cos\chi\cos 3\chi + 3\cos^2\chi)\right]$$
$$+\frac{\eta A G_m}{2}\left[\frac{1}{4}(\cos 3\chi + 3\cos\chi)\cos\phi\right. \qquad \text{(B. 10)}$$
$$\left.+\sin\chi\cos^2\chi\sin\phi\right] = G_m\left[\cos^2\chi\cos\phi\right.$$
$$\left.+\sin\chi\cos\chi\sin\phi\right]$$

Next, equation (B. 10) is averaged over one period, by integrating on χ from 0 to 2π. The functions $A(\tau)$ and $\phi(\tau)$ are assumed to be "slowly varying"; they are replaced in the integration by their average values, $\bar{A}$ and $\bar{\phi}$. Thus, (B. 10) yields

$$[1-\Omega^2]\bar{A} - 2\Omega\bar{A}\bar{\phi}_\tau - \frac{\eta^2\Omega^2\bar{A}^3}{4}$$
$$-\frac{3\eta^2\Omega\bar{A}^3\phi_\tau}{8} = G_m\cos\bar{\phi} \qquad \text{(B. 11a)}$$

Similarly, taking $\sin\chi$ times (B. 9), adding $-\Omega\cos\chi$ times (B. 8) and averaging over one period gives

$$-2\Omega\bar{A}_\tau - 2\beta\Omega\bar{A} - \frac{\eta^2\Omega\bar{A}^2\bar{A}_\tau}{8} = G_m\sin\bar{\phi} \qquad \text{(B. 11b)}$$

For steady-state vibrations, $\bar{A}$ and $\bar{\phi}$ are constant; in this case, $\bar{A}_\tau$ and $\bar{\phi}_\tau$ vanish identically, which causes (B. 11) to become

$$[1-\Omega^2]\bar{A} - \frac{\eta^2\Omega^2\bar{A}^3}{4} = G_n \cos\bar{\phi} \qquad \text{(B.12a)}$$

and

$$-2\beta\Omega\bar{A} = G_n \sin\bar{\phi} \qquad \text{(B.12b)}$$

Squaring and adding these gives

$$\left\{[1-\Omega^2]\bar{A} - \frac{\eta^2\Omega^2\bar{A}^3}{4}\right\}^2 + 4\beta^2\Omega^2\bar{A}^2 = G_n^2 \qquad \text{(B.13)}$$

For given values of G_n, η^2, and Ω, $\bar{A}$ can be computed from (B.13). Then $\bar{\phi}$ may be determined from (B.12b).

For $\beta = 0$, (B.12) reduces to

$$[1-\Omega^2]\bar{A} - \frac{\eta^2\Omega^2\bar{A}^3}{4} = G_n \qquad \text{(B.14)}$$

If β is very small, (B.14) gives results that are very close to (B.13) except in the vicinity of

$$[1-\Omega^2]\bar{A} - \frac{\eta^2\Omega^2\bar{A}^3}{4} = 0$$

i.e., near $$\Omega = 1 - \frac{\eta^2\bar{A}^2}{8} + \cdots$$

which is the so-called "backbone curve".

On the "backbone curve", (B.13) gives

$$4\beta^2\Omega^2\bar{A}^2 = G_n^2, \quad \text{i.e.,} \quad \bar{A} = \frac{G_n}{2\beta\Omega}$$

which may be substituted in (B.12b) to yield $\bar{\phi} = -\frac{\pi}{2}$. This corresponds to the resonance point in linear vibrations.

Finally, the approximate solution for φ becomes

$$\varphi(\tau) = \bar{A} \cos [\Omega \tau + \bar{\phi}]$$

with $\bar{A}$ and $\bar{\phi}$ determined from (B.12) and (B.11b) as indicated above. A typical response curve is shown in Fig. 3. As mentioned previously, the effect of the damping is to "round off" the peak response.

The method of averaging was used to analyze the equations which include the effects of extension (3.5) and tangential inertia (3.25 - 3.27). The results of those studies are presented in Section 2.3.2 and may be obtained in a manner similar to that described here.

APPENDIX C

In discussing the stability of the one and two-mode solutions (Sections 2.5.1a and 2.5.1c), it was necessary to omit many of the calculations and present only the results. The reader who is interested in the details of the analyses will find them included in the following paragraphs.

Approximate Stability Boundaries of Equation (5.6b)

$$x_{\tau\tau} + 2\beta_s x_\tau + x + \frac{\eta^2}{2} x \left[-\Omega^2 \bar{A}^2 \cos 2(\Omega\tau + \bar{\phi}) \right] + \frac{\eta x}{2} G_o \cos \Omega\tau = 0 \qquad (5.6b)$$

If G_o and β_s are both zero, (5.6b) is just the Mathieu equation. Similarly, when G_o and β_s do not vanish, it may be transformed to the more general Hill's equation. To do this, let

$$x(\tau) = u(\tau)\, e^{-\beta_s \tau} \quad \text{AND} \quad \tau = \frac{2z}{\Omega}$$

and define

$$\theta_o = \frac{4}{\Omega^2}(1-\beta_s^2) \qquad 2\theta_1 = \frac{2}{\Omega^2}\eta G_o \qquad 2\theta_2 = -2\eta^2\bar{A}^2$$

$$\epsilon_1 = 0 \qquad \epsilon_2 = \bar{\phi}$$

Then (5.6b) may be written as

$$0 = \frac{d^2u}{dz^2} + \left[\theta_o + 2 \sum_{m=1}^{2} \theta_m \cos(2mz + \epsilon_m) \right] u \qquad (5.10)$$

In the vicinity of the nth unstable region, u is approximated by

$$u(z) = e^{\mu z} \sin(nz - \sigma) \tag{C.1}$$

Substituting this into (5.10) and equating the coefficients of the first harmonic terms separately to zero, one finds

$$(\bar{\theta}_0 - n^2) = \theta_n \cos 2\sigma$$
$$2\mu n = \theta_n \sin 2\sigma$$

where $\bar{\theta}_0 = \theta_0 + \mu^2$

Squaring and adding gives

$$(\theta_0 + \mu^2 - n^2)^2 + (2\mu n)^2 = \theta_n^2$$

which leads to

$$\mu^4 + 2(\theta_0 + n^2)\mu^2 + (\theta_0^2 - 2n^2\theta_0 + n^4 - \theta_n^2) = 0$$

Solving this bi-quadratic results in

$$\mu^2 = -(\theta_0 + n^2) \pm [4n^2\theta_0 + \theta_n^2]^{1/2}$$

Now recall that

$$x(\tau) = u(\tau)\, e^{-\beta_s \tau} = e^{-\frac{\beta_s 2z}{\Omega}} e^{\mu z} \sin(nz - \sigma)$$

It is apparent that $x(\tau)$ will be unstable if

$$\mu > \frac{2\beta_s}{\Omega} \quad \text{i.e., if} \quad \mu^2 > \frac{4\beta_s^2}{\Omega^2}$$

Thus, the condition for instability of (5.6b) near the nth unstable region is

$$-(\theta_0 + n^2) \pm [4n^2\theta_0 + \theta_n^2]^{1/2} > \frac{4\beta_s^2}{\Omega^2} \tag{C.2}$$

Since $\theta_0 > 0$, $(\theta_0 + n^2)$ is also positive, and (C.2) is equivalent to

$$[\theta_n^2 + 4n^2\theta_0] > \left[\theta_0 + n^2 + \frac{4\beta_s^2}{\Omega^2}\right]^2$$

as the instability condition. Conversely, the requirement for stability is

$$4n^2\Theta_0 + \Theta_n^2 < \left[\Theta_0 + n^2 + \frac{4\beta_s^2}{\Omega^2}\right]^2 \tag{5.11}$$

Stability of the Solutions when both Self-Coupled Bending Modes are Excited

To investigate the stability of the solution (5.22b), the method of averaging was used. To apply this technique, let

$$\begin{aligned} \bar{A} &= \bar{A}_0 + a(\tau) \qquad \bar{\phi} = \bar{\phi}_0 + \varphi(\tau) \\ \bar{B} &= \bar{B}_0 + b(\tau) \qquad \bar{\psi} = \bar{\psi}_0 + \psi(\tau) \end{aligned} \tag{5.26}$$

where the steady-state solution has been redesignated by

$$\begin{aligned} \eta_c(\tau) &= \bar{A}_0 \cos[\Omega\tau + \bar{\phi}_0] \\ \eta_s(\tau) &= \bar{B}_0 \sin[\Omega\tau + \bar{\psi}_0] \end{aligned} \tag{5.27}$$

and a, b, φ, and ψ are perturbations in the amplitudes and phases of the steady-state solution.

To obtain the equations governing the perturbations, equations (5.26) are substituted into (5.15), and use is made of the fact that (5.27) satisfies (5.17). Only the first order terms in the perturbation quantities are retained, and the following equations result:

$$K_1 a + 4\Omega L_4 b + K_4 \frac{db}{d\tau} + [G_m \sin\bar{\phi}_0 + 4\Omega \bar{B}_0 K_4]\varphi - K_6 \frac{d\varphi}{d\tau} - 4\Omega \bar{B}_0 K_4 \psi + \bar{B}_0 K_8 \frac{d\psi}{d\tau} = 0 \quad \text{(C. 3a)}$$

$$4\Omega L_4 a - K_4 \frac{da}{d\tau} + M_3 b + 4\Omega \bar{A}_0 K_4 \varphi + \bar{A}_0 K_8 \frac{d\varphi}{d\tau} - 4\Omega \bar{A}_0 K_4 \psi - M_8 \frac{d\psi}{d\tau} = 0 \quad \text{(C. 3b)}$$

$$\frac{G_m \sin\bar{\phi}_0}{\bar{A}_0} a - L_2 \frac{da}{d\tau} - 4\Omega K_4 b + L_4 \frac{db}{d\tau} + [4\Omega L_4 \bar{B}_0 - G_m \cos\bar{\phi}_0]\varphi - 4\Omega L_4 \bar{B}_0 \psi - B_0 K_4 \frac{d\psi}{d\tau} = 0 \quad \text{(C. 3c)}$$

$$-4\Omega K_4 a - L_4 \frac{da}{d\tau} + N_4 \frac{db}{d\tau} + 4\Omega L_4 \bar{A}_0 \varphi - \bar{A}_0 K_4 \frac{d\varphi}{d\tau} - 4\Omega L_4 \bar{A}_0 \psi = 0 \quad \text{(C. 3d)}$$

where the following notation has been introduced:

$$K_1 = \frac{G_m \cos\bar{\phi}_0}{\bar{A}_0} - \frac{\epsilon\Omega^2 \bar{A}_0^2}{2}, \quad K_4 = \frac{1}{8}\epsilon\Omega \bar{A}_0 \bar{B}_0 \sin 2\bar{\Delta}_0$$

$$K_6 = \Omega \bar{A}_0 \left(2 + \frac{3\epsilon \bar{A}_0^2}{8}\right), \quad K_8 = -\frac{\epsilon\Omega \bar{A}_0 \bar{B}_0}{4}\left(1 - \frac{1}{2}\cos 2\bar{\Delta}_0\right)$$

$$L_2 = 2\Omega + \frac{\epsilon\Omega \bar{A}_0^2}{8}, \quad L_4 = \frac{1}{8}\epsilon\Omega \bar{A}_0 \bar{B}_0 \cos 2\bar{\Delta}_0$$

$$M_3 = -\frac{\epsilon\Omega^2 \bar{B}_0^2}{2}, \quad M_8 = \Omega \bar{B}_0 \left(2 + \frac{3\epsilon \bar{B}_0^2}{8}\right)$$

$$N_4 = 2\Omega + \frac{\epsilon\Omega \bar{B}_0^2}{8}$$

Equations (C. 3) form a linear system with constant coefficients; to solve them, one inserts

$$a(\tau) = a_1 e^{\lambda\tau} \qquad \varphi(\tau) = \varphi_1 e^{\lambda\tau}$$
$$b(\tau) = b_1 e^{\lambda\tau} \qquad \psi(\tau) = \psi_1 e^{\lambda\tau} \tag{5.29}$$

and requires a non-trivial solution. This results in an eigenvalue problem, whose determinant is given below:

$$0 = \begin{vmatrix} K_1 & (4\Omega L_4 + \lambda K_4) & (G_m \sin\bar{\phi}_o - 4\Omega \bar{B}_o K_4 - \lambda K_2) & (\lambda \bar{B}_o - 4\Omega \bar{B}_o K_4) \\ (4\Omega L_4 - \lambda K_4) & M_3 & (4\Omega \bar{A}_o K_4 + \lambda \bar{A}_o K_8) & (-\lambda M_8 - 4\Omega \bar{A}_o K_4) \\ \left(\frac{G_m \sin\bar{\phi}_o}{A_o} - \lambda L_2\right) & (\lambda L_4 - 4\Omega K_4) & (-G_m \cos\bar{\phi}_o + 4\Omega L_4 \bar{B}_o) & (-\lambda \bar{B}_o K_4 - 4\Omega \bar{B}_o L_4) \\ -(\lambda L_4 + 4\Omega K_4) & \lambda N_4 & (4\Omega \bar{A}_o L_4 - \lambda \bar{A}_o K_8) & -(4\Omega \bar{A}_o L_4) \end{vmatrix} \tag{C.4}$$

When this is multiplied out, a polynomial for λ results. The Routh-Hurwitz criteria (or some other stability criteria) can then be applied to the polynomial to determine if $\mathrm{Re}(\lambda) \gtrless 0$. This procedure must be carried out for each combination of $\bar{A}_o$, $\bar{B}_o$, $\bar{\phi}_o$, $\bar{\psi}_o$, G_n etc., to determine the stable and unstable regions of the solution (5. 22a).

An alternative procedure is to solve the eigenvalue problem numerically on a computer directly for the eigenvalues themselves. This approach was considered, but it has not been carried out.

Finally, one can obtain approximate stability boundaries by neglecting the effect of damping in (C. 4). Considerable simplification results, and the determinant may then be put in the form (5. 31). In

this case, it becomes practical to do the computations by hand, and a polynomial of the form

$$z^4 + 2\alpha^2(\alpha^2+\beta^2)z^2 + \alpha^2\beta^2(\alpha^2-\beta^2)^2 = 0 \qquad (5.32)$$

is obtained, where the substitution $z = 2\Omega\lambda$ has been used. For the roots of (5.32) to have non-negative real parts, the conditions

$$2\alpha^2(\alpha^2+\beta^2) \geq 0$$

and

$$4\alpha^8\left[1 + \left(\frac{\beta}{\alpha}\right)^2 + 3\left(\frac{\beta}{\alpha}\right)^4 - \left(\frac{\beta}{\alpha}\right)^6\right] \geq 0$$

must be satisfied.

Solving $\left(\frac{\beta}{\alpha}\right)^6 - 3\left(\frac{\beta}{\alpha}\right)^4 - \left(\frac{\beta}{\alpha}\right)^2 - 1 = 0$, one finds a positive real root, $\left(\frac{\beta}{\alpha}\right)^2 = 3.38$ and two negative roots; the latter have no physical significance. By examining (5.33) in the vicinity of $\left(\frac{\beta}{\alpha}\right)^2 = 3.38$, one can show that the inequality will be satisfied (and the two mode solution will be stable) if $\left(\frac{\beta}{\alpha}\right)^2 \leq 3.38$.

The above result was obtained by neglecting the damping terms in the stability determinant; from previous experience, one suspects that including damping will alter the undamped stability boundaries in a relatively small region. This is sketched qualitatively in Fig. 7.

TABLE I

EXPERIMENTAL RESPONSE SURVEY

Mode (s) Vibrating	Driving Frequency (cps)	Type of Response
n = 2	7.1	
n = 3	17.5	
n = 4	33.0	
n = 6	78.0	Resonance at the
n = 7	107.4	Driving Frequency
n = 8	139.2	
n = 9	179.6	
n = 10	222.8	
n = 3	8.8	Ultraharmonic, order 1/2
n = 4	11.1	Ultraharmonic, order 1/3
n = 7	213.0	Subharmonic, order 2
n = 8	69.8	Ultraharmonic, order 1/2
n = 8	47.6	Ultraharmonic, order 1/3
n = 9	92.3	Ultraharmonic, order 1/2

TABLE I (cont'd)

EXPERIMENTAL RESPONSE SURVEY

Mode (s) Vibrating	Driving Frequency (cps)	Type of Response
n = 3 n = 5	26.7	n = 3 at 26.7 cps, n = 5 at 53.4 cps
n = 4 n = 6	39.0	n = 4 at 39.0 cps, n = 6 at 78.0 cps
n = 4 n = 7	35.8	n = 4 at 35.8 cps, n = 7 at 107.4 cps
n = 4 n = 8	35.3	n = 4 at 35.3 cps, n = 8 at 141.2 cps
n = 5 n = 9	60.5	n = 5 at 60.5 cps, n = 9 at 181.5 cps

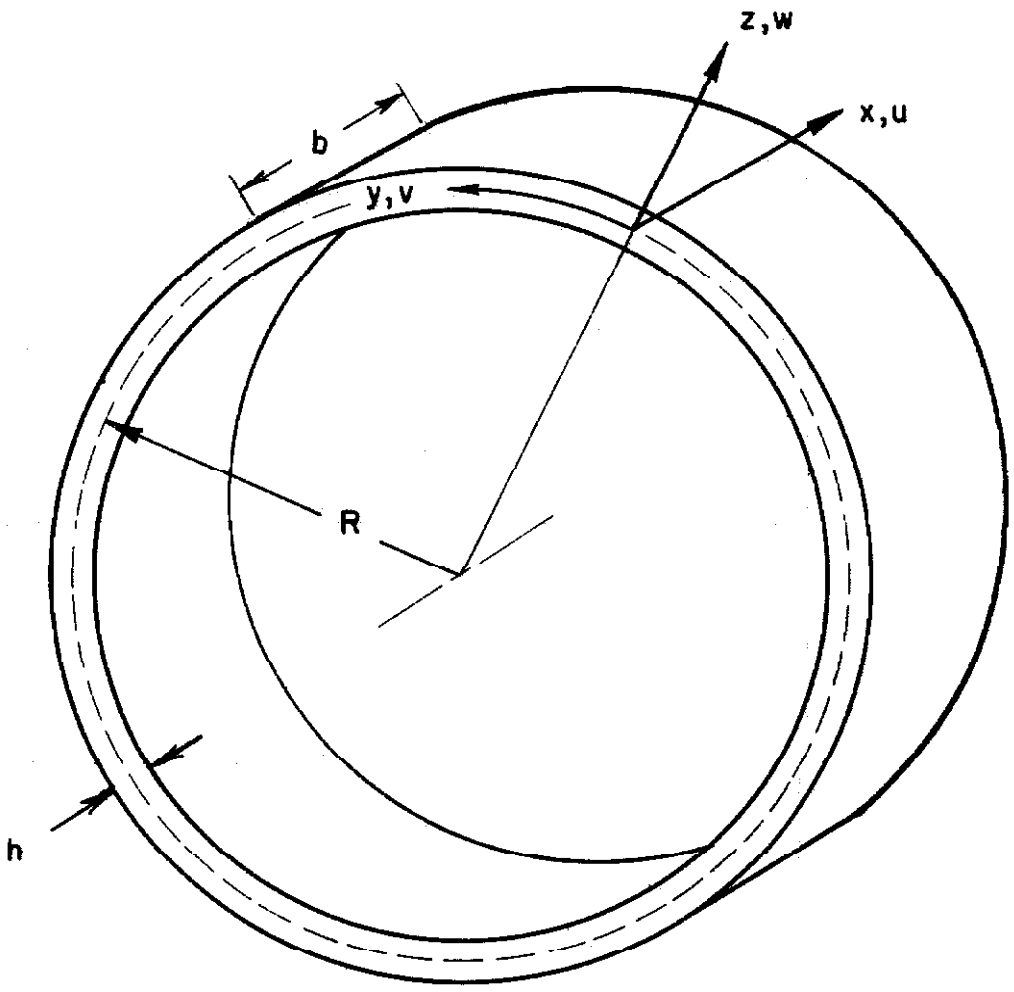

FIG. 1 RING GEOMETRY AND COORDINATE SYSTEM

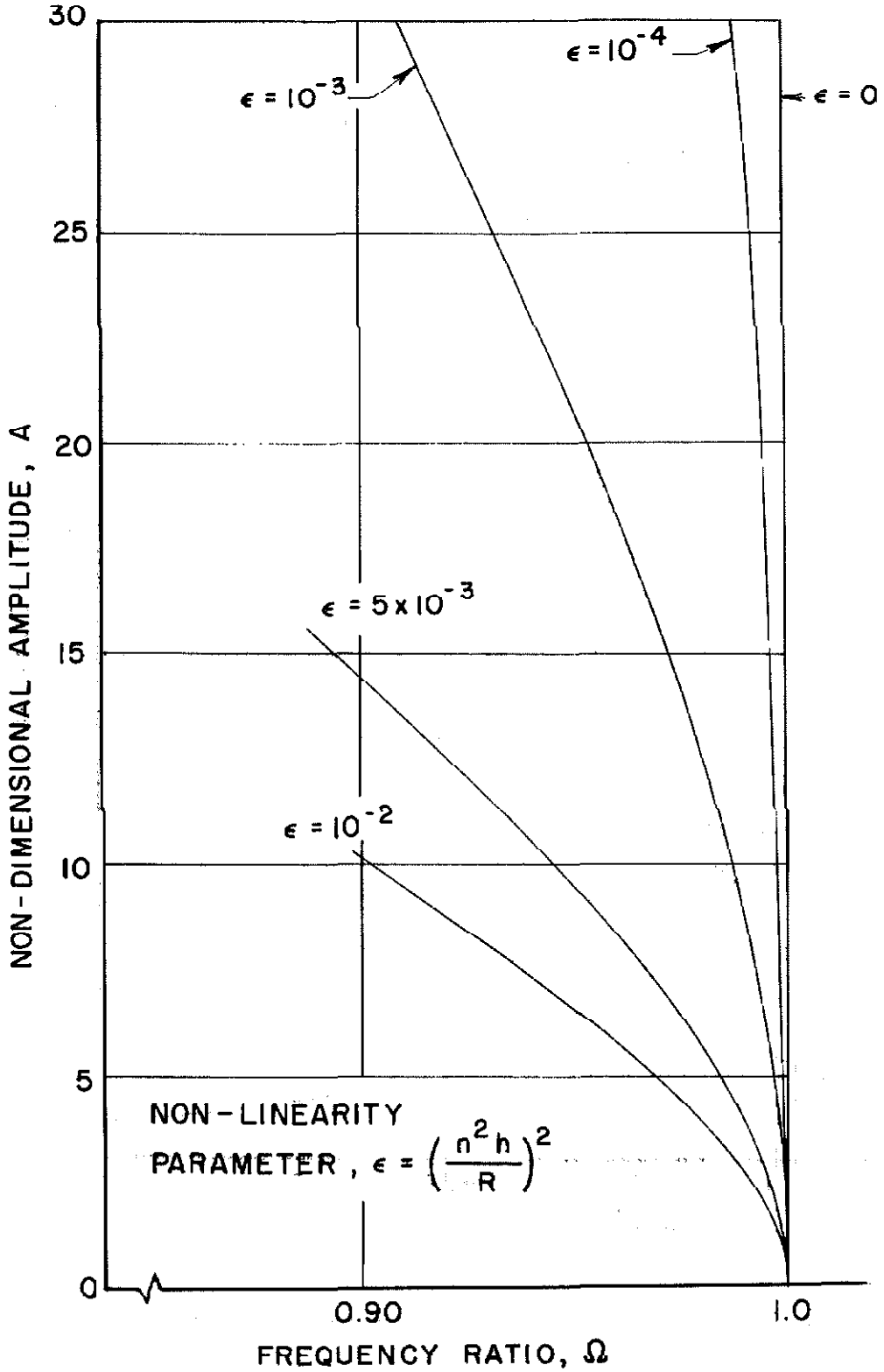

FIG. 2 BACKBONE CURVES FOR VARIOUS ϵ

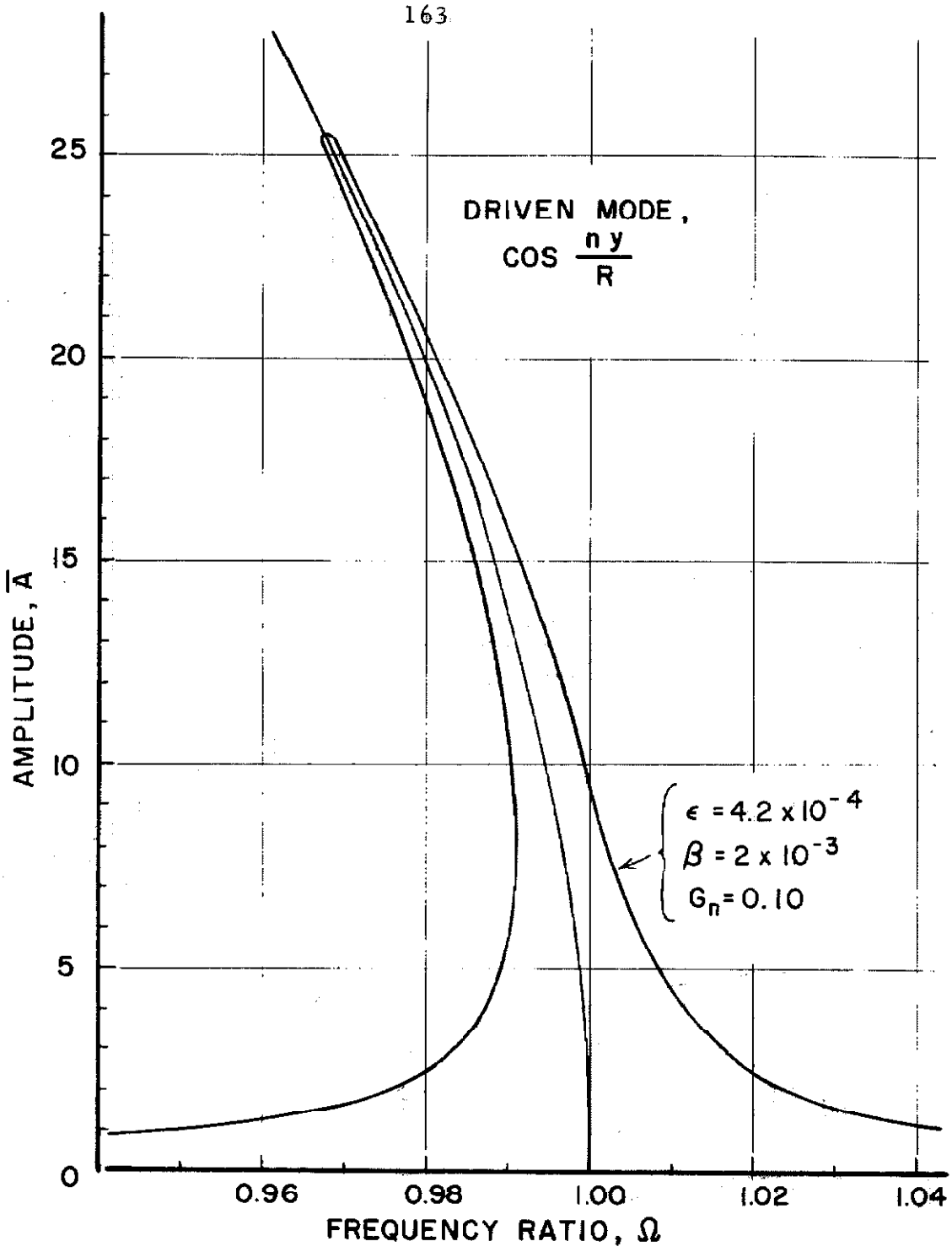

FIG. 3 TYPICAL SINGLE MODE RESPONSE

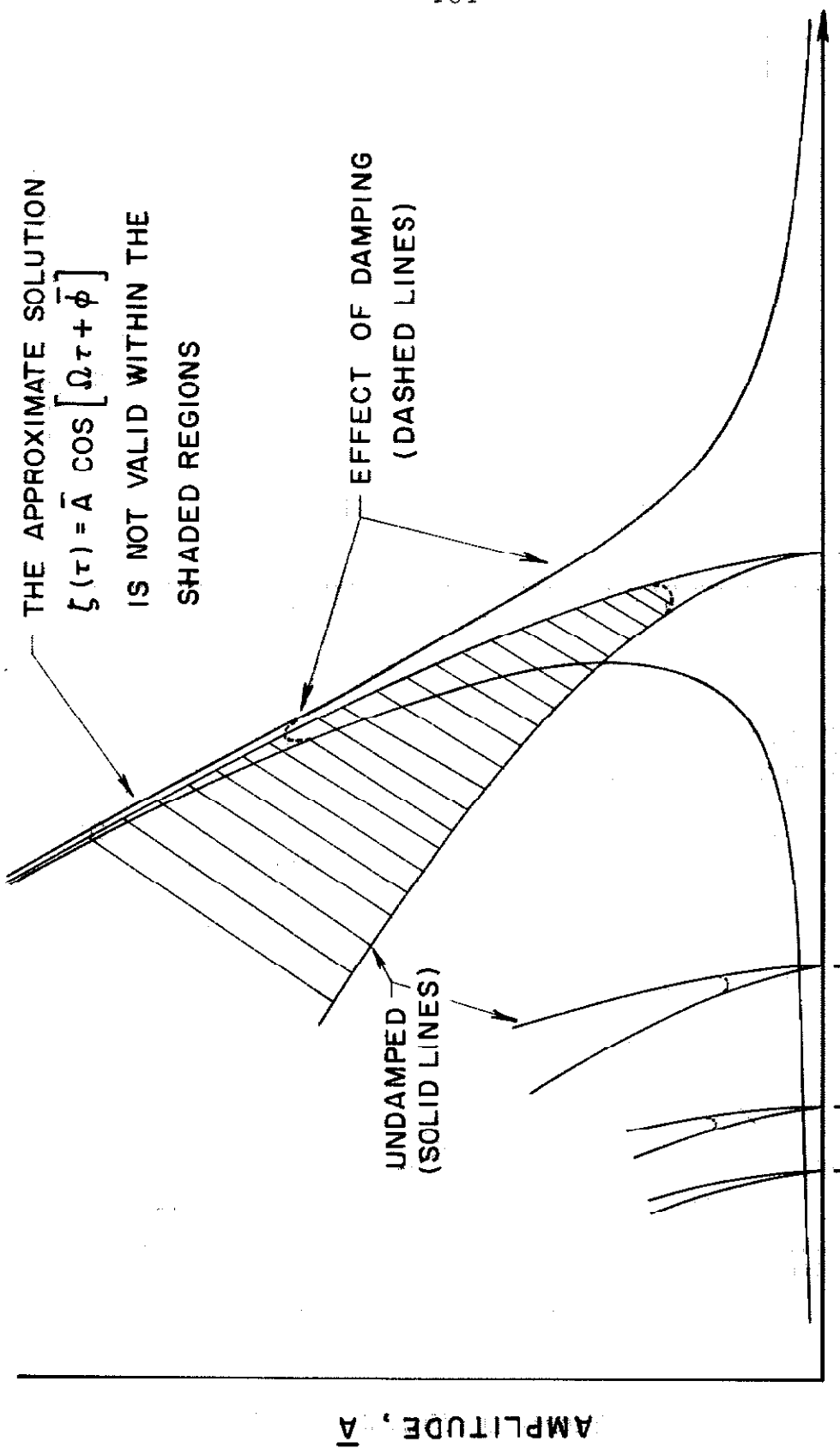

FIG. 4 RESULTS OF THE STABILITY ANALYSIS (ONE MODE)

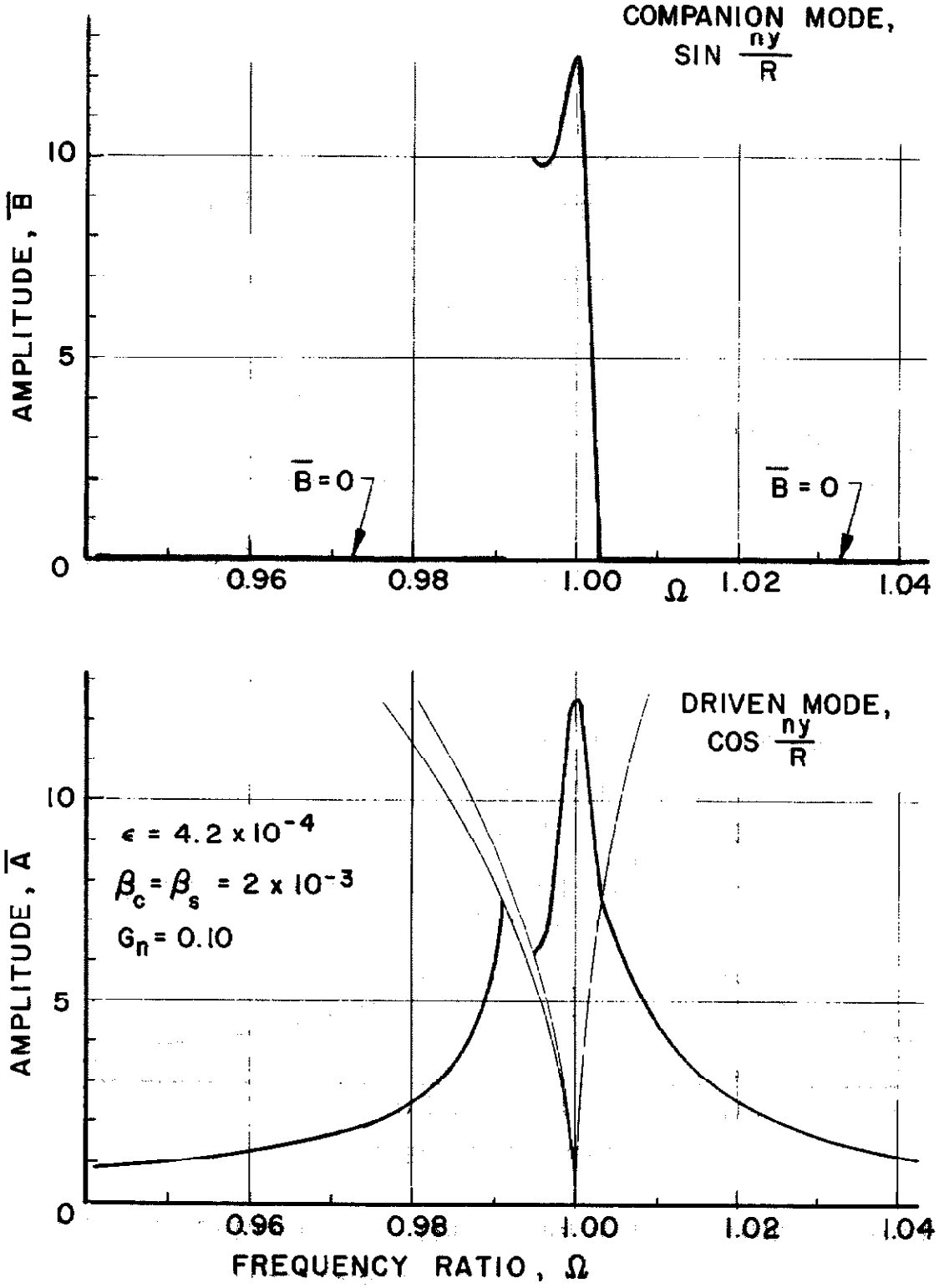

FIG. 5 TYPICAL COUPLED MODE RESPONSE

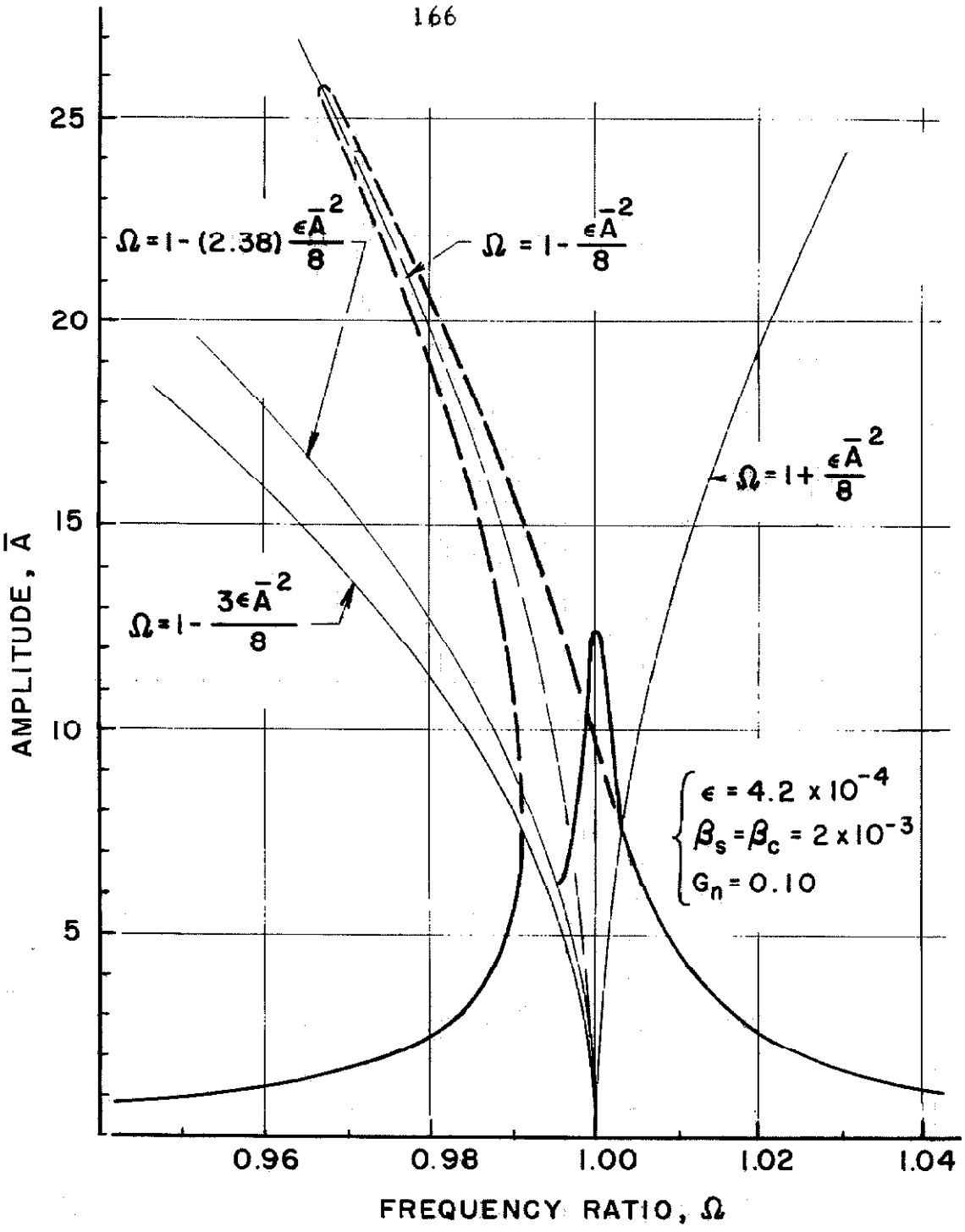

FIG. 6 COMPARISON OF THE SINGLE MODE AND COUPLED MODE RESPONSES

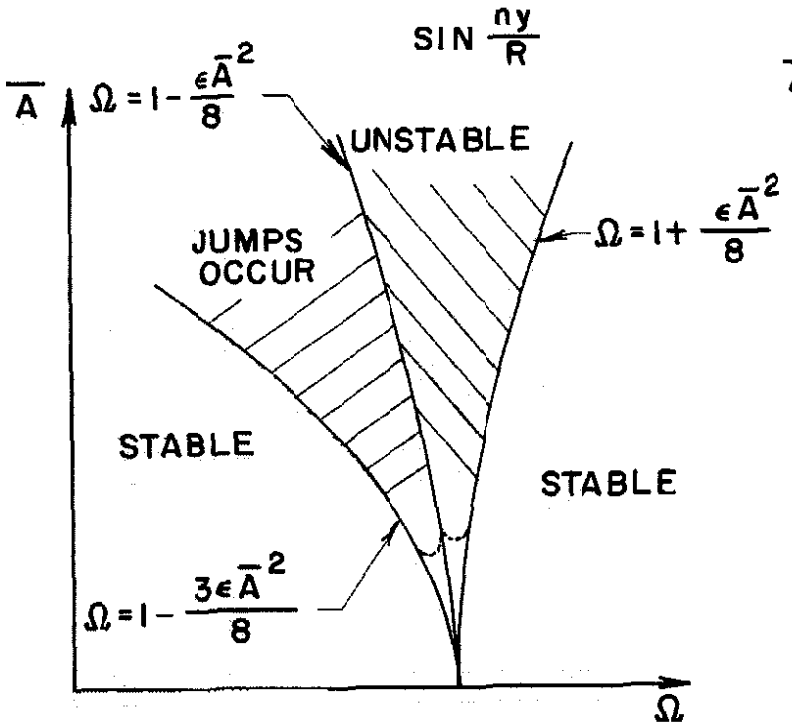

STABILITY DIAGRAM FOR THE SOLUTION

$$\zeta_c = \bar{A} \cos\left[\Omega\tau + \bar{\phi}\right]$$

$$\zeta_s = 0$$

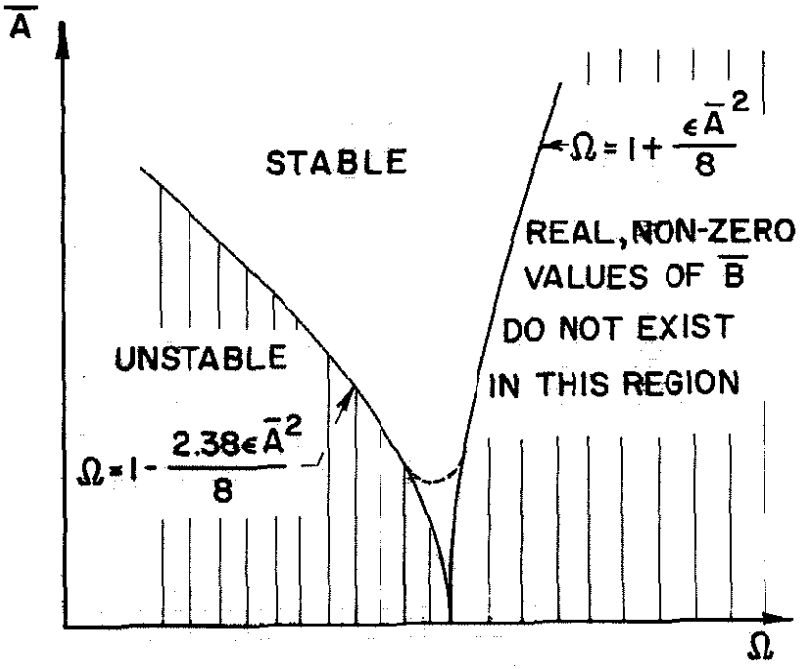

STABILITY DIAGRAM FOR THE SOLUTION

$$\zeta_c = \bar{A} \cos\left[\Omega\tau + \bar{\phi}\right]$$

$$\zeta_s = \bar{B} \sin\left[\Omega\tau + \bar{\psi}\right]$$

FIG. 7 SUMMARY OF THE STABILITY ANALYSES

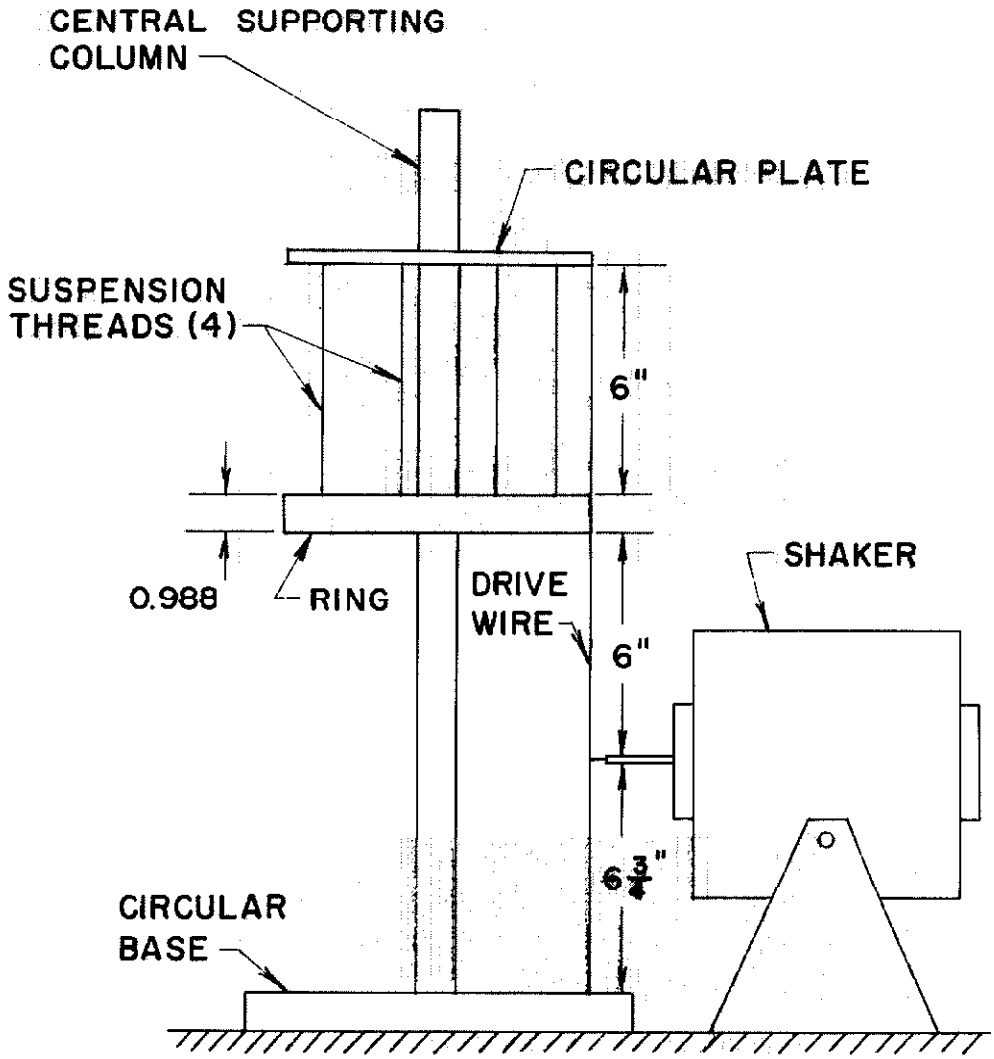

FIG. 8 DIAGRAM OF THE SUSPENSION AND DRIVE SYSTEM

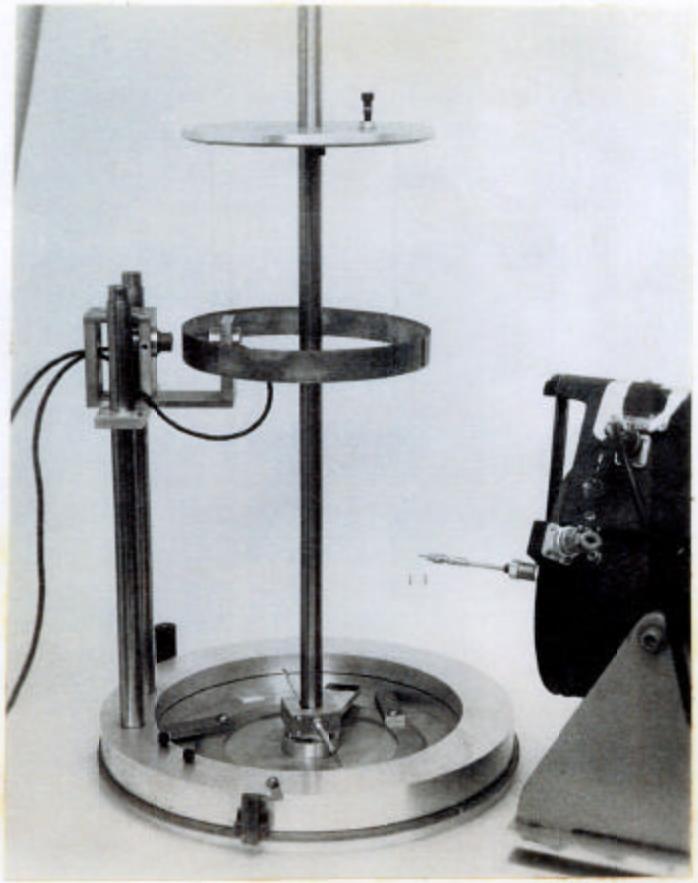

Fig. 9 Overall View of the Experimental Set-Up

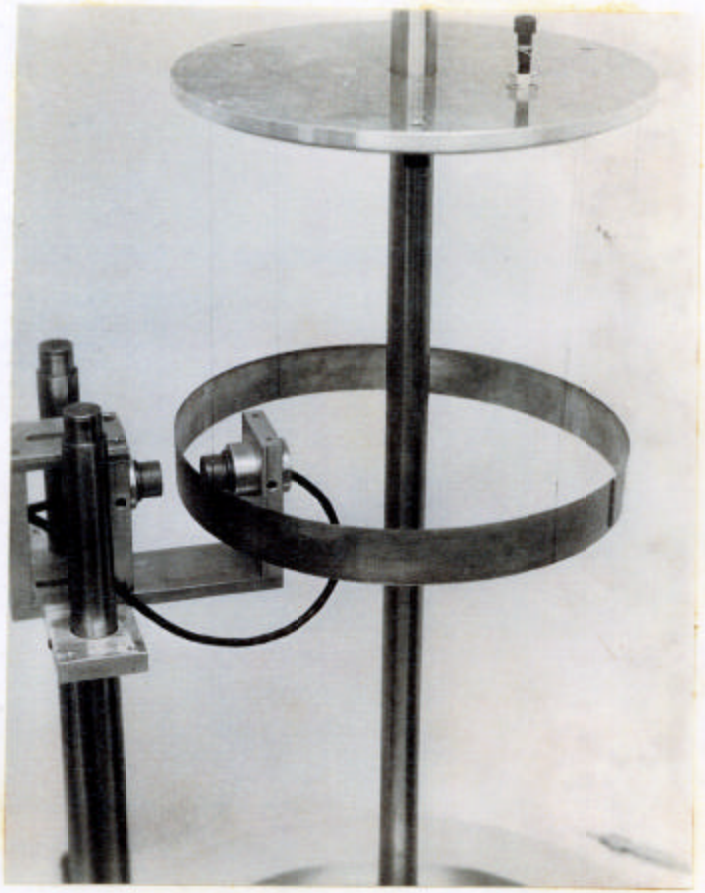

Fig. 10 Closeup of the Ring, showing the Displacement Pickups and the Suspension Threads

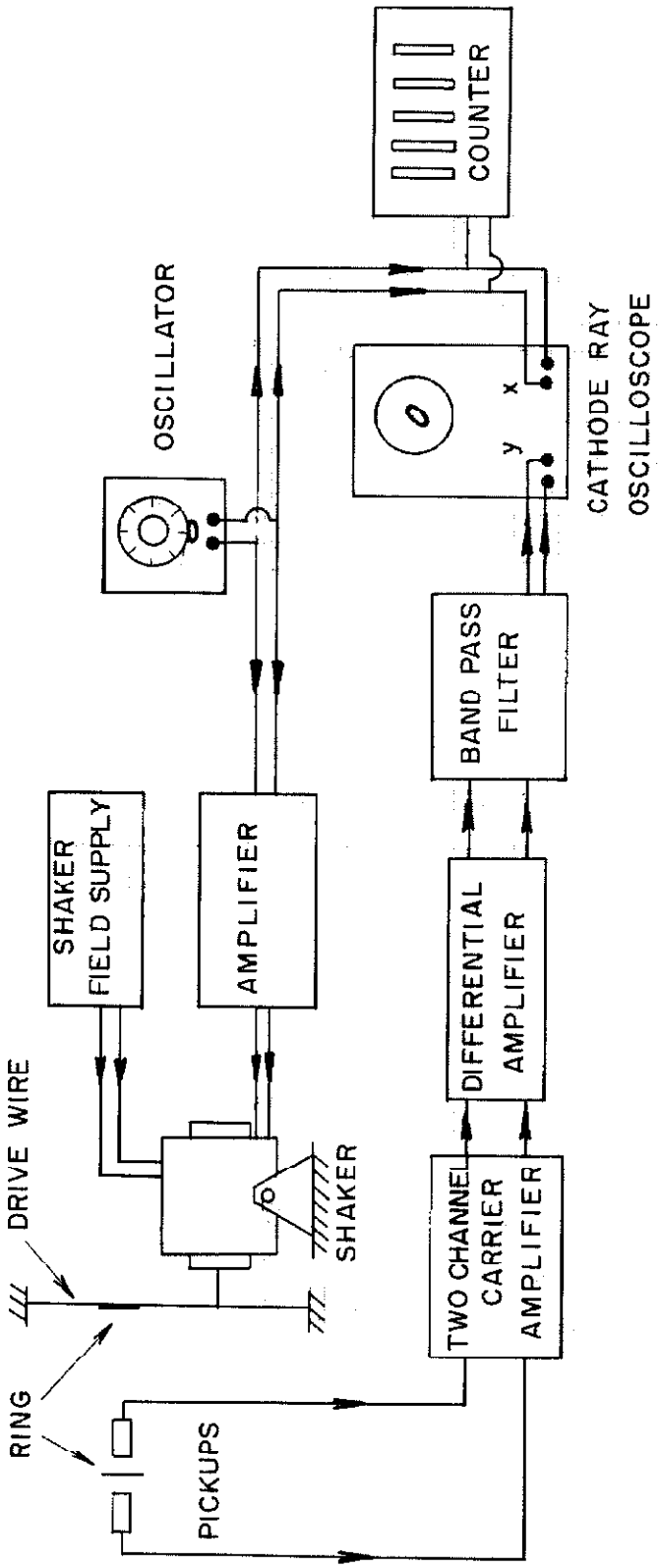

FIG. II BLOCK DIAGRAM OF THE EXPERIMENTAL SET-UP

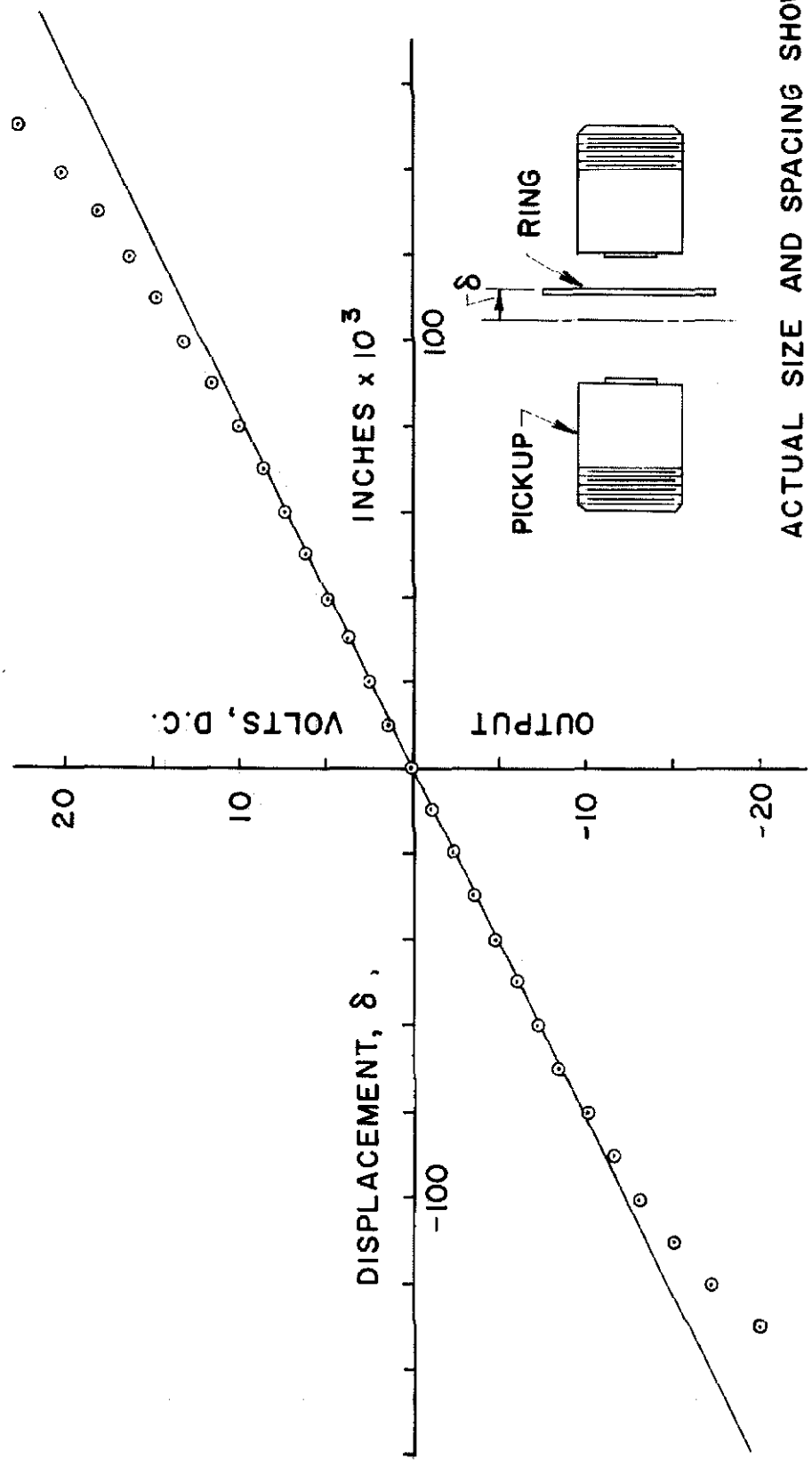

FIG. 12 CALIBRATION CURVE FOR THE PICKUP SYSTEM

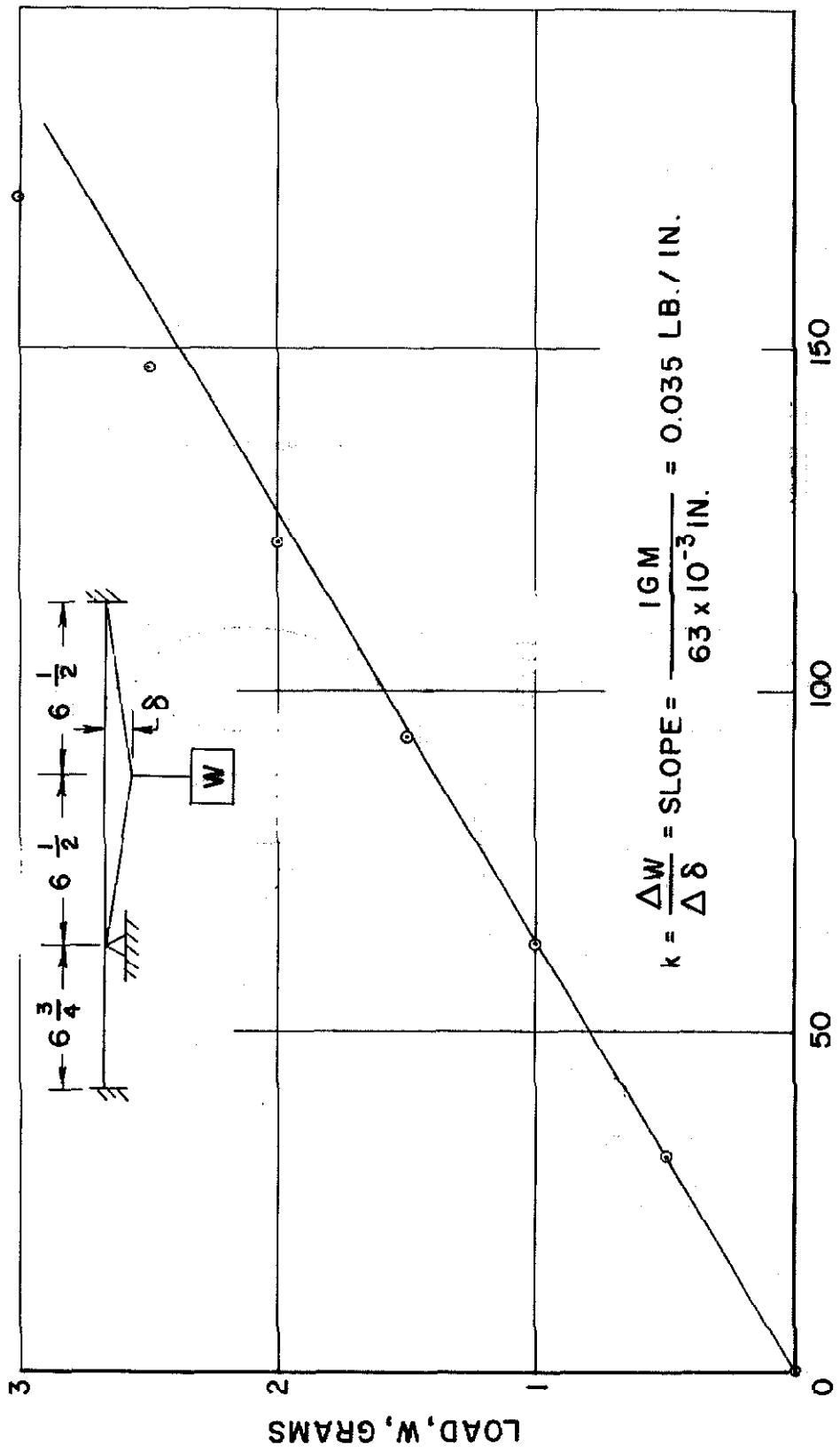

FIG. 13 CALIBRATION OF THE DRIVE WIRE

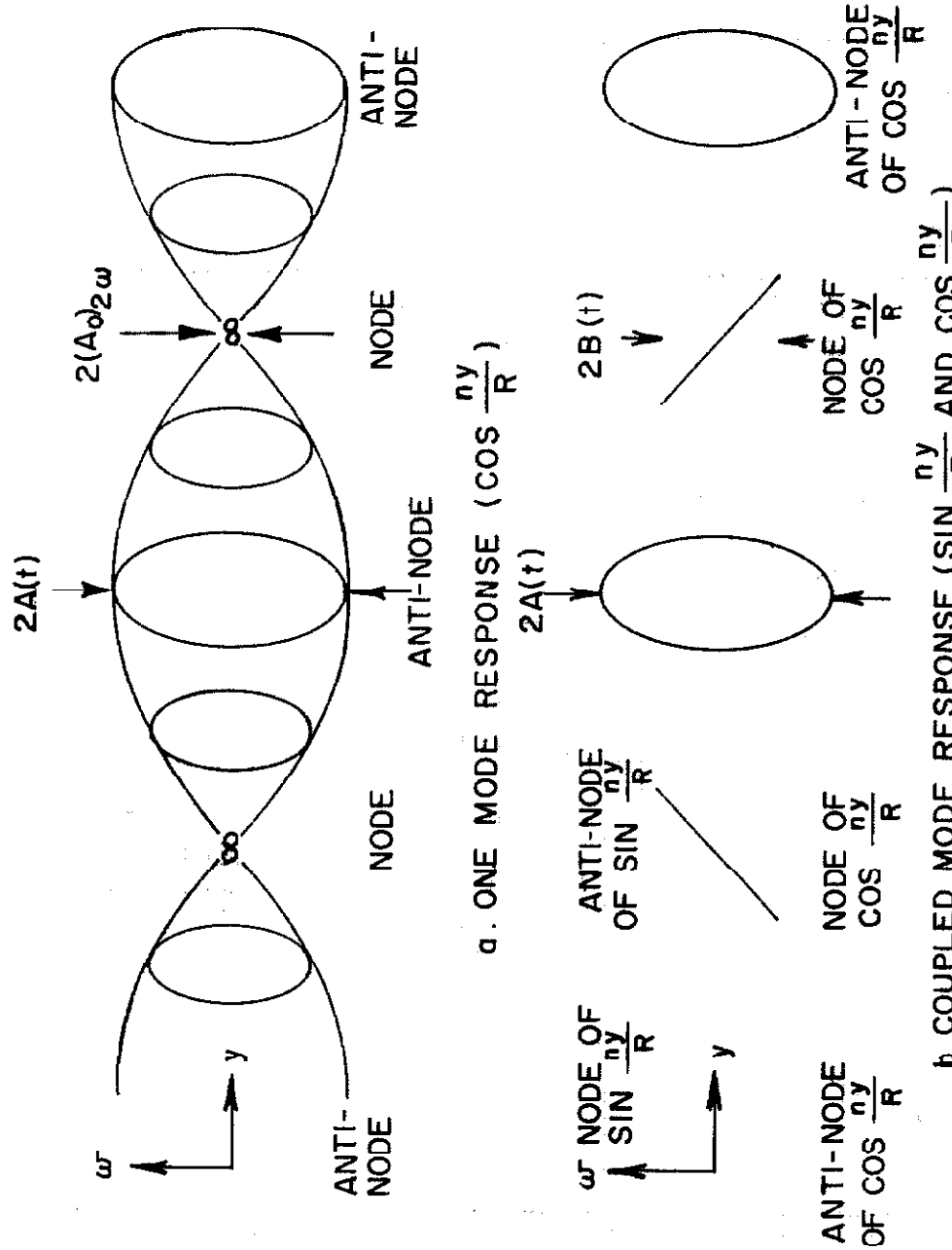

FIG. 14 CIRCUMFERENTIAL VARIATION OF THE LISSAJOUS FIGURES

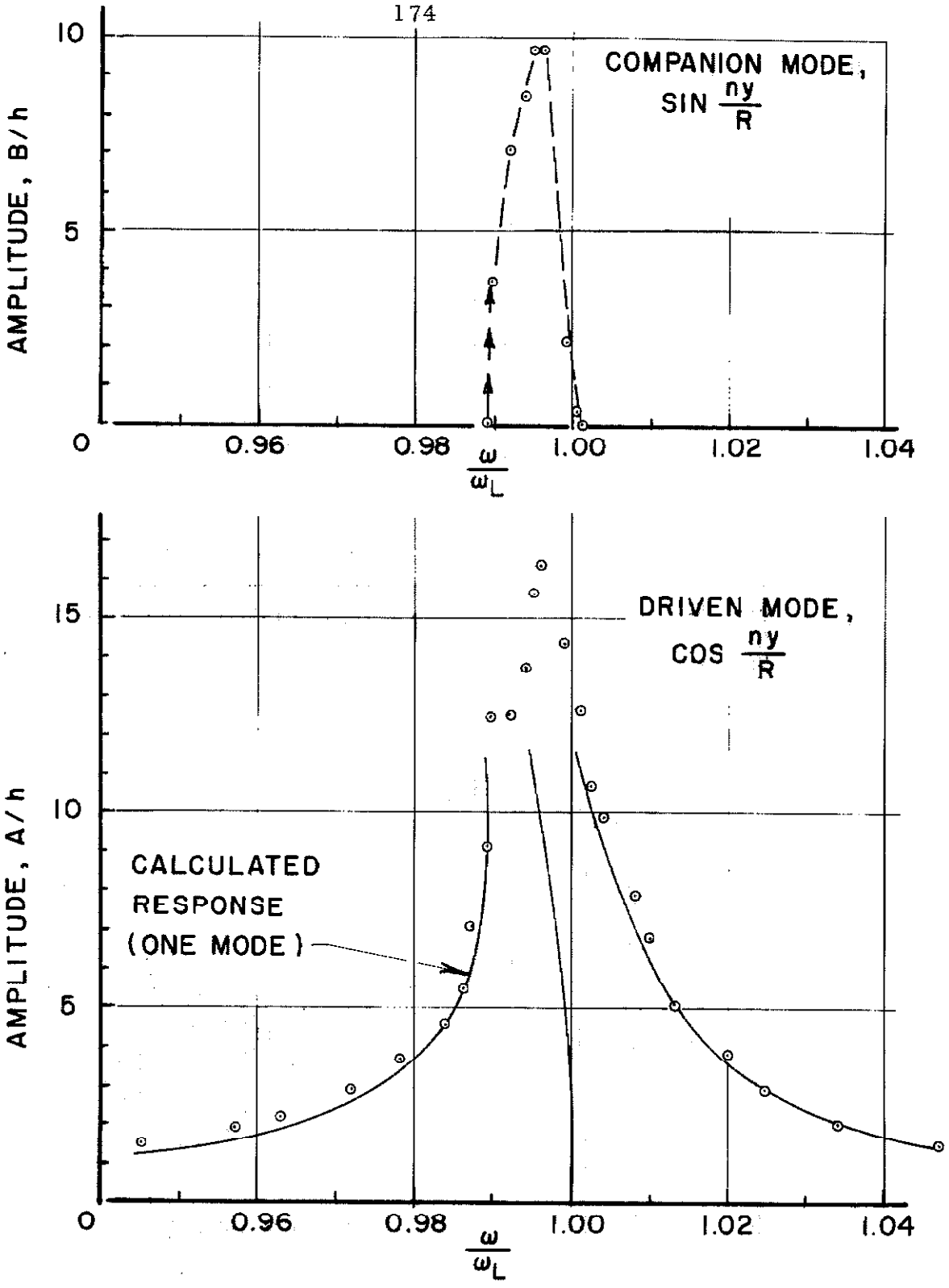

FIG. 15 n = 4 RESPONSE (NO MASS ADDED) SHAKER DISPLACEMENT : $2\delta_0 = 200 \times 10^{-3}$ IN.

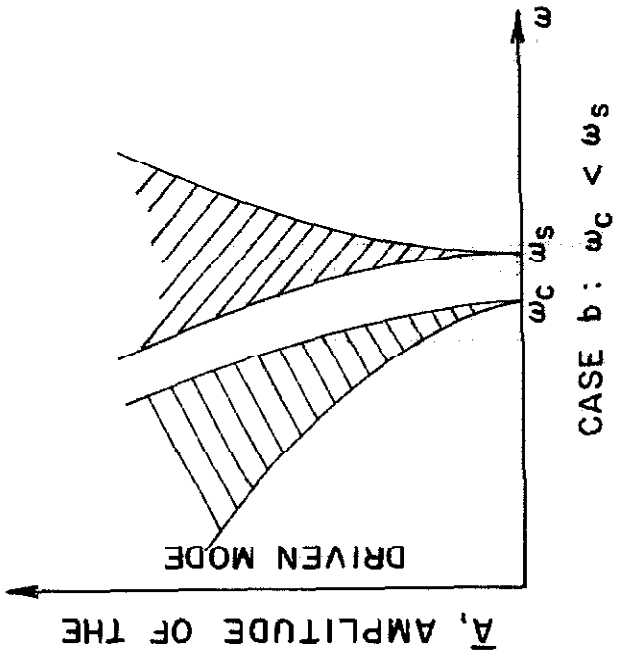

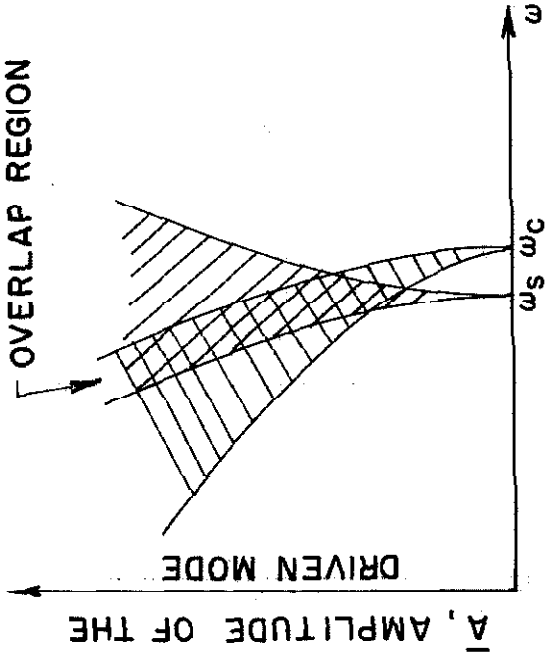

ω_c = LINEAR FREQUENCY OF COS $\frac{ny}{R}$

ω_s = LINEAR FREQUENCY OF SIN $\frac{ny}{R}$

▨ DRIVEN MODE IS UNSTABLE; "JUMPS" OCCUR

▨ COMPANION MODE IS EXCITED; BOTH MODES VIBRATE

FIG. 16 SHIFT OF THE INSTABILITY REGIONS DUE TO CHANGES IN NATURAL FREQUENCY

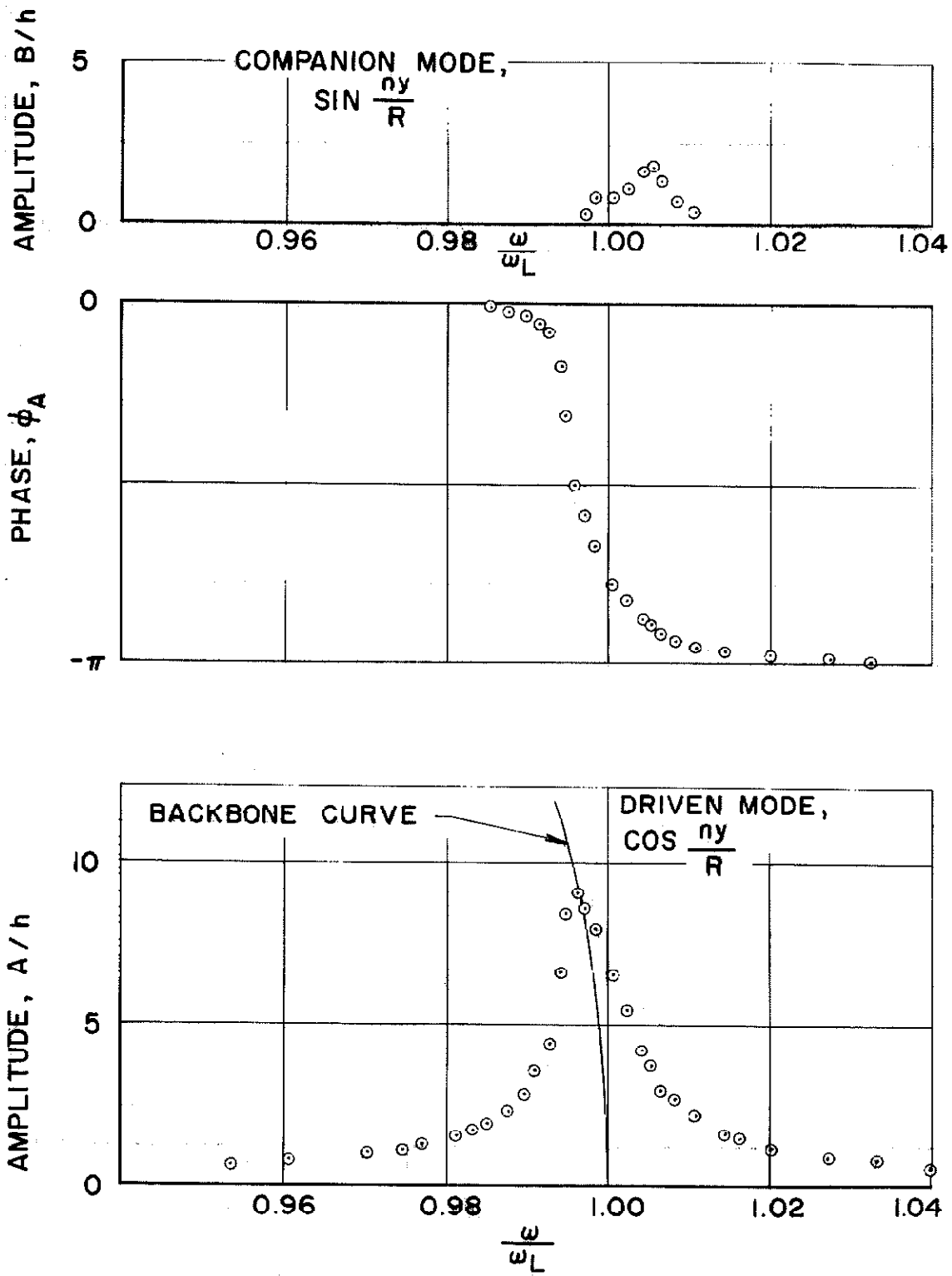

FIG. 17a n = 4 RESPONSE (MASS ADDED)
SHAKER DISPLACEMENT: $2\delta_0 = 100 \times 10^{-2}$ IN.

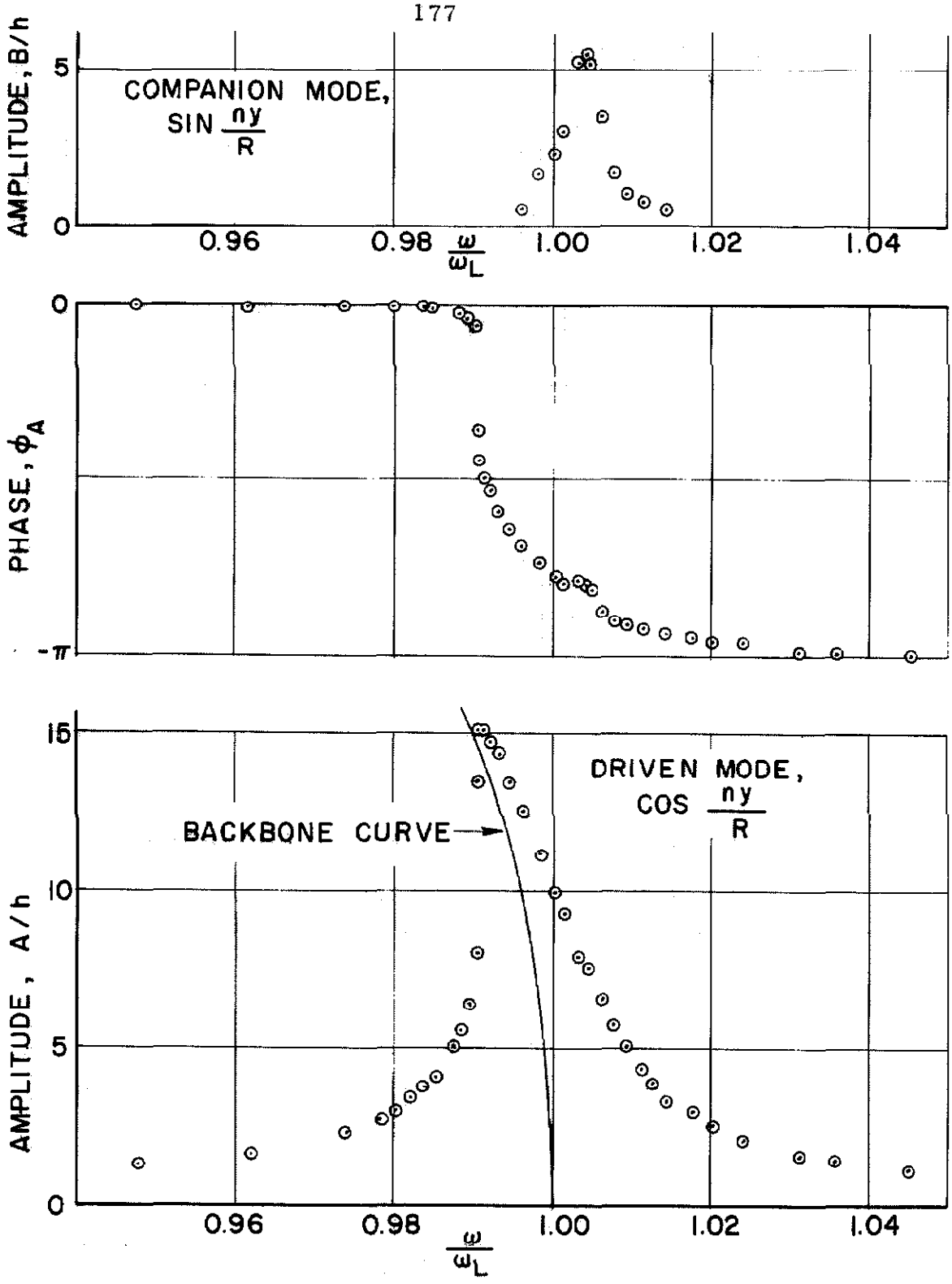

FIG. 17 b n = 4 RESPONSE (MASS ADDED)
SHAKER DISPLACEMENT: $2\delta_0 = 200 \times 10^{-3}$ IN.

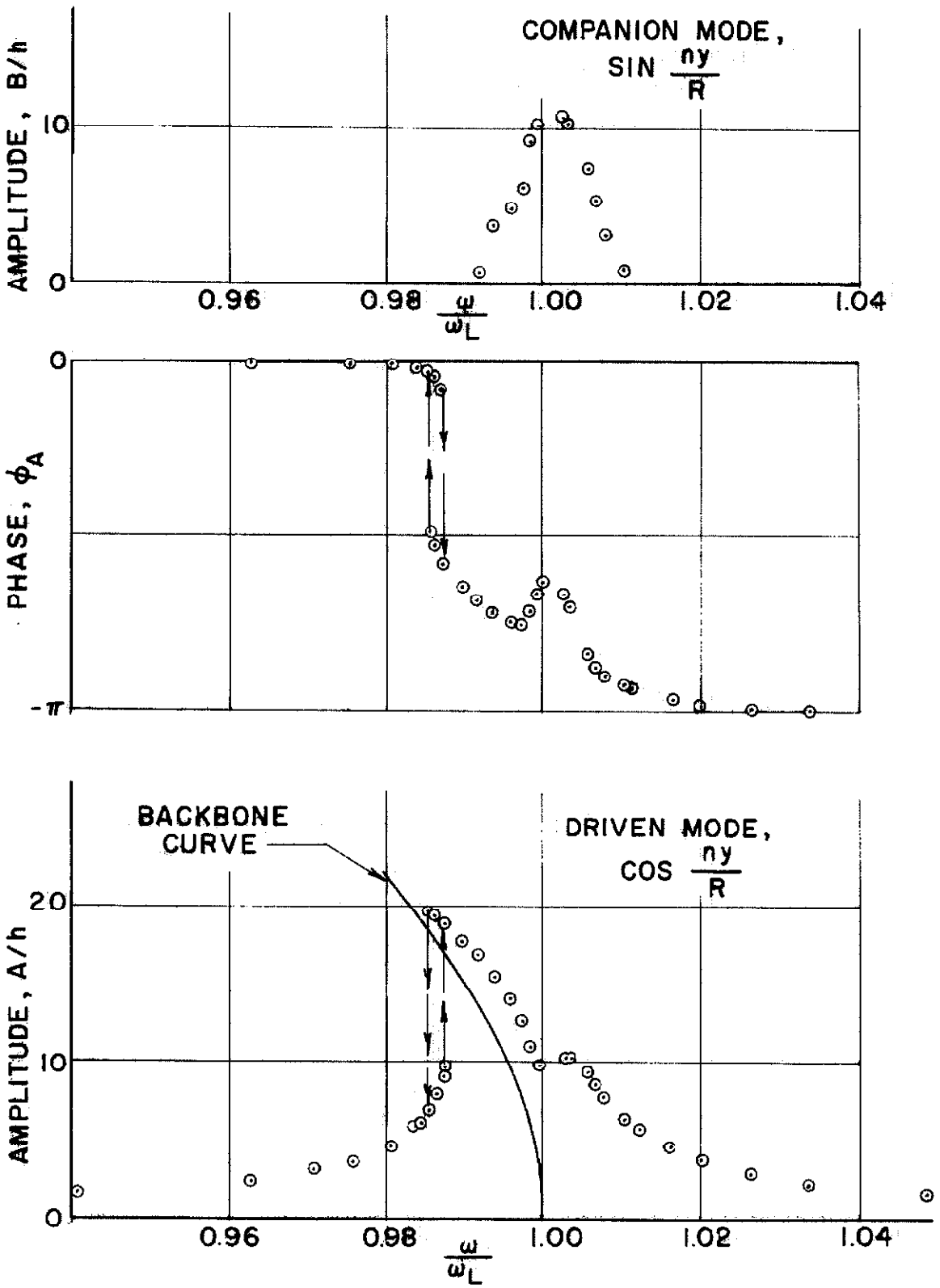

FIG. 17c n = 4 RESPONSE (MASS ADDED)
SHAKER DISPLACEMENT : $2\delta_0 = 300 \times 10^{-3}$ IN.

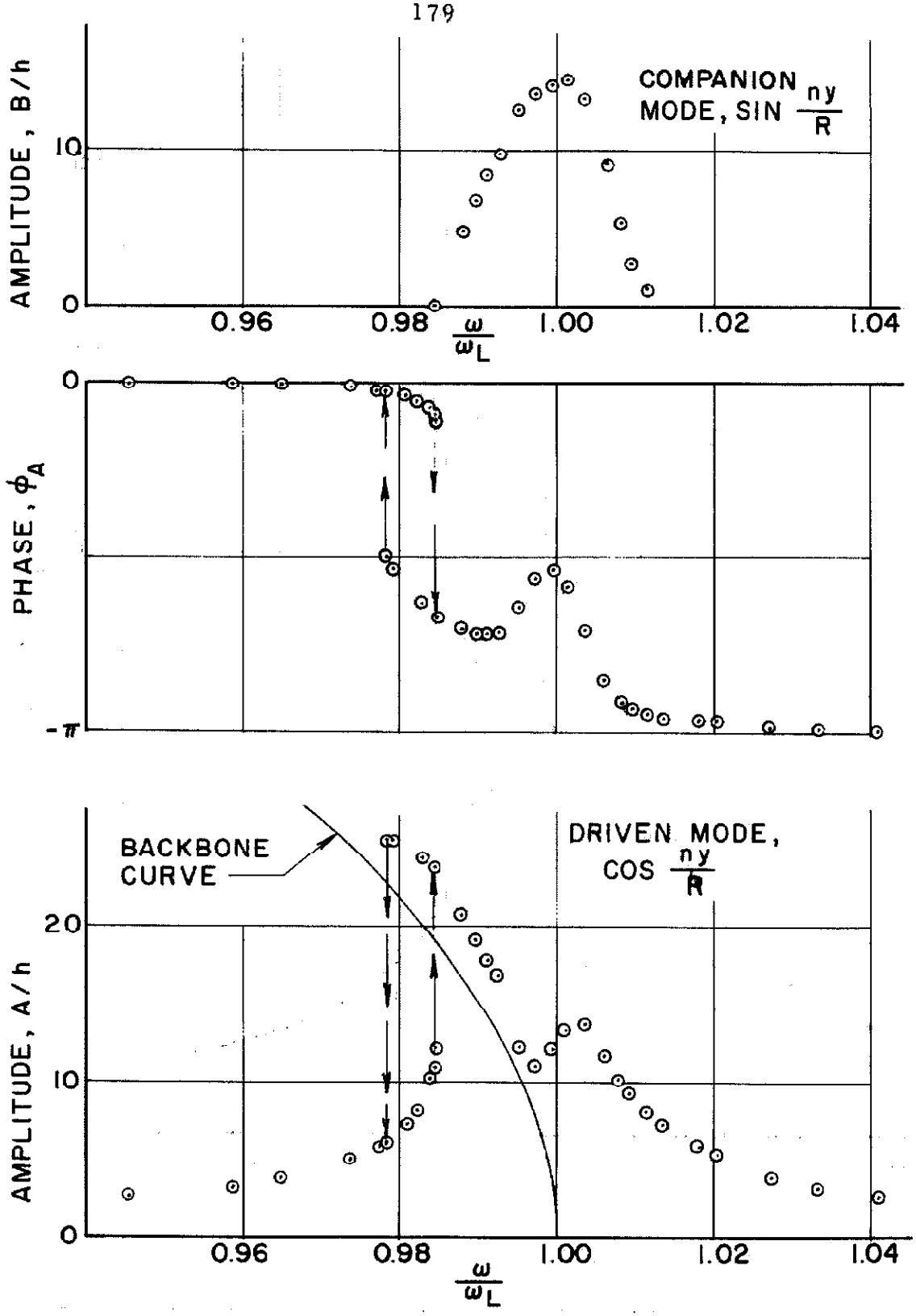

FIG. 17 d n = 4 RESPONSE (MASS ADDED)
SHAKER DISPLACEMENT : $2\delta_0 = 400 \times 10^{-3}$ IN.

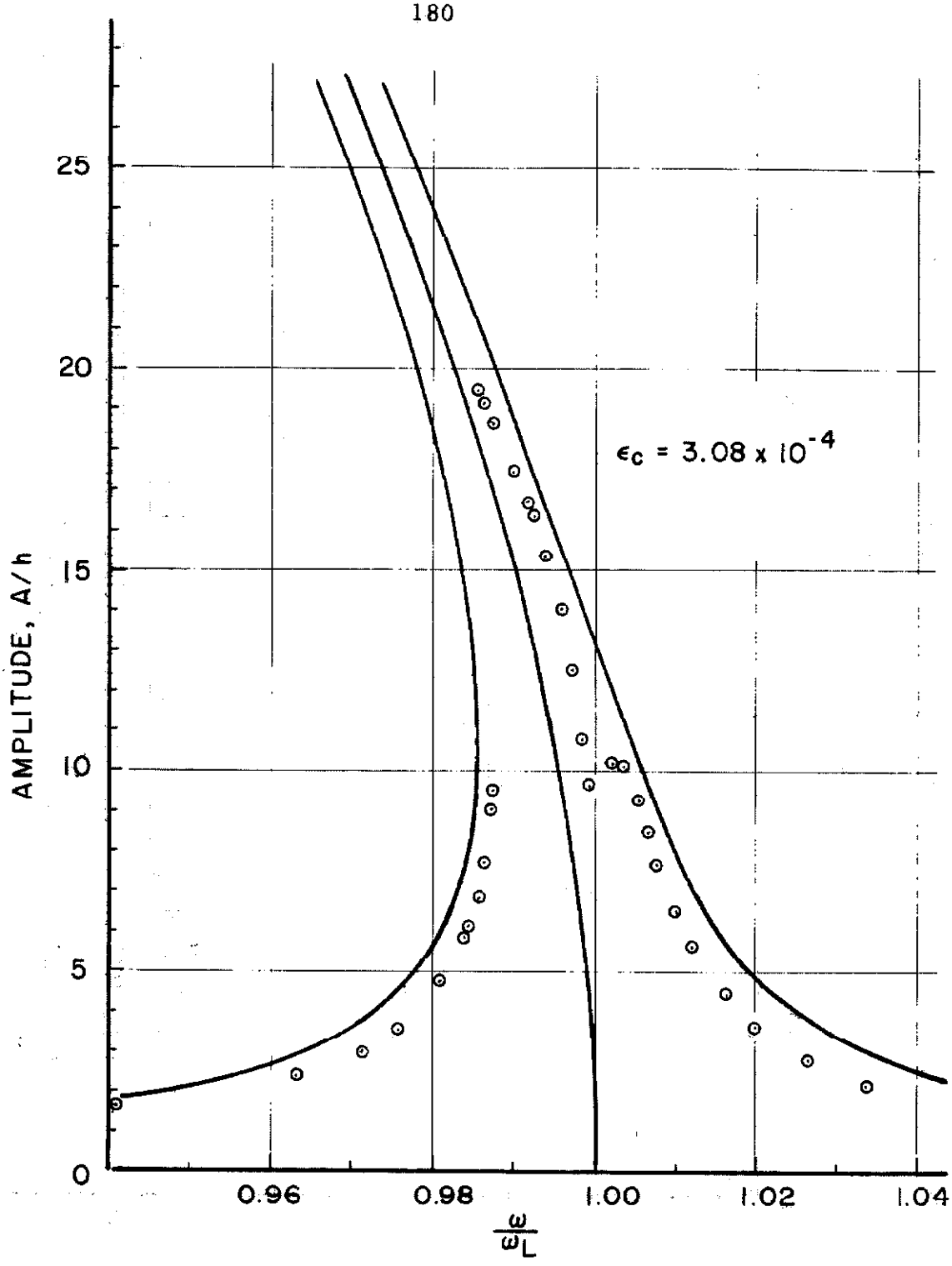

FIG. 17e CALCULATED AND MEASURED RESPONSE. n = 4, MASS ADDED, $2\delta_0 = 300 \times 10^{-3}$ IN.

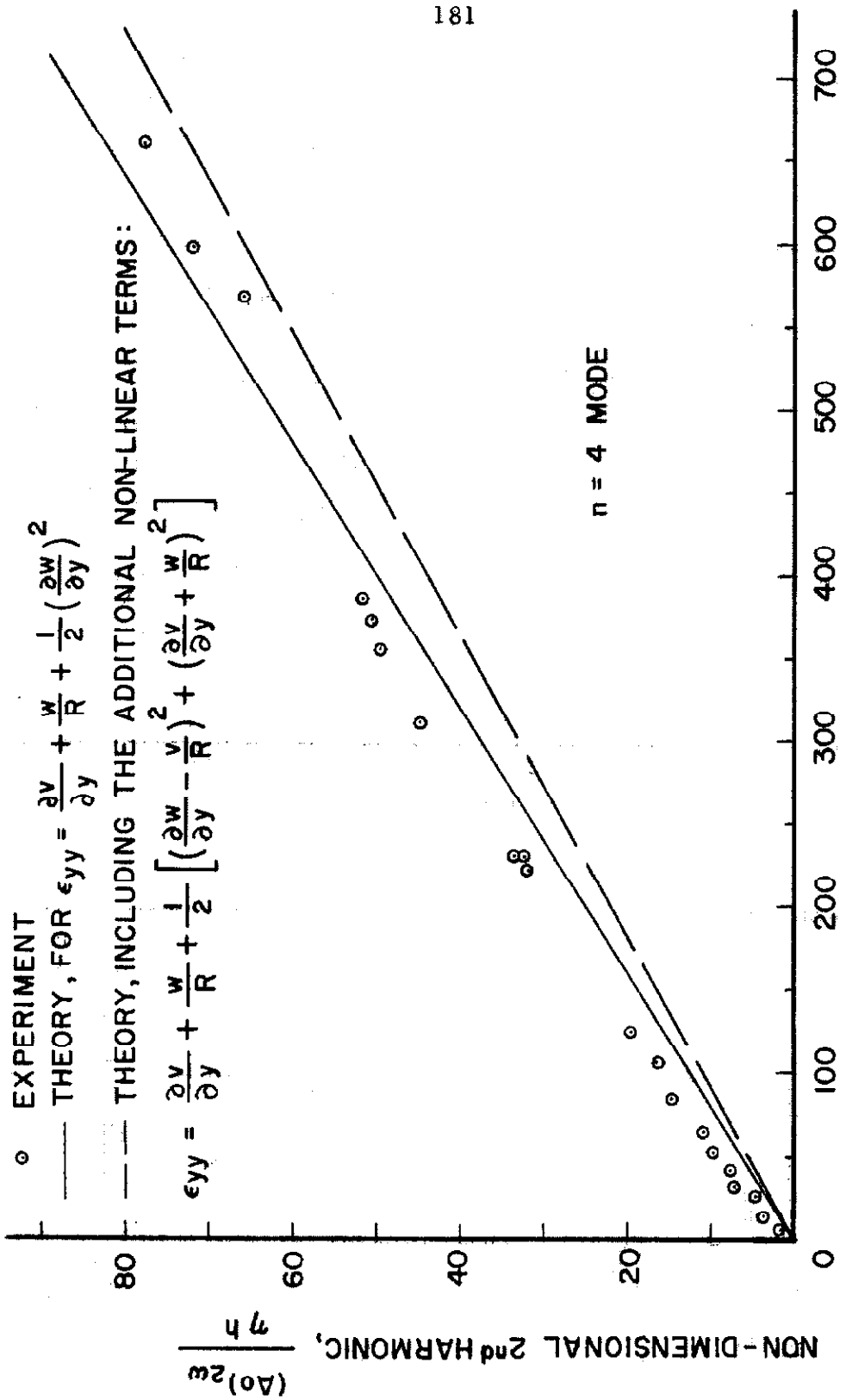

FIG. 17 f SECOND HARMONIC AT THE NODES VS (AMPLITUDE)^2

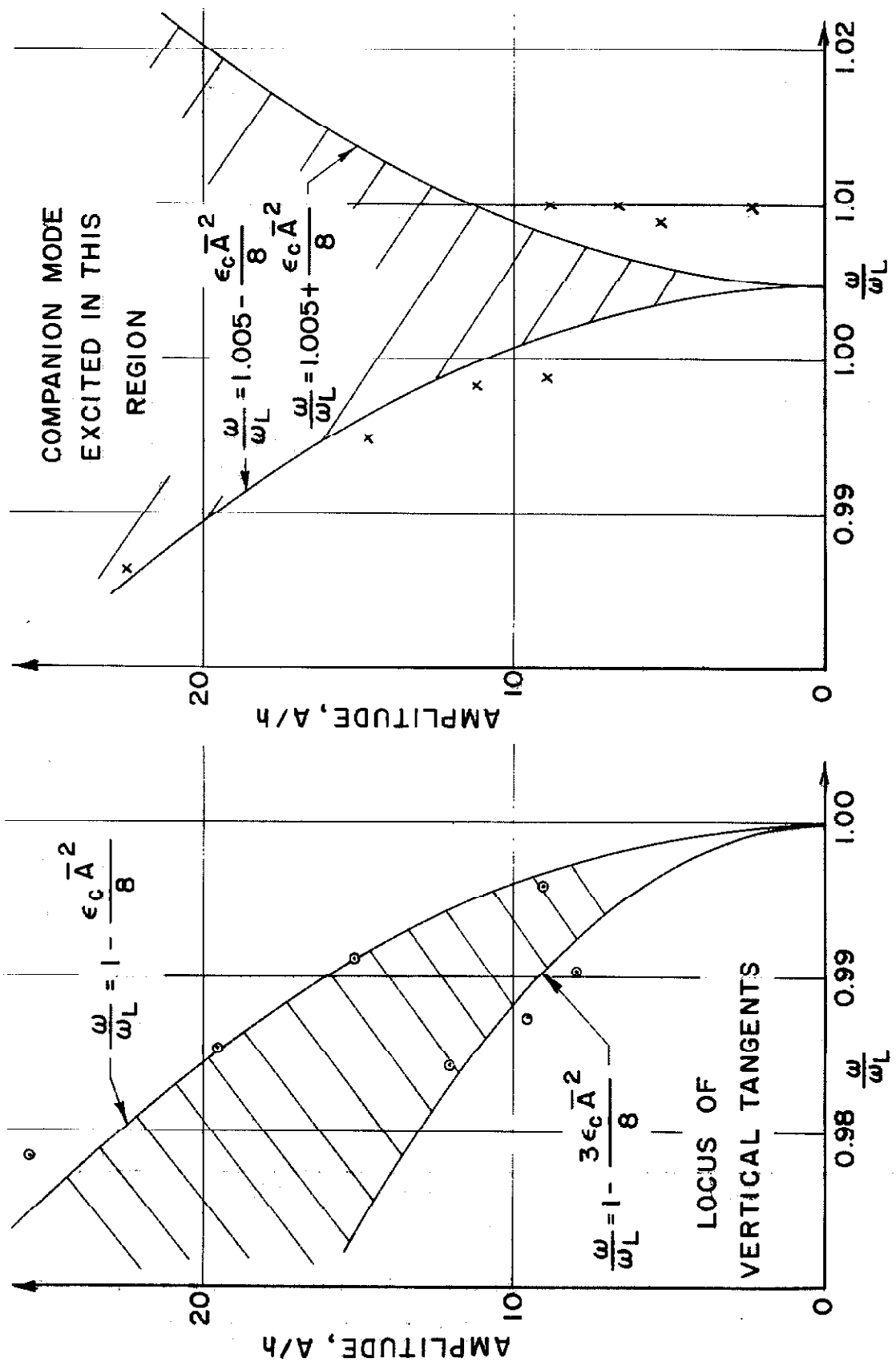

FIG.18 BOUNDARIES OF THE INSTABILITY REGIONS

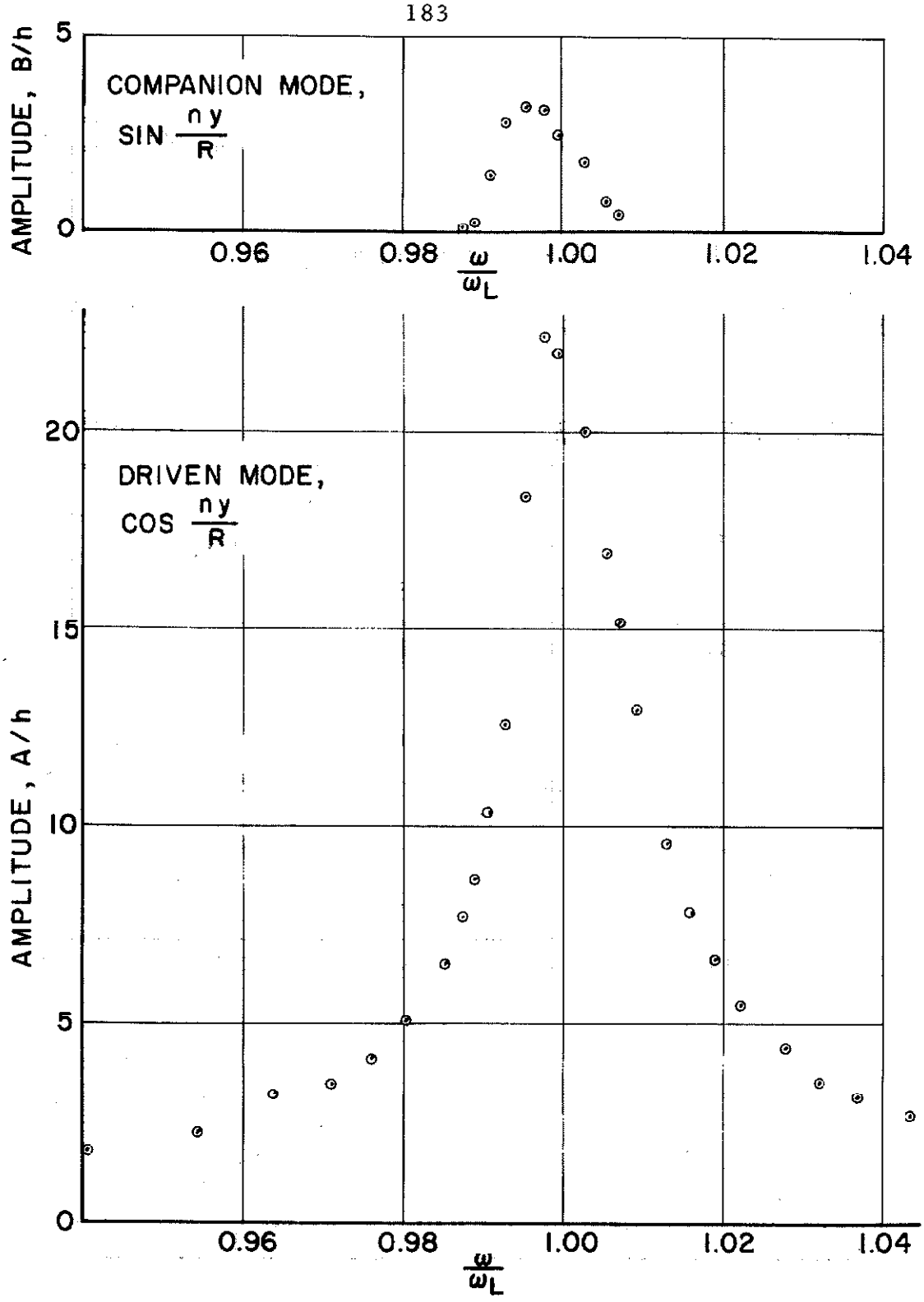

FIG. 19 n = 3 RESPONSE (MASS ADDED)
SHAKER DISPLACEMENT: $2\delta_0 = 100 \times 10^{-3}$ IN.

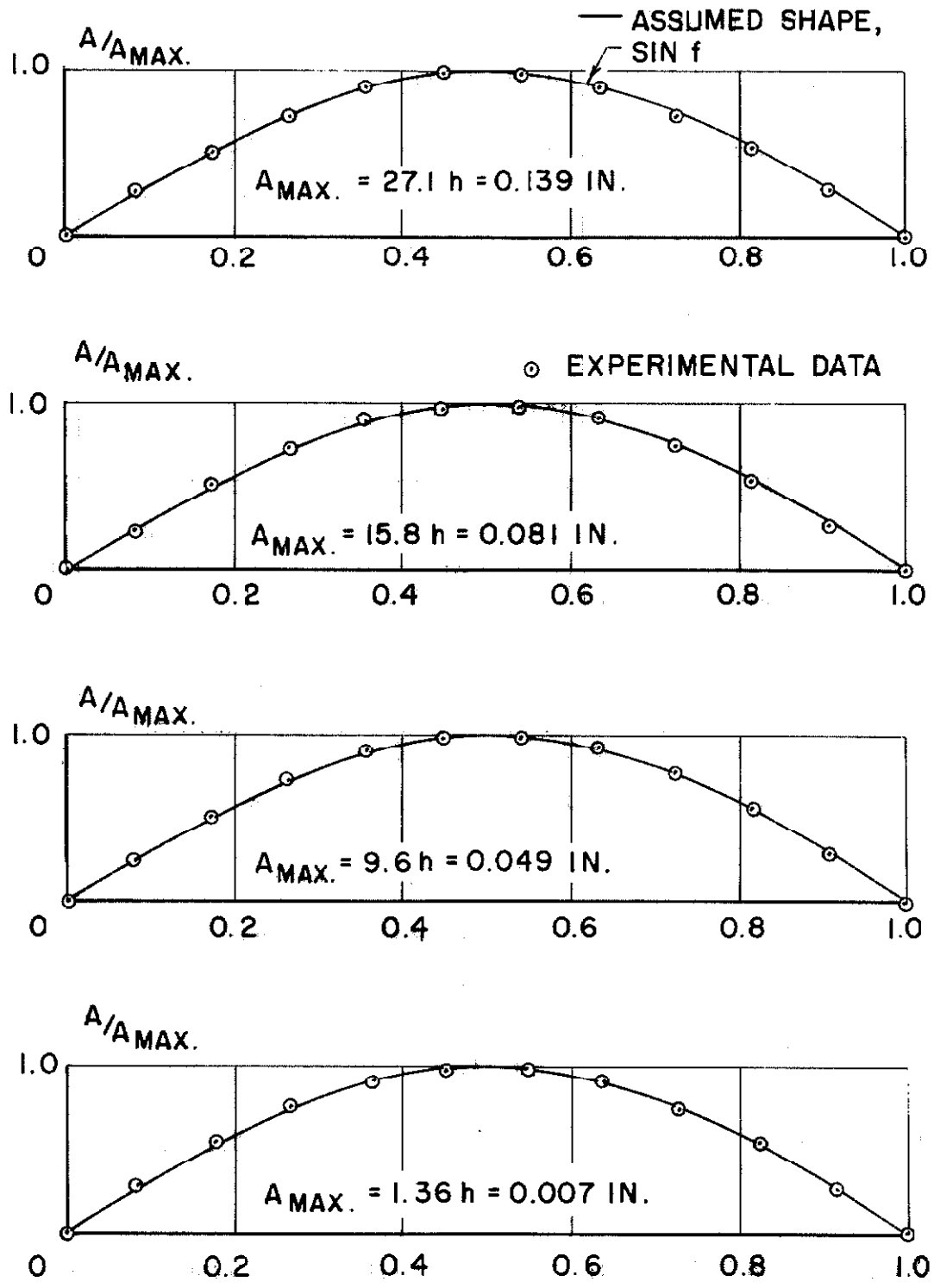

FIG. 20 DEFLECTION SHAPES

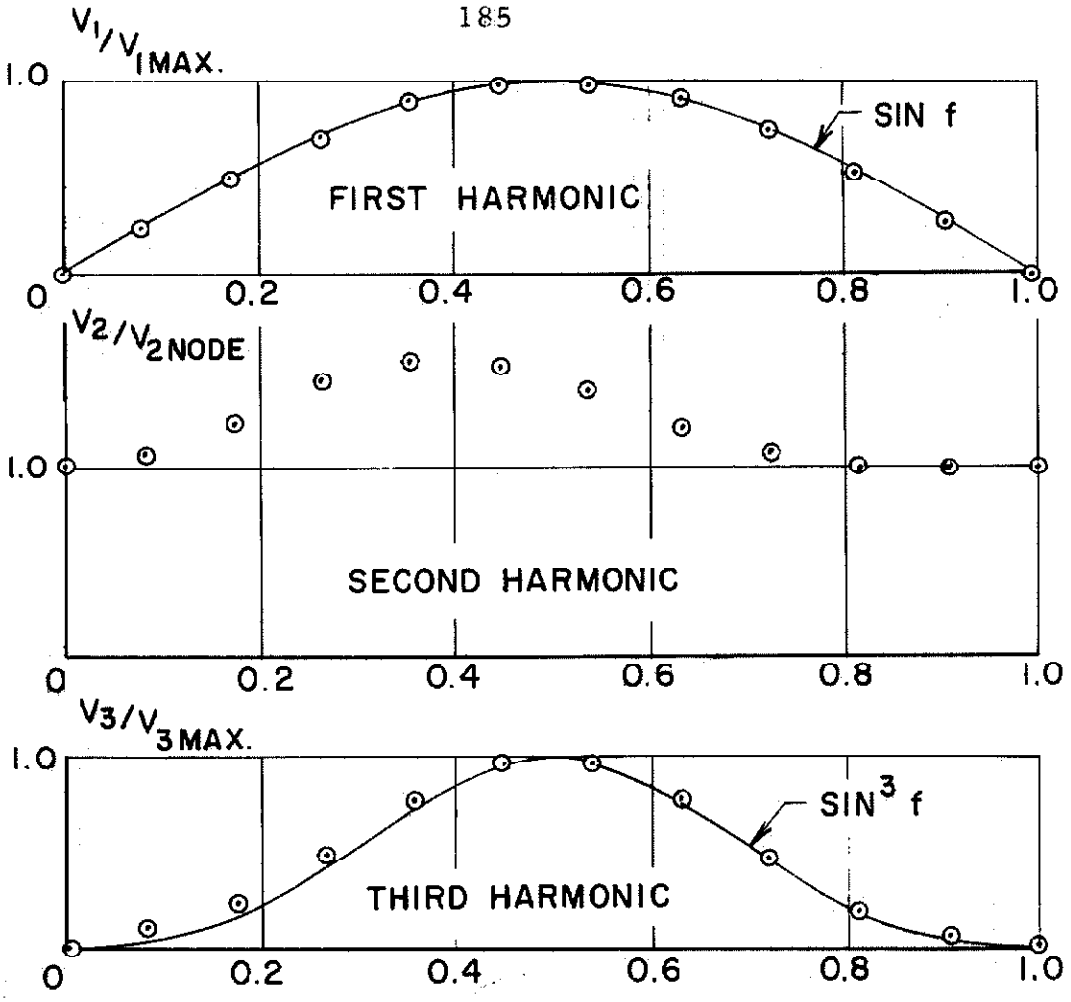

$$V(y,t) = V_1(y)\cos\omega t + V_2(y)\cos 2\omega t + V_3(y)\cos 3\omega t + \cdots$$

RATIO OF THE HARMONICS :

$V_{1MAX.} : V_{2NODE} : V_{3MAX.}$ AS 1 : 0.04 : 0.018

AMPLITUDE OF VIBRATION : $A_{MAX.} = 16.1\,h = 0.083$ IN.

FIG. 21 SPATIAL VARIATION OF THE RESPONSE VOLTAGE

DIAGRAM SHOWS THE LOCATION OF THE DRIVE WIRE AND THE NODES OF THE n = 4 MODE. SUPPORT THREADS WERE PLACED AT 1, 3, 5, AND 7.

MOST OF THE MEASUREMENTS (FIG.) WERE DONE ON THE HALF WAVE 2-3.

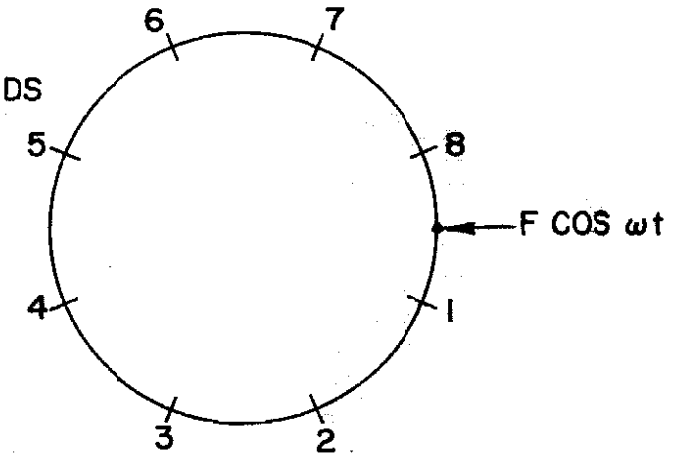

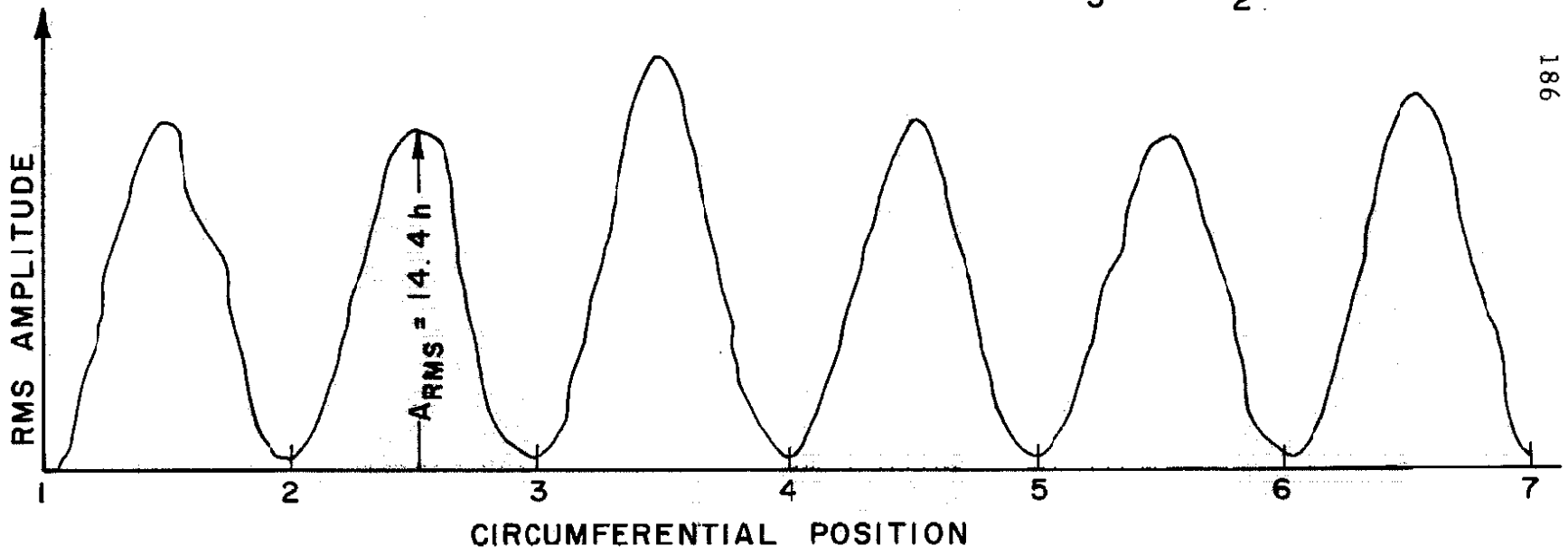

FIG. 22 CIRCUMFERENTIAL VARIATION OF THE RESPONSE

GROWTH OF THE COMPANION MODE (SIN $\frac{n y}{R}$)

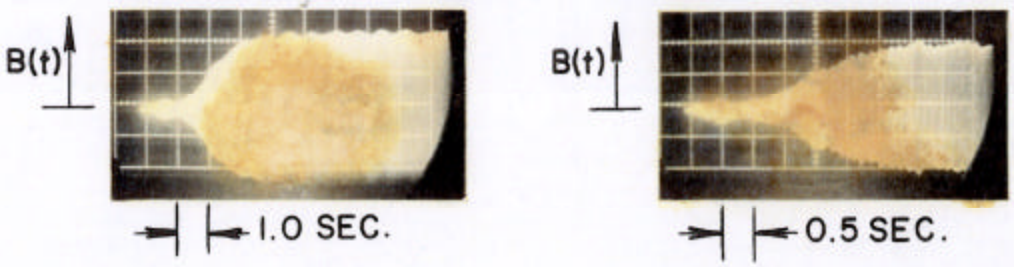

GROWTH OF THE DRIVEN MODE (COS $\frac{n y}{R}$)

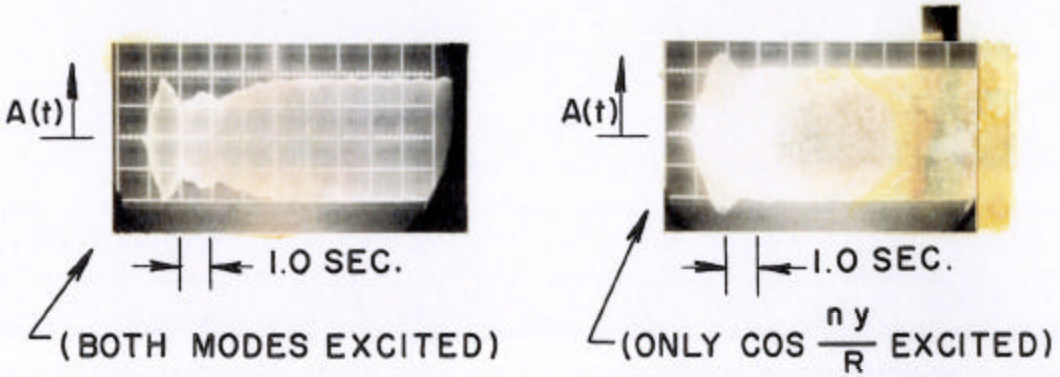

INITIAL GROWTH OF COS $\frac{n y}{R}$

START UP OF THE SHAKER (VELOCITY TRACE)

FIG. 23 STARTING TRANSIENTS

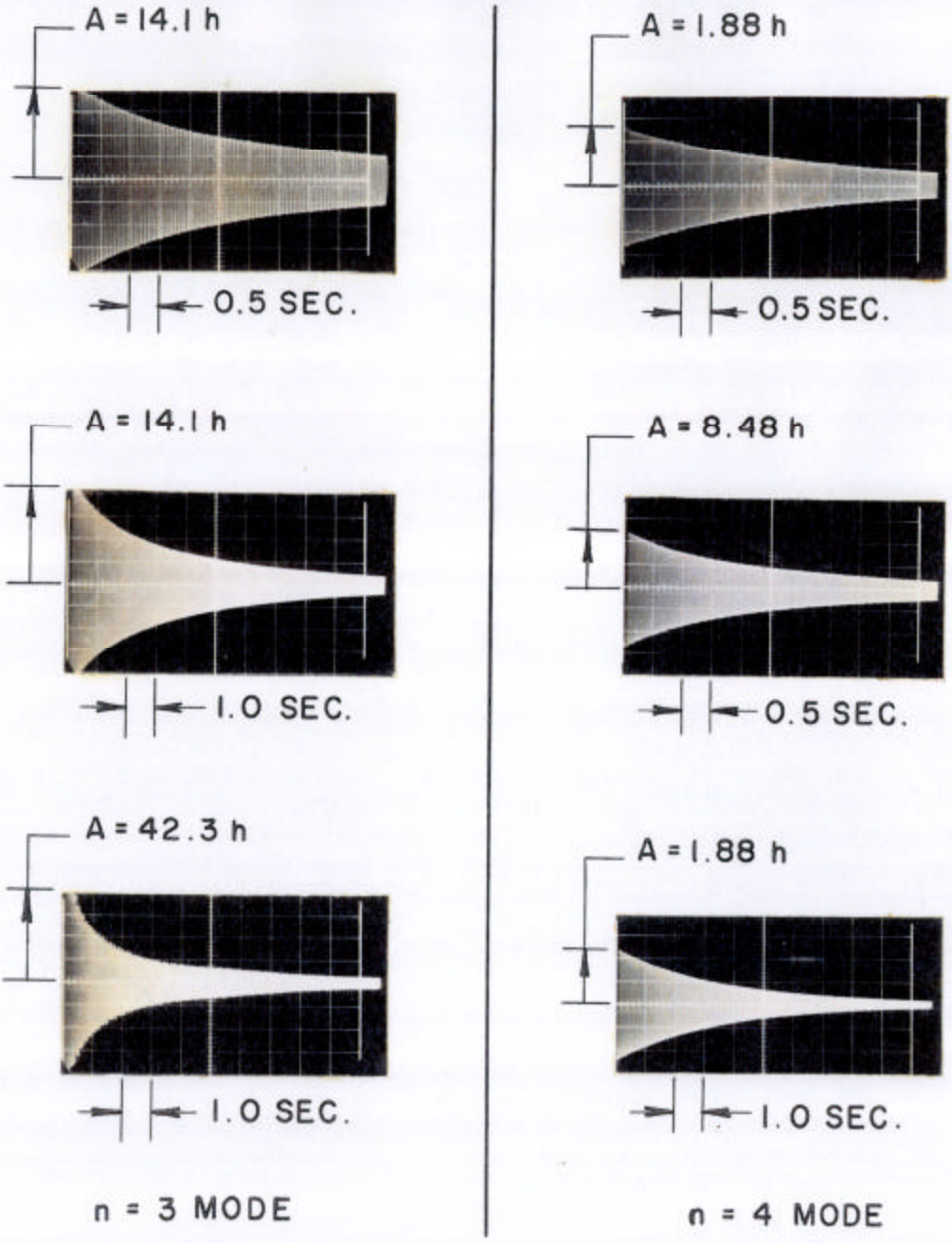

FIG. 24 DAMPING TRACES